

**EFFECT OF LOW LEVEL LASER THERAPY ON GENE
ACTIVATION, DNA DAMAGE AND REPAIR USING 5 OR
16 J/cm² ON WOUNDED HUMAN SKIN FIBROBLAST CELLS**

A dissertation submitted to the
Faculty of Health Sciences, University of Johannesburg, Johannesburg, in
fulfilment of the requirement for the degree of Master of Technology:
Biomedical Technology



by

Alwin B. Mbene

(Student number: 200582702)

Supervisor: _____

Prof. Heidi Abrahamse

_____ Date

Co-supervisor: _____

Dr. Nicolette Houeild

_____ Date

Johannesburg, 2008

DECLARATION

I, **Alwin Bilney Mbene** declare that this dissertation entitled “EFFECT OF LOW LEVEL LASER THERAPY ON GENE ACTIVATION, DNA DAMAGE AND REPAIR USING 5 OR 16 J/cm² ON WOUNDED HUMAN SKIN FIBROBLAST CELLS” is absolutely based on my own, unaided work unless where acknowledged. It is being submitted for the degree of Master of Technology: Biomedical Technology to the Faculty of Health Sciences, University of Johannesburg, Johannesburg. Neither this dissertation nor any part of has been submitted for any degree/diploma for any academic award anywhere before.

UNIVERSITY
OF
JOHANNESBURG



Alwin B. Mbene

12/08/08

Date

EXECUTIVE SUMMARY

Low level laser therapy, commonly known as LLLT or biomodulation, is a form of phototherapy which involves the application of low power monochromatic and coherent light to injuries and lesions to stimulate healing. In the medical field, lasers are classified as high power or surgical lasers and low level lasers which are used to stimulate cellular responses. Phototherapy has been successfully used for pain attenuation and induction of wound healing in non healing defects.

Even though phototherapy has been found to be beneficial in a wide variety of therapeutic applications, it has been shown that phototherapy can induce DNA damage; however this damage appears to be repairable (Hourelid and Abrahamse, 2008). DNA repair is vital to cells to avoid mutation. Literature reports show that red light or phototherapy up or down regulates genes involved in DNA repair (Zhang *et al.*, 2003). *N*-methylpurine DNA glycosylase (MPG) is involved in DNA repair by catalysing the excision of a variety of modified bases. The exact mechanism by which phototherapy works is still poorly understood.

Several authors have demonstrated that phototherapy enhances cell proliferation and migration. However, these cellular responses seem to confuse scientists as to whether wound healing is due to cell proliferation or migration or both. To determine the effect of phototherapy on cell proliferation or migration, a mini project was conducted (Zungu *et al.*, 2008). Thus, cell proliferation was arrested using 5 mM hydroxyurea (HU) which is an antiproliferative drug. Wounded (W) human skin fibroblast cells (WS1, ATCC

CRL 1502) were irradiated with 5 J/cm^2 using a Helium-Neon (He-Ne) laser with a wavelength (λ) of 632.8 nm on day 1 and 4. Cell morphology, viability and proliferation were measured 24 h post irradiation. Reports indicate that several cell culture studies have used HU to control proliferation (Cai *et al.*, 2000; Hamuro *et al.*, 2002).

Thereafter, the main study which was aimed at determining the effects of phototherapy on DNA damage and gene activation related to repair using 5 or 16 J/cm^2 on W human skin fibroblast (WS1) cells was performed. Both studies involved growing WS1 cells aseptically in complete minimum essential medium (MEM) with Earle's balanced salt solution and incubated at 37°C in 5% CO_2 and 85% humidity. Normal (N) and W cell cultures were irradiated with 5 or 16 J/cm^2 30 min and 72 h (day 1 and 4) post wounding. Non irradiated cells (0 J/cm^2) served as controls, while irradiated cells were the experimental groups. A wound was simulated by creating a central scratch across a monolayer of cells using a sterile 1 ml pipette. A 3 mW/cm^2 He-Ne laser, λ 632.8 nm, was used to irradiate cells. After a repair time of 1 or 24 h on day 4, cell morphology (microscopy), cell viability (Trypan blue exclusion test and ATP luminescent assay), proliferation (XTT assay) and DNA integrity (alkaline comet assay with and without Formamidopyrimidine glycosylase [Fpg]) were assessed. The up or down regulation of the DNA repair gene, MPG, and regulation of three reference genes namely; beta Actin (ACTB), Glyceraldehyde 3 phosphate dehydrogenase (GPDH) and Ubiquitin c (UBC) were assessed by real time reverse transcriptase polymerase chain reaction (real time RT-PCR).

Non irradiated HU treated cells had a reduced number of cells in the central scratch compared to non irradiated non treated cells, suggesting that HU inhibited cellular proliferation. Irradiated HU treated cells showed an increased number of cells in the central scratch compared to non irradiated treated cells. This observation proved that this increase was due to the stimulatory effect of irradiation with 5 J/cm^2 . The addition of HU had no significant effect on cell viability. The Trypan blue exclusion test showed no significant difference in percent viability between treated and non treated cells. Irradiated non treated cells showed a significant increase in the formazan dye, which is as a result of cleavage of XTT by the mitochondrial succinate dehydrogenase in actively proliferating cells, compared to non irradiated non treated cells ($P=0.01$).

W cells, which were not irradiated, showed incomplete wound closure at both 1 and 24 h, while W cells irradiated with 5 J/cm^2 showed complete wound closure. Similarly, W cells irradiated with 16 J/cm^2 showed incomplete wound closure at 1 and 24 h. Cell viability, proliferation and DNA integrity assays showed that irradiated and non irradiated N cells were not significantly affected at both 1 and 24 h post irradiation. W cells (1 h) irradiated with 5 J/cm^2 showed a significant increase in percentage cell viability and ATP compared to non irradiated W cells (1 h), ($P=0.05$ and $P=0.04$ respectively), while irradiation with 16 J/cm^2 showed a significant decrease ($P=0.014$ and $P=0.02$ respectively). W cells (24 h) irradiated with 5 J/cm^2 also showed a significant increase in percentage cell viability and ATP when compared to non irradiated W cells (24 h), ($P=0.006$ and $P=0.04$ respectively). Contrary, irradiation with 16 J/cm^2 showed a significant decrease ($P<0.001$ and $P=0.003$ respectively).

Cell proliferation results showed that irradiation with 5 J/cm² was stimulatory while 16 J/cm² was inhibitory. The comet assay demonstrated that N cells irradiated with 5 or 16 J/cm² exhibited an insignificant change in DNA damage at both 1 and 24 h when compared to their respective controls. This finding is in agreement with Karu *et al.*, (2003) who observed that phototherapy does not alter the biological activity of cells which at the time of irradiation are functioning normally. W cells (1 and 24 h) irradiated with 16 J/cm² showed a significant increase in DNA damage compared to their respective controls. However, there was a significant decrease in damage at 24 h compared to 1 h incubation due to the activation of DNA repair mechanisms. Though not significant, comet assay with Fpg (modified comet assay) showed more DNA damage compared to comet assay without the enzyme (conventional comet assay). It can be explained that the modified comet assay detected and cleaved oxidised bases in addition to single strand breaks, which the conventional comet assay detected, suggesting that the modified comet assay is more sensitive than the conventional comet assay.

After validation of the three reference genes, ACTB was chosen to be the gene with which to normalise MPG expression in WS1 cells. It was found to be the least variable; its expression was consistent in W cells as well as cells exposed to a He-Ne laser at a fluence of 5 or 16 J/cm². It produced an acceptable correlation coefficient ($R^2 > 0.999$) and PCR efficiency (94%). Conversely, other primers like GAPDH produced a low PCR efficiency (82%), while UBC produced a low R^2 (0.898). Wang *et al.*, (2006) recommends the value of R^2 to be more than 0.995 and a PCR efficiency of between 90 and 100% for PCR results to be reliable. Other researchers have not supported the use of ACTB as a reference gene, stating that it is highly regulated (Wang *et al.*, 2006), however this study showed that ACTB was not regulated by laser irradiation (632.8 nm at 5 or 16 J/cm²). The cell culture conditions and

laser irradiation in this study did not induce MPG expression; perhaps an alternative repair pathway might have been induced, and hence repaired the DNA damage.

In conclusion, the mini project demonstrated that HU is able to inhibit cell proliferation through its cytostatic effect without affecting the viability of W WS1 cells. This study also showed that irradiation of W cells with 5 J/cm^2 using the correct parameters enhances cell migration and proliferation as evidenced by the presence of more cells in the central scratch in HU treated cells, and a significant increase in cell proliferation as shown by the XTT assay in non treated cells respectively. Thus, migration and proliferation are the direct result of phototherapy as both are involved in wound closure. This study further confirmed that irradiation of W cells with 5 J/cm^2 stimulated ATP production, and hence cellular viability, as well as cell proliferation and migration.

Irradiation of cells with higher fluences such as 16 J/cm^2 is damaging to DNA and inhibitory to cell proliferation, migration and possibly to MPG expression. The study further showed that N cells are not stimulated by phototherapy, supporting the notion that lasers stimulate compromised cells. Thus, if they are growing normally there is nothing to stimulate. This understanding helps to clarify why N cells irradiated with 5 or 16 J/cm^2 had insignificant responses. Cell culture conditions, fluence and duration of exposures are important parameters that can affect gene expression, and hence documentation of all experimental conditions needs to be emphasised and published if reproducibility is to be achieved.

*DEDICATED TO MY DAUGHTER, MERVIS, AND WIFE,
THANDIE*



UNIVERSITY
OF
JOHANNESBURG

ACKNOWLEDGEMENTS

1. It is my pleasant duty to place on record my heart felt gratitude to Professor Heidi Abrahamse who is the Head, guarantor and supervisor of the Laser Research Group for introducing me in the area of Laser Research. I am indebted to her for her invaluable guidance, advice and encouragement which led to the completion of this dissertation.
2. I am grateful to Dr Nicolette N. Houreld, my co-supervisor and post doctoral fellow at the University of Johannesburg, for her assistance and support in my research work.
3. Financial assistance received from the University of Johannesburg (UJ), National Laser Centre (NLC), Medical Research Council (MRC), and National Research Foundation (NRF) for this project is thankfully acknowledged.
4. The management and staff at the National Laser Centre are also acknowledged for setting up lasers and provision of the laser safety course.
5. The University of Johannesburg and the African Laser Centre/CSIR for providing me with a bursary for the duration of the project.
6. I gratefully remember Dr Denise H. Hawkins Evans for her kind co-operation and helpful pieces of advice.
7. It is my pleasure to acknowledge my colleagues Messrs Innocent L. Zungu, Bernard D. Mvula, Sello L. Manotto, and Ms Tebogo Mathope for the support accorded to me in times of need.
8. Last, but not the least, I should thank my wife, Thandie, for her constant encouragement and accepting to stay alone in Malawi while I was studying in South Africa.
9. Special thanks are due to the University of Johannesburg technical staff: Messrs Alister Campbell, Mandhla Sibiya and Ms Lynca Viljoen who were always available and ready to assist.

TABLE OF CONTENTS

DESCRIPTION	PAGE
DECLARATION	ii
EXECUTIVE SUMMARY	iii
DEDICATION	viii
ACKNOWLEDGEMENTS	ix
LIST OF FIGURES	xiv
LIST OF TABLES	xvii
LIST OF SYMBOLS	xviii
PUBLICATIONS	xix
CHAPTER 1 INTRODUCTION	1
1.1 Introduction	1
1.2 Statement of the Problem	1
1.3 Aims	2
CHAPTER 2 LITERATURE REVIEW	3
2.1 Introduction	3
2.2 Ordinary Light	3
2.3 Laser Light	5
2.4 Science of Wound Healing	6
2.4.1 Chronic wound healing	9
2.5 Laser Light Tissue Interaction	10
2.6 Laser Therapy	12
2.7 DNA Damage and Repair	16
2.8 Gene Expression	21
2.9 Detection of Damaged DNA (Enzyme-Linked Comet Assay)	23

CHAPTER 3	MATERIALS AND METHODS	25
3.1	Cell Culture	25
3.1.1	Subculture	25
3.1.2	Cell model	26
3.2	Laser Irradiation	27
3.3	Cell Morphology	30
3.4	Cell Viability	31
3.4.1	Trypan blue exclusion test	31
3.4.2	ATP luminescent assay	33
3.5	Cell Proliferation	33
3.6	Genetic Integrity	34
3.6.1	Alkaline comet assay	34
3.7	Real Time Reverse Transcription PCR	38
3.7.1	Primers	39
3.7.2	Ribonucleic acid (RNA) isolation	40
3.7.3	cDNA synthesis	41
3.7.4	PCR	43
3.7.5	Melt curve analysis	45
3.7.6	Reference gene validation	46
3.7.7	REST program	46
3.7.8	Gel electrophoresis	47
3.8	Statistical Analysis	48
CHAPTER 4	RESULTS	49
4.1	Cell Morphology	49
4.2	Cell Viability	52
4.2.1	Trypan blue exclusion test	52
4.2.2	ATP luminescent assay	55

4.3	Cell Proliferation	57
4.4	Genetic Integrity	61
4.4.1	Alkaline comet assay	61
4.5	Real Time Reverse Transcription PCR	65
4.5.1	Reference gene validation	65
4.5.2	MPG expression	72
 CHAPTER 5 DISCUSSION AND CONCLUSION		 79
 REFERENCES		 94
 APPENDICES		 114
 APPENDIX A		 114
 MATERIALS AND METHODS		 114
A1	Flow Diagram	114
A2	Equipment Used	115
 APPENDIX B		 118
 MEDIA, SOLUTIONS AND CALCULATIONS		 118
B1	Cell Line Description	118
B2	Composition of Complete Media	118
B3	0.25% Trypsin in HBSS	119
B4	3% EDTA (Ethylenediaminetetracetic acid)	119
B5	Calculation of Cell Number and Seeding of Culture Dishes (Plates)	119
B6	ATP Assay	120
B7	XTT Assay	121
B8	Comet Assay Solutions	121
B8.1	Phosphate buffered saline (PBS), 1% Standard agarose and slide preparation	121
B8.2	1% Low melting point agarose	122
B8.3	Lysis solution	122

B8.4	Electrophoresis solution	122
B8.5	Neutralisation buffer	122
B8.6	Sodium hydroxide (NaOH) solution (10 M)	122
B8.7	Enzyme reaction buffer	123
B8.8	Formamidopyrimidine glycosylase (Fpg)	123
B8.9	4'6-diamidine-2-phenylindol dihydrochloride (DAPI)	123
B9	Real Time RT-PCR Solutions	124
B9.1	Tris-EDTA (TE) buffer, pH 8.0	124
B9.2	50x Tris acetate EDTA (TAE) buffer	124
APPENDIX C		125
REFERENCE GENE SEQUENCE		125
C1	MPG Gene Sequence	125
C2	ACTB Gene Sequence	126
C3	GAPDH Gene Sequence	127
C4	UBC Gene Sequence	128
APPENDIX D		129
CALCULATION AND CONCENTRATION OF cDNA		129
APPENDIX E		130
REAL TIME RT-PCR RESULTS		130
E1	Melt Report for ACTB	130
E2	Melt Report for GAPDH	134
E3	Melt Report for UBC	137
E4	Relative Expression Report for Reference Genes	140
E5	MPG Expression in W Cells Irradiated With 5 J/cm ² 1 h Incubation Post Irradiation	142
E6	MPG Expression in W Cells Irradiated With 16 J/cm ² 0 h Incubation Post Irradiation	145
E7	MPG Expression in W Cells Irradiated With 16 J/cm ² 3 h Incubation Post Irradiation	148
E8	MPG Expression in W Cells Irradiated on Day 1 With 16 J/cm ² 8 h Incubation Post Irradiation	151

LIST OF FIGURES

Figure 1	The electromagnetic spectrum showing the different types of electromagnetic radiation	5
Figure 2	A cutaneous wound three days after injury	8
Figure 3	Irradiation of cells with 5 J/cm^2 is stimulatory while irradiation with more than 12 J/cm^2 is inhibitory	15
Figure 4	A He-Ne laser (Spectraphysics, model 127) was used to irradiate cells at λ 632.8 nm	27
Figure 5	The laser beam was clipped with an iris at X and produced a spot size of 9.08 cm^2	29
Figure 6	A haemocytometer showing two chambers in which cells were counted using a light microscope	32
Figure 7	Cell DNA migration pattern produced by the comet assay as a result of strand breakage	36
Figure 8	Classes of comets (0-4) stained with DAPI ($1 \mu\text{g/ml}$)	37
Figure 9	Micrograph of irradiated and non irradiated normal (N) WS1 cells	50
Figure 10	Micrograph of irradiated and non irradiated wounded (W) WS1 cells	51
Figure 11	ATP luminescent assay graph	57
Figure 12	Cell proliferation as determined by XTT in normal (N) and wounded (W) cells	59
Figure 13	Hydroxyurea graph showing cell proliferation	60
Figure 14	Comet assay with and without Fpg	62
Figure 15	Standard curve for reference gene beta Actin (ACTB)	66
Figure 16	Standard curve for reference gene Glyceraldehyde 3 phosphate dehydrogenase (GAPDH)	67
Figure 17	Standard curve for reference gene Ubiquitin c (UBC)	67
Figure 18	A melt curve analysis for ACTB PCR product	68
Figure 19	A melt curve analysis for GAPDH PCR product	69
Figure 20	A melt curve analysis for UBC PCR product	69

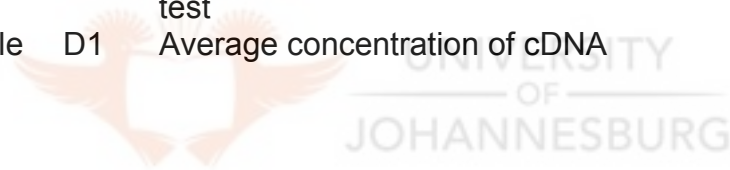
Figure 21	A 2% agarose gel was made to check PCR products of the reference genes	70
Figure 22	Relative gene expression for ACTB, GAPDH and UBC	71
Figure 23	A melt curve analysis for MPG and ACTB PCR products	72
Figure 24	A 2% agarose gel for MPG and ACTB PCR products	73
Figure 25	A melt curve analysis for MPG PCR products 0 h incubation post irradiation	74
Figure 26	A 2% agarose gel for MPG PCR products 0 h incubation post irradiation	75
Figure 27	A melt curve analysis for MPG PCR products 3 h incubation post irradiation	76
Figure 28	A 2% agarose gel for MPG PCR products 3 h incubation post irradiation	76
Figure 29	A melt curve analysis for MPG PCR products 8 h incubation post irradiation	77
Figure 30	A 2% agarose gel for MPG PCR products 8 h incubation post irradiation	78
Figure A1	Flow diagram of normal (N) and wounded (W) WS1 cells irradiated with a He-Ne laser (λ 632.8 nm) on day 1 and 4	114
Figure A2	An incubator in which cells were grown at 37 °C in 5% CO ₂ and 85% humidity	115
Figure A3	A centrifuge (DIGICEN-R, INSTRULAB S.A) used to spin cell culture suspensions at 2,200 rpm for 4 min	115
Figure A4	An inverted light microscope	116
Figure A5	A fluorescent microscope used to score comet assay slides stained with DAPI	116
Figure A6	A centrifuge used to spin samples during RNA and cDNA synthesis	117
Figure A7	The RotorGene thermocycler which was used for real time RT-PCR	117
Figure C1	MPG gene sequence showing forward (>>>>) and reverse primers (<<<<)	125
Figure C2	ACTB gene sequence showing forward (>>>>) and reverse primers (<<<<)	126

Figure C3	GAPDH gene sequence showing forward (>>>>) and reverse primers (<<<<)	127
Figure C4	UBC gene sequence showing forward (>>>>) and reverse primers (<<<<)	128



LIST OF TABLES

Table 1	Proteins which repair DNA damage	17
Table 2	Gene activation in wound healing	22
Table 3	Irradiation parameters using the He-Ne laser	28
Table 4	PCR primer sets and product sizes for the gene of interest and reference genes	39
Table 5	Genomic DNA elimination	41
Table 6	Reverse transcription reaction	42
Table 7	PCR reaction components	44
Table 8	Three step PCR cycling program	45
Table 9	Gel loading	47
Table 10	Percent cell viability as determined by the Trypan blue exclusion test in normal (N) and wounded (W) WS1 cells	52
Table 11	Total number of viable and non viable cells as determined by the Trypan blue exclusion test	54
Table D1	Average concentration of cDNA	129



LIST OF SYMBOLS

J/cm^2	joules per square centimetre
mW	milliwatts
mA	milli amperes
nm	nanometre
CO ₂	carbon dioxide
Min	minute(s)
h	hour(s)
s	second(s)
WS1	human skin fibroblast cell line
ATCC	American Type Culture Collection
ml	millilitre
mg	milligram
ATP	adenosine triphosphate
μ l	microlitre
μ g	microgram
μ M	micromole
ng	nanogram
M	molarity
mM	millimole
v/v	volume by volume
rpm	revolutions per minute
X g	gravitational force
rRNA	ribosomal ribonucleic acid
E. coli	<i>Escherichia coli</i>
e.g.	example
~	approximately
λ	Wavelength(s)

PUBLICATIONS

Mbene, A.B., Zungu, I.L., Houreld, N.N., Hawkins, D. and Abrahamse, H. (2006) Adaptive Response After 632.2 nm Laser Irradiation Decreases Cellular Damage in Diabetic Wounded Fibroblast Cells. *Medical Technology SA* **20**(1): 21-24

Zungu, I., Mbene, A., Houreld, N., Hawkins, D. and Abrahamse, H. (2008) Phototherapy promotes cell migration in the presence of hydroxyurea. *Lasers in Medical Science* **DOI**: 10.1007/s10103-007-0533-z

The other paper emanating from this study is in the draft form ready to be submitted to the journal:-

Mbene, A.B., Houreld, N.N. and Abrahamse, H. (2008) DNA damage and gene activation related to DNA repair after phototherapy in wounded fibroblast cells. *Photochemistry and Photobiology B: Biology*

CHAPTER 1 INTRODUCTION

1.1 Introduction

Phototherapy or biomodulation is a remarkable therapy that has become more popular and widely used in the treatment of a variety of medical conditions, such as slow to heal wounds, pain, soft tissue injuries, arthritis and skin trauma. Although the mechanism is not very well understood, it is known that light energy passes through a cell and photonic energy is absorbed by the mitochondria. This absorbed light stimulates a cascade of photobiological events. The effects of phototherapy are photochemical, not thermal (Matic *et al.*, 2003).

1.2 Statement of the Problem

Even though phototherapy has been found to be beneficial in a wide variety of therapeutic applications, it has been shown that phototherapy can induce DNA damage; however this damage appears to be repairable (Hourelid and Abrahamse, 2008). It might be that phototherapy helps the patient at first glance and damages DNA at the same time, thereby increasing the risk of therapy induced disease up to an increased cancer risk (Greulich, 2003). The restorative capacity of DNA damage is important for progress of life. If DNA damage repair mechanisms are compromised, mutation, death or extinction of the species may occur. The exact mechanism by which phototherapy influences DNA repair is not known. However, literature indicates that irradiation at 628 nm upregulates genes involved in DNA repair (Zhang *et al.*, 2003).

Despite extensive research in the field of phototherapy, literature still remains contradictory; some authors have found positive, negative or no effect at all in wound healing. This discrepancy has been largely attributed to poor records and lack of proper controls. Furthermore, little research has been done on DNA repair genes related to phototherapy and hence this study would add knowledge to the public on the molecular biology of phototherapy. Lastly, in South Africa not many people are aware of phototherapy as an alternative treatment modality for the various ailments and as such its study would help patients and healthcare practitioners understand and make informed choices. If the treatment is accepted, healthcare practitioners would incorporate it in their treatment plans to enhance the healing of slow to heal wounds.

1.3 Aims

The aims of this study were to:

- assess the effects of phototherapy on wounded WS1 cells by investigating DNA damage and methylpurine DNA glycosylase (MPG) gene activation related to DNA repair using a He-Ne laser (λ 632.8 nm) with fluences of 5 or 16 J/cm²;
- attempt to bridge the gap in knowledge which might have been created due to modern advances in cellular and molecular biological research techniques associated with laboratory experiments in wound healing and the clinical application of this knowledge;
- compare the effect of phototherapy on the expression of MPG in WS1 cells at 1 and 24 h post irradiation and
- assess the sensitivity of the comet assay with and without Fpg.

CHAPTER 2 LITERATURE REVIEW

2.1 Introduction

There are conflicting reports in the literature about the effectiveness of low level laser therapy (LLLTT), commonly known as phototherapy, in wound healing; some researchers reported beneficial or inhibitory effects, while others have reported no effect at all (Allendorf *et al.*, 1997; Flemming and Cullum, 2000; Hall *et al.*, 1994; Kopera *et al.*, 2005; Damante *et al.*, 2004). Most researchers agree that the differences in the findings might have been due to a number of conditions and amongst them were poor records, cell culture conditions, methods of assessing results, and lack of proper control groups and theoretical understanding (Karu, 1990; Vincky *et al.*, 2003).

More research is being done in wound healing using phototherapy, and there are numerous reports that its application enhances wound healing (Conlan *et al.*, 1996; Mester *et al.*, 1971; Mester *et al.*, 1985). Karu (2003) observed that in laser therapy, the question is no longer whether light has biological effects but rather how irradiation from therapeutic lasers and light emitting diodes (LED's) work at the cellular and organism level and what the optimal light parameters are for different uses of these light sources.

2.2 Ordinary Light

Light therapy, which has also been called photon therapy (Streeter *et al.*, 2004) has been used for healing purposes for thousands of years (Karu, 2003). The ancient Egyptians were the first to recognise the beneficial effect

of sunlight on humans. In 525 B.C., Herodot correlated the strength of the human skull to the degree of sun exposure. The ancient Greeks (Hippocrates 460-375 B.C. and Oribasius of Pergamon 325 A.D.) used the sun to treat a variety of illnesses including oedema and diseases of the abdomen and kidneys (Kai, 2002; Karu, 2003). Furthermore, scientists demonstrated that vitamin D, which is acquired through exposure to the sun, can be used to increase bone strength and simulated sunlight in the form of bright light has been shown to reduce psychological stress.

Today, researchers are trying to reproduce light's healing properties using devices such as low level lasers (Coulter, 2003). Present scientists have come to understand more about the nature of light and its restorative capacity and thus techniques and devices like lasers, that use light as part of the healing process, have been developed in the last few years. People had forgotten about the restorative capacity of sunlight. After noting that lasers can be used for treatment, the present generation is reminded of the past when sick people would be taken into the sunlight for treatment. Phototherapy, healing with light, could be one of the first natural therapies (Coulter, 2003). Enwemeka (2004) wraps it all up by saying "sunny days are exciting and dull ones depressing".

Normal daylight, which falls in the visible range, is incoherent (travels in all directions) and has a thermal effect. It consists of ultra violet light (300 to 400 nm range) as well as all the colours of the rainbow (polychromatic light), with wavelength (λ) from 400 nanometre (nm), where the light is blue in colour, to the rich red λ of 700 nm (Figure 1).

2.3 Laser Light

The laser is a device that emits a special form of light, which does not exist in nature and the word LASER is an acronym for **L**ight **A**mplification by **S**timulated **E**mission of **R**adiation (Tunér and Hode, 2002; Coulter, 2003; Carroll and Humphreys, 2006). Radiation refers to the coherent light (travels in a straight line) energy which is released. Light beams which fall between 400 to 700 nm form part of the visible spectrum of the electromagnetic radiation spectrum (Figure 1), while ultraviolet (UV) light forms part of the invisible spectrum (5 to 400 nm) beyond the violet ends of the visible spectrum. On the opposite end, infrared (IR) light is the portion of the invisible electromagnetic spectrum consisting of radiation with λ 750 nm to 1 mm, between light and radio waves.

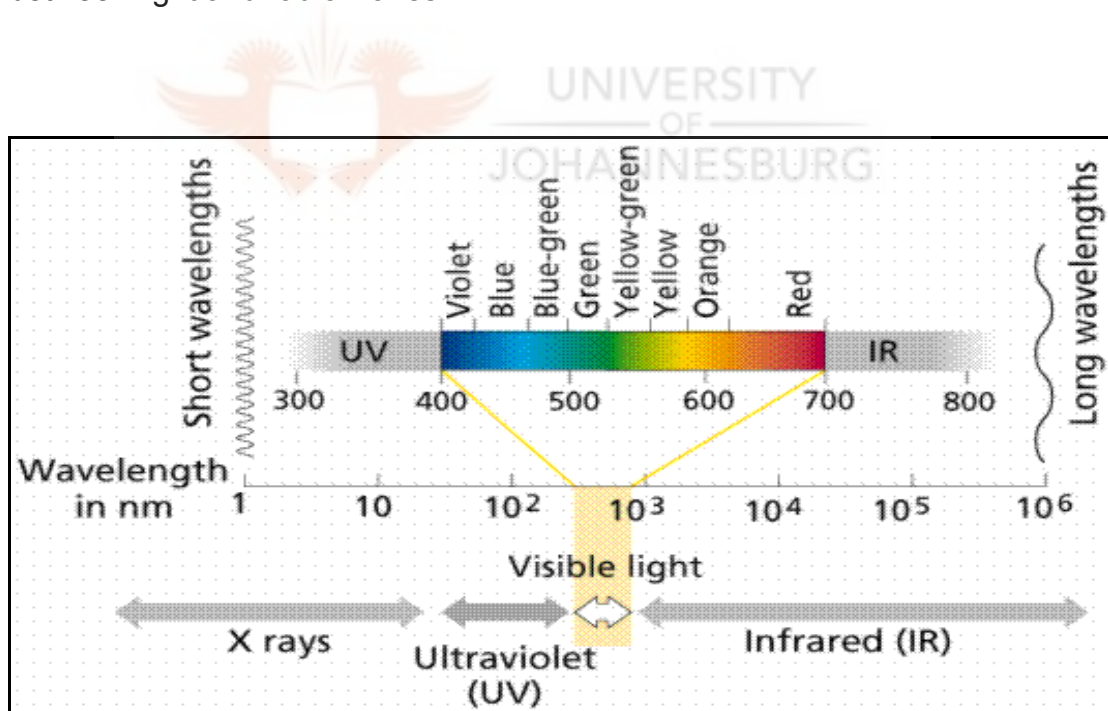


Figure 1 The electromagnetic spectrum showing the different types of electromagnetic radiation. The longer the λ of visible light the more red it appears. Wavelengths longer than red are referred to as infrared, while those shorter than violet are ultraviolet. A He-Ne laser falls in the visible range (Streeter *et al.*, 2004).

Laser light is monochromatic (has one precise colour or wavelength), it is coherent (travels in a straight line) and collimated (beam is concentrated in a defined location or spot), (Csele, 2004). These three properties make laser light to be considered as a disciplined light, because other light sources such as the sun and conventional light scatter in many directions and have no relationship to other light rays emitted from the same source (Gregory, 1998).

Lasers consist of three basic components namely: a power supply (energy source), a lasing or amplifying medium (solid, gas or liquid), which consists of molecules or atoms that store and release energy, and thirdly a resonating cavity or reflecting mirrors that return the photons to the lasing medium until they are released from the laser in the form of laser energy (Gregory, 1998; Tunér and Hode, 2002; Carroll and Humphreys, 2006). The principle on which lasers are based was postulated in 1917 by Albert Einstein. In 1959, 32 years after the concept of stimulation emission had been proposed, Theodore Maiman successfully developed a device known as a laser by utilising the technique of concentrating and amplifying monochromatic light which had originally been produced by two teams of researchers. Because the beam could be concentrated to a minute surface area, surgical applications were developed (Soet, 2005).

2.4 Science of Wound Healing

Anatomically, the skin is partitioned into two layers. The outermost layer is the epidermis, consisting of densely packed keratinocytes and the underlying layer is the dermis, which is composed of fibroblast cells, extracellular matrix and blood capillaries. The primary function of the skin is to serve as a protective barrier against the environment. Loss of the integrity of large

portions of the skin as a result of injury or illness may lead to major disability or even death (Singer and Clark, 1999). Diegelmann and Evans (2004) described the disruption of the normal anatomical structure and more importantly, the function as a wound. The primary function of treating a wound is to rapidly restore the anatomical structure and function.

Wound healing is a dynamic, interactive process involving soluble mediators, blood cells, extracellular matrix and parenchymal cells. A wound is a highly complex biological system, and hence detailed studies of repair processes are vital if progress is to be made in wound healing. This process of wound repair is the focus of intense research, with the goal of developing more rapid and long lasting treatments for chronic wounds. Because of that, considerable studies with phototherapy as a treatment modality have been done for the past four decades.

The healing process has a number of overlapping phases: inflammation, formation of granular tissue with angiogenesis (proliferation) and scar formation (remodelling) (Clark, 1996; Dyson, 1991; Singer and Clark, 1999; Gál *et al.*, 2006). Each component of the wound healing process plays a key role through several mediators. Inflammation is the normal acute reaction of tissues after any injury and occurs through the actions of neutrophils, macrophages and lymphocytes; all mediated by growth factors and proteases (Yilmaz *et al.*, 2006). The earliest circulating cell fragment detected at the injury site is platelets, which are involved in haemostasis and initiation of the inflammatory phase. Activated platelets become sticky and aggregate to form a plug that temporarily occludes small vessels (Figure 2). Fibroblasts also migrate into the wound site 24 h after injury.

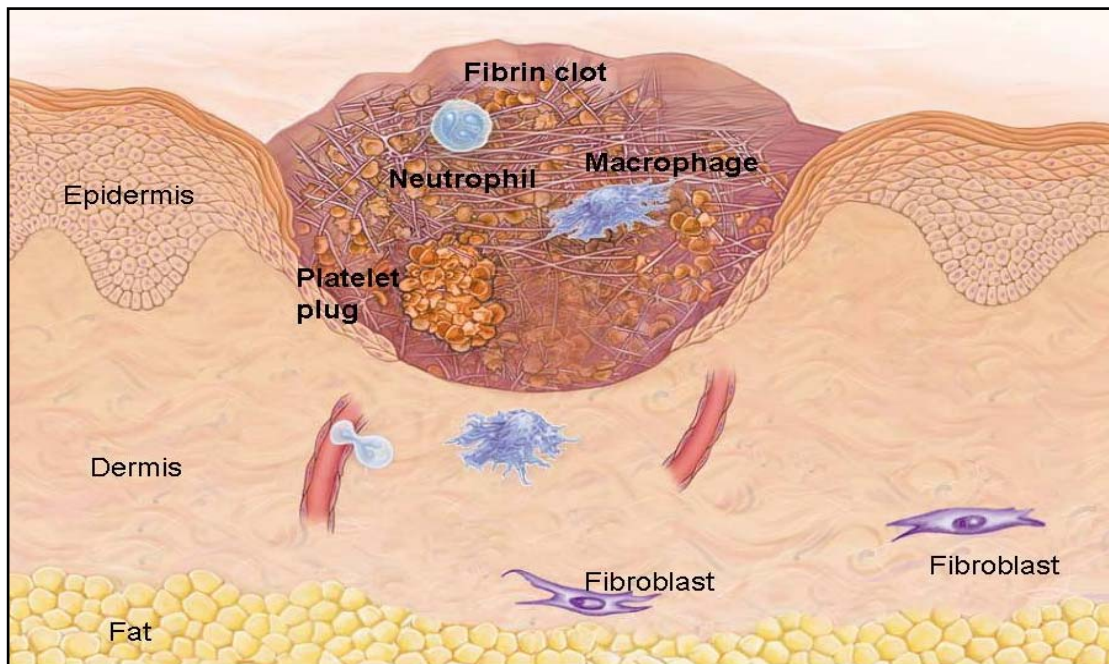


Figure 2 A cutaneous wound three days after injury. A platelet plug is formed to occlude the haemorrhage. Neutrophils and macrophages produce growth factors which stimulate fibroblast proliferation (Singer and Clark, 1999).

During the phase of healing (4 to 21 days), fibroblasts are activated and undergo a burst of proliferative and synthetic activity, initially producing high amounts of fibronectin and then other proteins including collagen and elastin (Abrahamse *et al.*, 2006; Singer and Clark, 1999). The fibroblasts align themselves along the wound axis and form cell to cell links, which contribute to the contraction of the wound (Calvin, 1998). Finally, remodelling is provided by collagen cross linking. Usually, natural healing of a wound takes time, and humans quickly become impatient, and hence seek alternative remedies such as medicine and a range of natural and synthetic materials in an attempt to speed healing (Demir *et al.*, 2004). Patients and healthcare practitioners who are aware of phototherapy as a treatment modality look for this intervention.

Even though there is no general agreement about the exact way in which phototherapy influences the process of wound healing, literature indicates that laser photobioactivation accelerates inflammation, modulates the level of prostaglandin, enhances the action of macrophages, promotes fibroblast proliferation, facilitates collagen synthesis, fosters immunity and therefore in the process, accelerates the healing process (Dyson, 1991; Saygun *et al.*, 2008). However, there are some studies which have found negative or no effect at all between He-Ne irradiated groups and control wounds. This is in sharp contrast to the general trend regarding phototherapy as a biostimulator.

2.4.1 Chronic wound healing

Wound healing is a repair process that begins immediately after the wounding event. Due to various reasons, some wounds take longer to heal, and hence wounds are often classified as acute or chronic. Acute wounds take less than 8 weeks to heal and have not yet completed the natural healing cycle. Lazarus *et al.*, (1994) defines a chronic wound as one that fails to proceed through an orderly and timely process to produce anatomic and functional integrity, or one that proceeds through the repair process without establishing a sustained anatomic and functional result. Chronic wounds either require a prolonged time to heal, do not heal completely, or recur frequently.

A large number of factors can impede wound healing and may predispose a patient to the development of chronic wounds (Williams and Barbul, 2003). For instance, if the inflammatory phase persists beyond its normal physiological limits, a chronic wound is generated (Ennis *et al.*, 2007). Chronic wounds usually attract macrophages which produce matrix metalloproteinase. This protein is associated with inflammation. Thus as long

as there is inflammation reactive oxygen species (ROS), which damage DNA, are produced (de Bont and Larebeke, 2004). Phototherapy is known to be associated with the reduction of inflammation.

Chronic wounds are an economic burden to the family as well as the government because patients suffering from these wounds are most of the time semi incapacitated, if not completely, and thus have to be cared for. If admitted, they also spend more time in the hospital. Previous studies indicate that phototherapy enhances wound healing (Conlan *et al.*, 1996) and could thus decrease this burden by saving valuable time and resources for both patients and healthcare facilities. Furthermore, improved wound healing would reduce the risk of infection for the patient, decrease the amount of costly dressings required, and more quickly return the patient to a pre-injury/illness level of activity.

2.5 Laser Light Tissue Interaction

Light or laser light can interact with tissue in four ways namely: transmission, reflection, scattering and absorption. Transmission refers to the passage of light through a tissue without having any effect on that tissue or on the properties of the light. The transmission of laser radiation in tissues is related to its wavelength. Reflection refers to the repelling of light off the surface of the tissue without entering the tissue. Scattering of light occurs after it has entered the tissue, whereby the beam of light is spread out within the tissue resulting in irradiation of a larger area than anticipated (Carroll and Humphreys, 2006). Absorption is a process by which a photon gives up energy to its surrounding medium. This energy is ultimately responsible for photobiostimulation (Streeter *et al.*, 2004).

According to the Grothus-Draper law light must be absorbed by tissue to produce an effect in that tissue. Light absorbing tissue components are known as chromophores. Laser transforms light into electrical energy which is applied to tissue to accomplish a task. If properly applied, the task can be accomplished precisely with great benefit and few adverse effects (Gregory, 1998). Thus absorption of the photons of laser light is responsible for the effects on the tissue; cell metabolism activation via the respiratory chain occurs in all cells susceptible to light irradiation. Susceptibility to irradiation and capability of activation depends on the physiological status of irradiated cells; cells whose overall redox potential is shifted to a more reduced state (e.g. in a pathological state) are sensitive to irradiation (Karu, 1988; Karu 2003). Mester *et al.*, (1991) states that photons absorbed by tissue are thought to cause biological effects by two mechanisms: non specific photothermal effects caused by kinetic excitation and specific photochemical effects caused by electronic excitation of chromophore molecules. Thus, a fundamental understanding of laser tissue interactions is vital for the proper and appropriate use in clinical practice (Carroll and Humphreys, 2006).

Although several types of lasers exist, two lasers are commonly used in therapy namely: infrared and He-Ne lasers, with infrared being the most common. Infrared laser irradiation shows a higher penetration into tissues than laser light in the red region of the visible spectrum. A He-Ne laser has an indirect penetration depth of 1 to 1.5 cm and a direct penetration of 0.5 cm (Hartley, 2004). Laser therapy has proved useful in the treatment of skin and mucosal disorders (Mester *et al.*, 1985). The He-Ne laser has been used for wound healing for more than 30 years (Tunér and Hode, 2002). The long duration of use of the He-Ne laser has been attributed to the fact that it was the first commercially available source of coherent red light (Karu, 1990).

The beam of a low energy laser produces a temperature change confined in the range from less than 0.1 to 0.5 °C in the irradiated tissues (Basford, 1989; Yu *et al.*, 2003). The properties of lasers allow laser light used in phototherapy to penetrate the surface of the skin with no heating effect, no damage to the skin and no known side effects. Therefore, biological effects are derived directly from the radiation itself rather than from thermal influence (Yu *et al.*, 1996). Laser light directs biostimulation light energy to the body's cells, which the cells then convert into chemical energy to promote natural healing and pain relief.

2.6 Laser Therapy

While other researchers were busy with military applications, Endre Mester suspected that the laser could have a more human application; the destruction of malignant tumours. Mester's research did not work as anticipated; he found that the treatment was ineffective against malignancies. However, he observed that the incisions made to implant malignant cells in test animals appeared to heal faster in treated animals than in the control animals that were not treated. At last, he discovered that his laser was underpowered and hence could not destroy the cancerous tissue but could stimulate healing (Soet, 2005).

In the medical field, the application of laser therapy started with the eye (Steen, 2003). This therapy has been divided into two major categories namely; High Level Laser Therapy (HLLT) and LLLT. High level lasers are also known as surgical lasers because they can replace the knife of a surgeon; they can burn, cut and ablate (Damante *et al.*, 2004). In order for a laser to be used as a surgical laser it must be powerful enough to heat up the

tissues to a temperature of over 50 °C (Tunér and Hode, 2002). HLLT, as a surgical knife, has shown certain advantages over the scalpel blade because surgery using lasers is a non contact method, bloodless, precise, has minimum post operative oedema, painless healing and is without complication (Takac *et al.*, 1998).

In a different way, LLLT, which is a branch of phototherapy, utilises low power energy for biostimulating target cells or altering cellular behaviour (Damante *et al.*, 2004). The energy range for low level lasers lies between 1 to 500 mW, while for surgical lasers the energy ranges between 3,000 to 10,000 mW. The use of HLLT as a surgical tool is established while LLLT, as a biostimulator, is not really established. There are controversies with the application of LLLT in biostimulation (Soet, 2005) and more studies are being pursued to have LLLT established.

Reports by Mester and colleagues in the late 1960's and early 1970's showed that 1 to 4 J/cm² of laser irradiation induced healing of chronic non healing soft tissue ulcers and formed the genesis of clinical laser therapy (Mester *et al.*, 1971; Schindl *et al.*, 2000). Since then, over 2,000 studies have been published, producing a wide range of results (Papillion *et al.*, 2004). Lasers have been found to be beneficial in a wide variety of therapeutic applications such as treatment of dermatological conditions, dental problems, tumours, surgical cases and reducing pain.

Even though laser medicine has been in existence for more than four decades, it is still unclear as to its effects on human cells, and therefore studies are still on-going to find effects of phototherapy on cells. Reports

contradict on the effects of phototherapy and this has been attributed to difficulties in identifying its effect on cells (Carnevali *et al.*, 2003; Allendorf *et al.*, 1997). Literature has shown that even though phototherapy has been found beneficial in a wide variety of therapeutic applications, it can induce DNA damage; however this damage appears to be repairable (Hourel and Abrahamse, 2008). It might be that phototherapy helps the patient at first glance and damages DNA at the same time, thereby increasing the risk of therapy induced disease up to an increased cancer risk (Greulich, 2003). Kujawa *et al.*, (2004) had similar sentiments by stating that even though phototherapy is used in the biomedical treatment of many diseases, the possible molecular mechanisms of laser actions remain unclear and the damaging effects of laser irradiation are still controversial.

Simunovic (2000) observed that a cell without adenosine triphosphate (ATP) cannot maintain life, and therefore activities of the cell correlate to the amount of ATP which can be influenced by laser irradiation. Other studies proposed that phototherapy increases ATP production in the mitochondria, and that with more energy available the cell utilises this fuel to operate more efficiently (Karu, 1988). That is, it might be able to synthesise more proteins involved in cellular repair and enhance proliferation. Not only does laser irradiation increase ATP at the cellular level, researchers have also shown that it causes stimulation of the mitochondria, cellular enzymes, macrophage activation, collagen synthesis, significant increase of granulation tissue, increased permeability of cell membranes, increase in serotonin and endorphin levels with decreased fibre activity and bradykinin. The mentioned stimulatory effects of phototherapy make it a useful remedy for treatment of slow to heal wounds. Phototherapy is an effective therapy, working in harmony with the body's own healing and relieving mechanism (Hartley, 2004).

Biostimulatory effects of lasers are governed by the Arndt-Schultz law of biology; weak stimuli excite physiological activity while strong stimuli retard or abolish activity (Figure 3), (Sommer *et al.*, 2001). The optimal energy density for biostimulation in the Laser Research Group is 5 J/cm^2 and fluences more than 10 J/cm^2 cause DNA damage and hence inhibit growth of cell cultures (Mbene *et al.*, 2006; Zungu *et al.*, 2008; Houreld and Abrahamse, 2008).

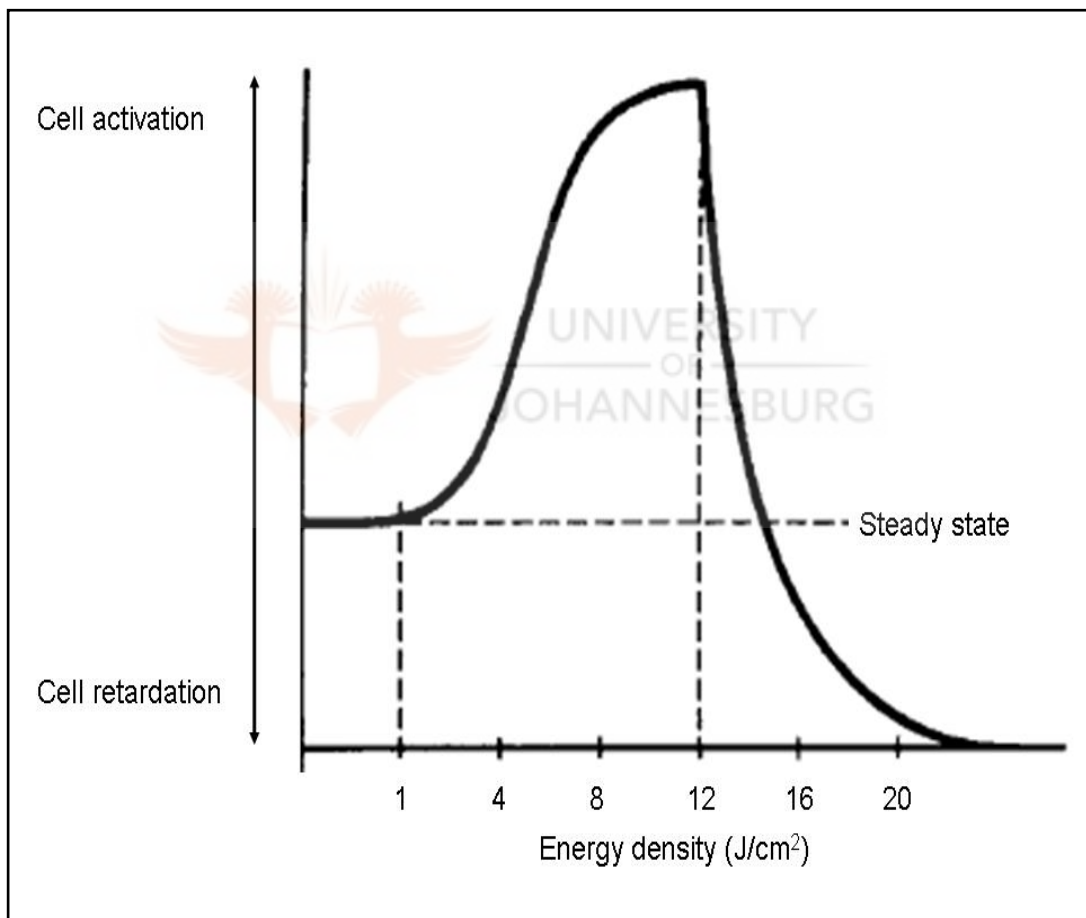
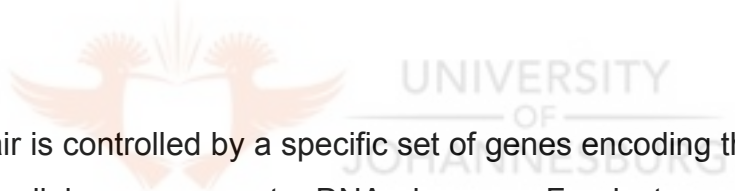


Figure 3 Irradiation of cells with 5 J/cm^2 is stimulatory while irradiation with more than 12 J/cm^2 is inhibitory. Basic Arndt-Schultz rule asserts that there is an ideal dosage for a best possible response and that too little energy will have no effect, while too much will be suppressive (Adapted from Sommer *et al.*, 2001).

2.7 DNA Damage and Repair

The human genome is continuously exposed to exogenous and endogenous alkylating and oxidative agents that result in DNA damage. This damage interrupts the continuity of genetic information by inhibiting or preventing transcription, DNA replication, and cell division. Exogenous sources include UV radiation from the sun, ionising radiation, aflatoxin from fungi, burning tobacco and many chemotherapy drugs. On the other hand, endogenous sources include oxidative metabolism and spontaneous alterations of DNA. DNA damage produced by ROS is the most frequently occurring damage. If the damage is unrepaired, it can lead to the production of mutations by insertion of incorrect bases, or cell death by blocking DNA replication and ageing (Livneh, 2001; Dale and Park, 2004; Wood, 1994).



DNA repair is controlled by a specific set of genes encoding the enzymes that catalyse cellular response to DNA damage. For instance, when DNA is damaged by radiation, enzymes within the cell nucleus attempt to repair the damage. These DNA repair mechanisms are an important component of the cell's defences against a variety of agents that damage the DNA (Dale and Park, 2004), (Table 1). It appears phototherapy can be used in maintaining proper functions of the body. Thus, the study of genes involved in DNA repair can have an important impact in phototherapy.

Ruttan and Glickman (2002) observed that dozens of genes are involved in DNA damage repair to maintain genomic stability through different pathways, including direct repair, base excision repair, nucleotide excision repair, mismatch repair and double strand DNA break repair. The genetic alterations of these genes may affect the function of their proteins and lead to

development of diseases or cancers (Friedberg, 2003; Goode *et al.*, 2002). Ronen and Glickman (2001) observed that about 125 human genes were directly involved in five major DNA repair pathways. With this in mind, the study of genes related to DNA repair would expose more insights in the field of molecular biology and phototherapy.

Table 1 Proteins which repair DNA damage.

PROTEIN	SUBSTRATE	REFERENCE
Fpg	Oxidised purine	Buschini <i>et al.</i> , (2007)
uvrABC	UV damage	Houten <i>et al.</i> , (2005)
3 methyladenine DNA glycosylase*	3 methyladenine sites	Samson <i>et al.</i> , (1991)
7 methylguanine DNA glycosylase*	7 methylguanine sites	
Uracil DNA glycosylase	Misincorporated uracil	Krokan <i>et al.</i> , (1997)
hOGG1	Oxidative DNA damage	Sidorenko <i>et al.</i> , (2008)

* Commonly known as methylpurine DNA glycosylase; hOGG1 (human oxoguanine DNA glycosylase 1); Fpg (Formamido pyrimidine glycosylase); uvrABC (ultraviolet radiation A, B, C).

MPG is involved in DNA repair by catalysing the excision of a variety of modified bases. Increased expression of MPG has been observed in high risk human papilloma virus (HPV) infected tissues and breast cancers when compared to normal primary epithelial cells (Sohn *et al.*, 2001; Cerda *et al.*, 1998). This finding suggests the role of MPG in DNA repair. MPG is the major repair protein in mammalian cells that is responsible for the removal of a variety of alkyl and cyclic ethanoabase adducts in the cellular genome (Roy *et al.*, 1997). Thus, studies of regulation of MPG expression in mammalian cells are highly significant so as to check the correlation of DNA damage due to

phototherapy and repair. It has been noted that under expression of MPG in rats renders them susceptible to mutation (Holt *et al.*, 2000). Other studies indicated that over expression of MPG did not increase tolerance to alkylating agents, but increased the number of apurinic sites and lead to a higher incidence of sensitised sister chromatid exchanges (Fishel *et al.*, 2003). The presence of accumulated apurinic/aprimidinic (AP) sites may lead to a miscoding or further stress in downstream base excision repairs. The above observation suggests that increased expression of MPG does not necessarily protect cells, but could in some instances lead to a decrease in resistance to environmental stress.

There are also reports that MPG removes intact bases in addition to damaged ones. Therefore at higher than physiological levels, this promiscuity could become significant (Fishel *et al.*, 2003; Berdal *et al.*, 1998). With this observation, the expression of MPG is expected to be highly regulated in order to protect both against external exposure to DNA damaging agents and to reduce induction of spontaneous mutations.

To prevent the potentially deleterious effects of DNA lesions, cells have evolved sophisticated DNA repair systems (base excision repair [BER], nucleotide excision repair [NER] and DNA repair methyltransferase [Mtase]), (Friedberg *et al.*, 1995). BER is initiated by DNA glycosylases, a class of enzymes that recognise a specific set of modified bases such as 7,8-dihydro-8-oxoguanine (8-oxoG) or thymine glycol (Croteau and Bohr, 1997).

Lesions that cause greater disturbances to double helical DNA are corrected by NER, which removes a segment of DNA surrounding the alteration. Contrary, simple modifications to single damaged bases are dealt with by BER, which sequentially removes the modified base and deoxyribose sugar. In both excision repair processes, the missing bases are resynthesised by a DNA polymerase, using the complementary strand as a template (Wood, 1994). Methyltransferases are enzymes found in many organisms that remove methyl groups from the susceptible positions. Each enzyme transfers a methyl group to one of its own cysteine residues. Human cells lacking this enzyme are more susceptible to alkylation than normal (Wood, 1994).

Most damage or inappropriate bases in DNA are removed by excision repair, while a minority are repaired by direct damage reversal (Lindahl and Wood, 1999; Sancar *et al.*, 2004). MPG is one of the DNA glycosylases, which is involved in BER. It is a broad spectrum excision repair protein which recognises a wide variety of damaged bases (Rinnie *et al.*, 2004). There are two classes of DNA glycosylases; the monofunctional, exhibiting only the glycosylase activity, such as MPG and uracil DNA glycosylase, which use an activated water molecule as a nucleophile to generate an AP site in DNA (Adhikari *et al.*, 2008), and the bifunctional such as human oxoguanine DNA glycosylase 1 (hOGG1) and human endonuclease III, which are glycosylases/AP lyases. The later possess both an activity to remove the substrate bases and an activity to incise the phosphodiester backbone. In human cells, an example of the first category is the 3-methyladenine DNA glycosylase and the alkyl *N*-purine DNA glycosylase (ANPG) protein. The second category has hOGG1 which excises the potent premutagenic lesion, 8-oxoG (Croteau and Bohr, 1997; Blainey *et al.*, 2006).

MPG is responsible for the hydrolysis of the deoxyribose *N*-glycosyl bond, excising 3-methyladenine and 3-methylguanine from the damaged DNA. The resulting AP site is further processed by an AP endonuclease which cleaves 5' to the AP site and a phosphodiesterase releases the remaining 5'-deoxyribose phosphate to leave a nucleotide gap in the DNA that is filled by the repair DNA polymerase, and thus the remaining nick is sealed by a DNA ligase (Seeberg *et al.*, 1995).

MPG has been studied and detected in humans as well as other organisms. In both cases it has been shown to be involved in DNA repair whereby it catalyses the excision of a variety of modified bases (Olsen *et al.*, 2001). Zheng *et al.*, (2006) observed that MPG could not be associated with the initiation and development of astrocytoma because there was no significant difference in its expression in all the grades.

Intermediates formed during BER can be more deleterious to the cell than the initial damage if repair is not completed. In many cases, damaged DNA bases are less toxic, but lead to mutagenesis during DNA replication. On the other hand, unrepaired AP sites are cytotoxic lesions that block DNA replication. Also, single stranded breaks (SSBs) can form at AP sites that may lead to double stranded breaks during replication (Maher *et al.*, 2007). Fan and Wilson (2005) observed that BER pathways must be coordinated to ensure that the repair process is completed so as to minimise the aforementioned circumstances.

2.8 Gene Expression

Gene expression analysis provides significant insight to understanding regulatory mechanisms of cell biology. According to the literature, phototherapy is known to increase cell proliferation, viability, enhance wound healing and reduce stress (Atabey *et al.*, 1995; Damante *et al.*, 2004). However, the mechanism by which phototherapy provides these beneficial effects is not clearly known. It has been shown that phototherapy up regulates genes involved in cell proliferation such as Platelet Derived Growth Factor c and Mitogen Activated Protein Kinase II and antioxidant related genes which include Selenoprotein W 1, just to mention a few (Zhang *et al.*, 2003).

Whelan *et al.*, (2003) observed that mouse tissue regenerating genes were significantly up regulated upon LED treatment when compared to the untreated sample. Examples of these genes include Integrins, Nidogen, Laminin, Actin and Kinesin motor proteins. These genes were identified upon gene array experiments with RNA isolated from sponges from the wound site, with and without LED treatment. In the same study, cell death associated genes were down regulated upon LED treatment, which increased proliferation. This shows that depending on the regulation of genes, the normal function may be increased or slowed down. For instance if MPG is optimally up regulated, the excision of oxidised bases would be increased (Table 2) whereas the down regulation of Cullin 1 enhances cell growth (Zhang *et al.*, 2003). The down regulation of genes enhancing apoptosis genes slows down apoptosis.

Table 2 Gene activation in wound healing.

GENE	FUNCTION	REFERENCE
N-methylpurine DNA glycosylase (MPG)	DNA synthesis and repair	Zhang <i>et al.</i> , (2003)
Nucleoside diphosphate linked moiety X type motif 1 (NUDT1)		Zheng <i>et al.</i> , (2006)
Adenine phosphoribosyltransferase (APRT)		Samson <i>et al.</i> , (1991)
Heat shock 70 kD protein 1A (HSPA1A)	Apoptosis and stress protein	Zhang <i>et al.</i> , (2003)
Caspase 6 (CASP6)		
Serum response factor (SRF)	Cell proliferation	Schratt <i>et al.</i> , (2001)
Platelet derived growth factor c (PDGFC)		Iyer <i>et al.</i> , (1999)
Leukocyte receptor cluster (LRC) member 5 (LENG5)	Immune inflammation and cytokine	Martin <i>et al.</i> , (2002)
E74 like factor 1 (ELF1)		Peng, (2004)
Septin 6 (SEP2)		Senese <i>et al.</i> , (2007)

MPG, nucleoside diphosphate linked moiety X type motif 1 (NUDT1) and adenine phosphoribosyltransferase (APRT), just to mention a few, are some of the genes involved in DNA repair or removal of oxidised bases incurred due to ROS or irradiation. Zhang *et al.*, (2003) demonstrated that red light (λ 628 nm) up regulated these genes. Phototherapy has also been linked to the up regulation of the production of growth factor genes such as fibroblast growth factor-2 (FGF-2), transforming growth factor-beta (TGF-b), epidermal growth factor (EGF) and growth factor receptors, which are directly involved in cell proliferation. It is in view of this that this study was conceived to look at the effects of phototherapy on gene activation related to DNA repair.

2.9 Detection of Damaged DNA (Enzyme-Linked Comet Assay)

The comet assay, also known as single cell gel electrophoresis (SCGE), (Andreoli *et al.*, 1999; Wang *et al.*, 2007), when linked with enzymes produce models of greater specificity and sensitivity. It is then also known as the modified comet assay because of an additional step of enzyme treatment to incise the DNA strand at the site of the damage (Collins *et al.*, 1996; Møller *et al.*, 2000). In addition to SSBs, double strand breaks (DSBs) and AP sites, other types of damage such as oxidised bases or ultraviolet-induced dimers, which do not cause strand breaks, exist. These types of damage cannot be detected unless lesion specific enzymes are added at the post lysis stage to create breaks at the sites of damage.

Enzymes that have been used in the comet assay to date include endonuclease III, which detects oxidised pyrimidines (Collins *et al.*, 1993), formamidopyrimidine glycosylase (Fpg), which detects oxidised purines, uvrABC, an enzyme complex that can be used to detect UV damage on bulky lesions (Dušinská and Collins, 1996), 3-methyladenine DNA glycosylase II (AlkA) that reveals 3-methyladenine sites (Collins *et al.*, 2001), and uracil DNA glycosylase (UDG), which exposes sites of misincorporated uracil. Smith *et al.*, (2006) also demonstrated that hOGG1 is more specific to oxidative DNA damage than other enzymes. Many studies have used the modified comet assay to investigate DNA damage *in vitro* for over 10 years because of its simplicity, sensitivity and the large number of samples that can be examined at once (Collins *et al.*, 2001; Collins *et al.*, 1993; Møller *et al.*, 2000). On the other hand, the end point measured by the traditional comet assay is a mixture of direct strand breaks and DNA damage that is converted to strand breaks by alkaline treatment (Møller *et al.*, 2000).

Although studies in both laboratory conditions and clinical settings seem to show that phototherapy is an effective treatment for enhancing wound healing in different types of wounds, the molecular mechanisms induced by low level laser irradiation are still poorly understood. This study is therefore justified as it is apparent that there is a need for more molecular and cellular research into laser biology in order to elucidate the effects of phototherapy on human cells.



CHAPTER 3 MATERIALS AND METHODS

3.1 Cell Culture

This study received ethical approval from the University of Johannesburg, Faculty of Health Sciences Ethics Committee (approval clearance reference number 06/06). All materials and cells used were supplied by Scientific Group Adcock Ingram S.A., unless specified otherwise. A flow diagram of the study design can be seen in Appendix A1. Human skin fibroblast cells, WS1, (ATCC, CRL 1502), (Appendix B1) were cultured in minimum essential medium (MEM) with Earle's balanced salt solution (INV/32360-026). The medium was modified to contain 2 mM L-glutamine (INV/25030-O24), 1.0 mM sodium pyruvate (INV/11360-039), 0.1 mM nonessential amino acids (INV/11140-053), 1% v/v Penicillin Streptomycin Fungizone (INV/17-745E), and supplemented with 10% v/v foetal bovine serum (FBS), (INV/10108-165). This modified media was called complete media (Appendix B2). Stocks of WS1 cells were stored in liquid nitrogen, when required, cells were rapidly thawed at 37 °C, added to 10 ml complete media and spun in a centrifuge (Digicen-R, Instrulab SA) at 2,200 rpm for 4 min. The supernatant was discarded; the cell pellet was resuspended in 25 ml complete media and seeded into a 75 cm² flask. WS1 cells were incubated aseptically in 5% carbon dioxide (CO₂) and 85% humidity at 37 °C (Figure A2).

3.1.1 Subculture

When cells reached a confluence of 90%, cells were subcultured according to standard cell culture techniques. The media in which cells were growing was discarded and the monolayer cell sheet was rinsed twice with Hanks

Balanced Salt Solution (HBSS), (INV/14170-0881) to remove traces of FBS which interfere with trypsinisation. Cells were then trypsinised (1 ml/25 cm²) using a 0.25% v/v trypsin-0.03% EDTA solution and incubated at 37 °C for 4 min to facilitate detachment of cells. Thereafter, an equal amount of 10% FBS in MEM was added to the cell suspension to inactivate trypsin which is toxic to cells. The suspension was poured into a 50 ml centrifuge tube (Scientific Group Adcock Ingram S.A., CR/430829), gently mixed and spun in a centrifuge (Digicen-R, Instrulab SA) for 4 min at 2,200 rpm (Figure A3). The supernatant was discarded and the cell pellet resuspended in 5 ml complete media. The suspension was then added to 70 ml of complete media in a 175 cm² flask and cultured. After growing to 90% confluence, cells were harvested, resuspended and split into four equal volumes. Two volumes were used for conducting tests, the third volume was cultured again in a 75 cm² flask for propagation of cells and was given a consecutive passage number. The fourth volume was frozen in cryopreservative media for future use.

3.1.2 Cell model

For the experiments, 20 µl of resuspended trypsinised cells was mixed with an equal volume of 0.4% Trypan blue (Sigma-Aldrich S.A., T-8154) and the number of viable cells was determined (see 3.4.1 and Appendix B7). Approximately 6 x 10⁵ cells in 3 ml culture medium were grown in 3.4 cm diameter culture dishes. Normal (N) and wounded (W) cells were used in this study as shown in the flow diagram (Appendix A1). A central scratch was made across a monolayer of cells using a 1 ml sterile pipette to simulate a wound according to Rigau *et al.*, (1995). Several studies have used this wound model to study the effect of phototherapy using a He-Ne laser (Abrahamse *et al.*, 2006; Hamuro *et al.*, 2002; Hawkins and Abrahamse, 2007a; Mbene *et al.*, 2006; Pullar *et al.*, 2006; Yarrow *et al.*, 2004).

3.2 Laser Irradiation

The He-Ne laser is the most common and familiar type of laser. This laser was developed between 1960 and 1961 (Siegman, 1986) and it is one of the earliest lasers to be made (Hartley, 2004). It produces visible red light in a continuous wave (CW). A CW laser emits a constant (or slowly changing) power for a period of more than half of a second (King, 1989) and may result in non selective injury (Carroll and Humphrey, 2006).

Lasers were supplied and set up by the National Laser Centre (NLC) S.A. Normal and wounded WS1 cells were irradiated with a He-Ne laser (Spectraphysics, Model 127) at λ 632.8 nm with a fluence of 5 or 16 J/cm² (Figure 4). Laser parameters are shown in Table 3.



Figure 4 A He-Ne laser (Spectraphysics, model 127) was used to irradiate cells at λ 632.8 nm. This laser has a spot size of 9.08 cm². He-Ne gas is the amplifying medium in this laser.

Table 3 Irradiation parameters using the He-Ne laser.

VARIABLE	PARAMETERS
Wavelength	632.8 nm
Wave emission	Continuous wave (CW)
Power density	1 - 3 mW/cm ²
Spot size	9.08 cm ²
Fluence	5 or 16 J/cm ²
Cells	N and W (WS1)
No. of exposures	2
Days exposed	1 and 4
Duration of effect	1 or 24 h post irradiation

N = normal; W = wounded

All irradiations were performed from the top with the culture plate lid off in a temperature controlled room (21 °C) with the lights off so as to minimise interference from other light sources. The visible red laser beam was expanded using a concave lens and reflected downwards towards the cells using a mirror and clipped with an iris to produce a truncated Gaussian beam with a spot size of 9.08 cm² (Figure 5). The area of the beam is the same as the area of the culture dishes. Carroll and Humphreys (2006) observed that the spot size of a laser is equivalent to the laser beam cross section and directly affects the fluence and the irradiance of a laser beam. A power meter (Fieldmate) was used to measure the power output prior to irradiation; the value obtained was used to calculate the duration of laser exposure as follows:

$$\frac{X \text{ mW} \times 4}{\pi (\text{Diameter})^2} = \text{mW/cm}^2$$

$$\text{Time (s)} = \frac{\text{Energy density (J/cm}^2\text{)}}{\text{Work (W/cm}^2\text{)}}$$

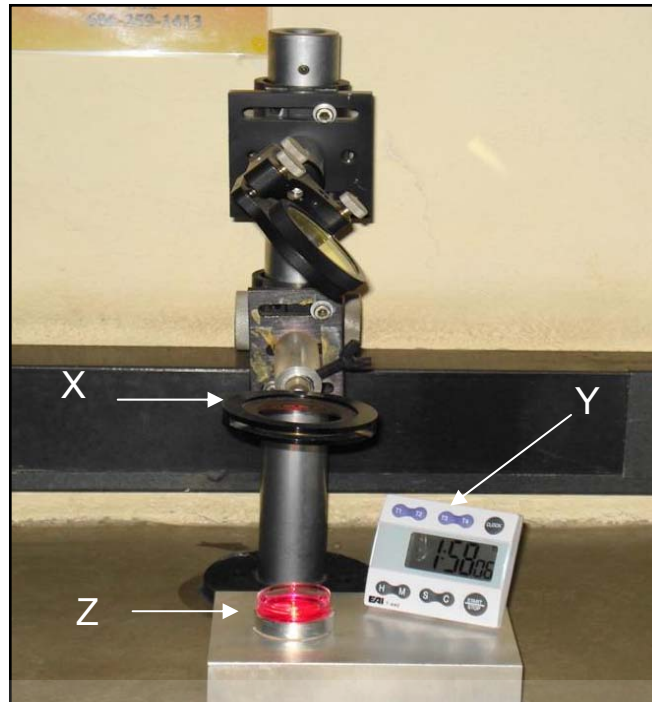


Figure 5 The laser beam was clipped with an iris at X and produced a spot size of 9.08 cm^2 . The timer (Y) was used to time duration of laser exposure. WS1 cells were irradiated in a 3.4 cm diameter culture plate (Z).

On average the power output for the two lasers used during the study was 20 mW and 15.9 mW. However, due to expansion and reflection of the laser beam, power density at the level of the cells decreased to 78.7% and 87.1% respectively. Thus, the power density at the cellular level was determined by multiplying the power output by either 0.787 or 0.871 and divided by the area of the culture dish (9.08 cm^2). This then translated to a power density of 1.7 mW/cm^2 and 1.5 mW/cm^2 respectively. The average irradiation time to achieve a fluence of 5 J/cm^2 was calculated to be 45 min 18 s and 51 min 29 s respectively, while for 16 J/cm^2 irradiation time was calculated to be 2 h 24 min 57 s and 2 h 44 min 55 s respectively. Control cells were treated in the same manner but were not irradiated.

Cells were irradiated 30 min and 72 h (day 1 and 4) post wound induction using 5 or 16 J/cm². Hawkins and Abrahamse (2005) and Houreld and Abrahamse (2008) demonstrated that 5 J/cm² promoted healing while 16 J/cm² produced a significant amount of cellular and molecular damage. Therefore, 5 J/cm² was selected with the view that it would equally stimulate healing while 16 J/cm² would have a damaging effect therefore provide a good comparison for (1) comet assay with and without Fpg and (2) the up or down regulation of MPG using 5 or 16 J/cm².

3.3 Cell Morphology

Cellular and molecular responses were assessed on day 4 at 1 or 24 h post irradiation. Abrahamse *et al.*, (2006) observed that irradiation of cells with 5 or 16 J/cm² and measuring responses 24 h post irradiation produced stimulatory and inhibitory effects on irradiated cells respectively. Kreisler *et al.*, (2003) reported that cells showed increased proliferation and viability 24 h post irradiation. Therefore, it was with this understanding that 24 h was chosen as cells seem to have maximum time to repair while 1 h seems not enough time for cells to repair. This provided a way of comparing responses at 1 or 24 h.

N and W human skin fibroblast cells were observed for changes in cell morphology using an inverted light microscope (Olympus CKX 41), (Figure A4). Observation was focussed on colony formation (cell regrouping at wound margin), haptotaxis (cell orientation) of the edge fibroblast cells, chemotaxis (cell migration across the central scratch) and number of cells in the central scratch (Rigau *et al.*, 1995). A camera (Olympus Camedia C-3030 zoom) attached to an inverted microscope was used to digitally record the behaviour of cells on day 1 and 4.

3.4 Cell Viability

There are various methods of assessing cell viability. In this study, the Trypan blue exclusion test and ATP luminescent assay were used. Trypan blue is used to examine the integrity of the cell membrane and thus viability, while the ATP luminescent assay measures the mitochondrial activity of the cell. ATP is the primary energy unit for cells and levels of this compound offer a potential marker for cell viability and growth. The availability of a luminescent assay allows a rapid, sensitive, and reproducible measurement of ATP (Riss *et al.*, 2002).

3.4.1 Trypan blue exclusion test

Trypan blue is a vital stain used to determine the number of viable cells present in a cell suspension. Due to the selectivity in staining, this assay is also called the dye exclusion test (Ridder *et al.*, 1988). The test is based on the principle that live cells possess an intact cell membrane that exclude certain dyes, such as Trypan blue, eosin or propidium, whereas dead cells allow the stain to penetrate. The chromophore in Trypan blue is negatively charged and does not interact with the cell nucleus unless the membrane is damaged. Thus viable cells remain colourless, while non viable cells stain blue.

Itoh and Linn (2005) and Ridder *et al.*, (1988) used the Trypan blue exclusion test to determine cell viability by looking at permeability. Azevedo *et al.*, (2006) also used the Trypan blue exclusion test with a haemocytometer to determine the number of human gingival fibroblast cells. In this study an equal volume (25 µl) of a 0.4% Trypan blue in HBSS and cell suspension was

added and incubated at room temperature for 5 min. Ten microlitres was then loaded on either side (chamber) of the haemocytometer (Figure 6a). Viable and non viable cells were counted in the 1 mm centre square (C) and four 1 mm corner squares (W), (Figure 6b).

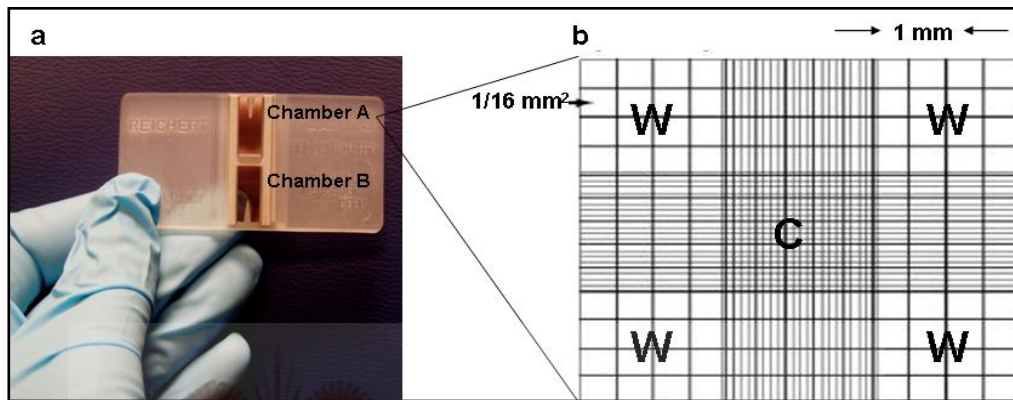


Figure 6 A haemocytometer showing two chambers in which cells were counted using a light microscope. A mixture of the cell suspension was loaded on either side (chamber). Both chambers were counted and a total cell count per ml was calculated. Chamber A has been enlarged so as to show the 5 big squares in which cells were counted; one centre square (C) and 4 corner squares (W). Each square has an area of 1 mm² and has 16 tiny squares. When the chamber is charged, it has a depth of 0.1 mm.

Cells touching the top and left lines of each small square were counted, leaving out cells which touched the bottom and right sides so as not to count the same cells twice. This procedure was repeated for the other chamber (B). The total number of viable and non viable cells was recorded and the number of cells per ml was calculated (Appendix B5). The percentage of viable cells for each chamber was then calculated as follows:

$$\text{Viable cells (\%)} = \frac{\text{total number of viable cells per ml of aliquot}}{\text{total number of cells per ml of aliquot}} \times 100$$

3.4.2 ATP luminescent assay

The CellTiter-Glo luminescent cell viability assay (Whitehead Scientific S.A., Promega G7571) is based on the quantification of ATP present, which signals the presence of metabolically active or viable cells (Riss *et al.*, 2002). Equal volumes (50 µl) of cell suspension (7×10^4) and CellTiter-Glo reagent were added and mixed using an orbital shaker for 2 min to induce lysis. The tube was incubated at room temperature for 10 min for the signal to stabilise. Luminescence was measured in reading light units (RLU) using the Junior EG and G Berthold luminometer. The reading from the negative control (CellTiter-Glo reagent and media without cells) was subtracted from each sample's raw data to eliminate background absorbance due to media and other substances.

3.5 Cell Proliferation

The XTT, (Roche S.A., 1465015), (Sodium 3' - (1 - (phenylaminocarbonyl) - 3, 4 - tetrazolium) - bis (4 - methoxy - 6 - nitro) benzene sulfonic acid hydrate) assay was used to assess cell proliferation. Mitochondrial succinate dehydrogenase in metabolically active cells cleaves the yellow tetrazolium salt (XTT) forming an orange formazan dye. The formed dye is soluble in aqueous solutions and was spectrophotometrically quantified using a BIO-RAD Benchmark plus microplate reader. The absorbance is directly proportional to the number of proliferating cells. Lewis *et al.*, (2001) used this test to determine cell proliferation on the effects of ketamine administration in high concentrations on cultured cells.



To determine the effect of phototherapy on migration and proliferation, a mini project was done. Hydroxyurea (HU), (Sigma-Aldrich S.A., H8627) was added to experimental cells to a final concentration of 5 mM in 3 ml complete media. Cells were then incubated overnight and irradiated with 5 J/cm² on day 1 and 4. The mode of action of HU includes inhibition of DNA synthesis without affecting RNA or protein synthesis in a fluence dependent manner. HU at a final concentration of 5 mM has been used in many studies to inhibit proliferation (Hamuro *et al.*, 2002; Sarkar *et al.*, 1996; Yabro *et al.*, 1965).

A total of 2 X 10⁴ cells/ml (20 µl) in 80 µl of original media, was added to the wells of a sterile tissue culture grade 96 well microtitre plate (Flat bottom, AEC-Amersham S.A., 167008). The same culture media (80 µl) was used so as to maintain the same environment. Cells were incubated for 3 h to allow attachment. The reaction reagent was made by adding 1 µl of PMS (N-methyl dibenzopyrazine methyl sulphate), a coupling reagent, to 50 µl of XTT. Thereafter, 50 µl of the reaction reagent was added to the respective wells. The mixture was incubated for a further 3 h at 37 °C to allow cells to react with the reagent. Prior to reading absorbance, the microtitre plate was gently shaken so that the dye could be evenly distributed. The absorbance was read at A_{450 nm} and corrected at A_{630 nm}.

3.6 Genetic Integrity

3.6.1 Alkaline comet assay

The comet assay is a single cell based technique that allows detection and quantification of DNA damage. The principle of the assay is based on the ability of denatured, cleaved DNA fragments to migrate out of the cell nucleus

under the influence of an electric field, whereas undamaged DNA migrates slower and remains within the confines of the nucleoid. The comet assay without Fpg (conventional) detects SSBs while the comet assay with Fpg (modified) detects and cleaves oxidised bases, thereby inducing additional strand breaks (Collins, 2000). The specificity of the comet assay can be enhanced to investigate specific types of DNA damage by adding DNA modifying enzymes. Fpg (Mut M) is amongst the enzymes which have been successfully used in the comet assay to investigate oxidative damage. The comet assay protocol has four steps namely: lysis, DNA unwinding, electrophoresis and neutralisation.

Prior to commencement of the comet assay, reagents were prepared (Appendix B8) and slides coated with 1% standard agarose and left to dry overnight at room temperature. Slides and tubes were then labelled in duplicate with the respective sample numbers for the modified and conventional comet assay. Since cells which were used for the comet assay were stored in liquid nitrogen, they were rapidly thawed and 100 µl of cell suspension (2×10^4 cells/ml per sample) was spun in a centrifuge (Harneus Fresco 17, Separation Scientific SA) at 3,000 rpm for 3 min at 4 °C to remove cryoprotective media which is toxic to cells at room temperature. The cell pellet was washed twice in phosphate buffered saline (PBS) by centrifugation. After the last wash, the supernatant was discarded and the pellet resuspended in the remaining PBS. Cell suspensions rested on ice between centrifugations to minimise DNA degradation. Thereafter, 140 µl of 1% low melting point agarose (37 °C) was added to each of the cell suspensions and gently mixed with a pipette. Two equal drops of the suspension were placed on each of the pre-coated slides with the respective sample numbers. Coverslips (22 X 22 mm) were placed on top of each gel so as to evenly spread the sample and slides were then left at 4 °C to let the agarose set.

After the agarose had set, coverslips were removed from the slides and cells were lysed in lysis solution for 1 h at 4 °C. Lysis solution contains high salt concentrations and detergent (2.5 M NaCl, 0.1 M EDTA, 10 mM Tris, pH 10 and 1% Triton X-100 added prior to use). Slides were then rinsed in three changes of enzyme reaction buffer at 4 °C for 5 min each (40 mM HEPES, 0.1 M KCl, 0.5 mM EDTA, 0.2 mg/ml bovine serum albumin, pH 8). Thereafter, one set of slides was incubated with 50 µl of Fpg (Sigma-Aldrich S.A., F3174), diluted 1:3,000 in enzyme reaction buffer at 37 °C for 30 min to allow the enzyme to react with the DNA strands. The other set which acted as a control was incubated with 50 µl enzyme reaction buffer only. Slides were incubated in a humidifying chamber which was warmed prior to incubation. Slides were then transferred to a horizontal electrophoresis tank containing electrophoresis buffer (0.3 M NaOH, 1 mM EDTA), where damaged DNA underwent alkaline unwinding for 40 min at 4 °C. During electrophoresis (in the same buffer) at 4 °C at a power of 300 mA (BIO-RAD, Power Pac 300), relaxed coils were pulled towards the anode forming the tail of a comet like image (Figure 7). After electrophoresis, cells were rinsed in three changes of neutralisation buffer (0.4 mM Tris, pH 7.5) for 5 min each and then in distilled water for the same period to remove salts. Slides were then left to dry.

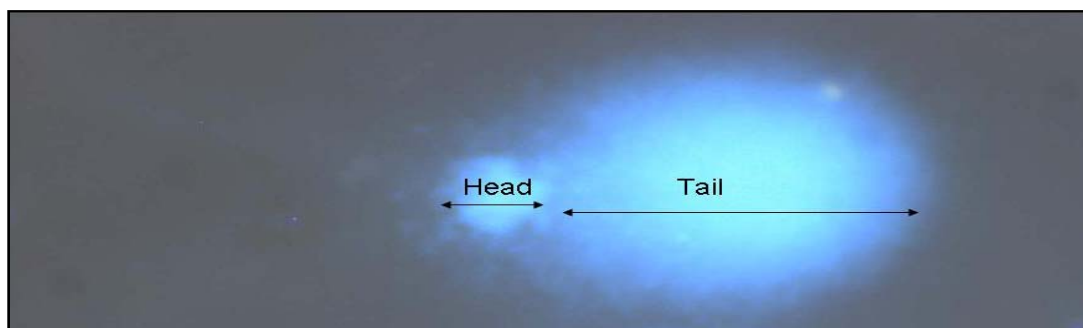


Figure 7 Cell DNA migration pattern produced by the comet assay as a result of strand breakage. The cell looks like a comet hence the name “comet assay”. Damaged DNA is pulled towards the anode during electrophoresis. The more the damage the longer the tail (400x magnification).

Slides were stained with 20 μ l of 1 μ g/ml 4'6 diamidine-2-phenylindol dihydrochloride (DAPI), (Sigma-Aldrich S.A., D9564). Stained slides were examined at 400x magnification using a fluorescent microscope (Olympus BX41/BX51), (Figure A5) and an epifluorescent microscope (Olympus BH2-RFCA) was used to record the digital images. One hundred randomly selected comets per gel were visually analysed and scored according to the five recognisable classes of comets ranging from class 0 to 4, with the most damage in class 4 (Figure 8).

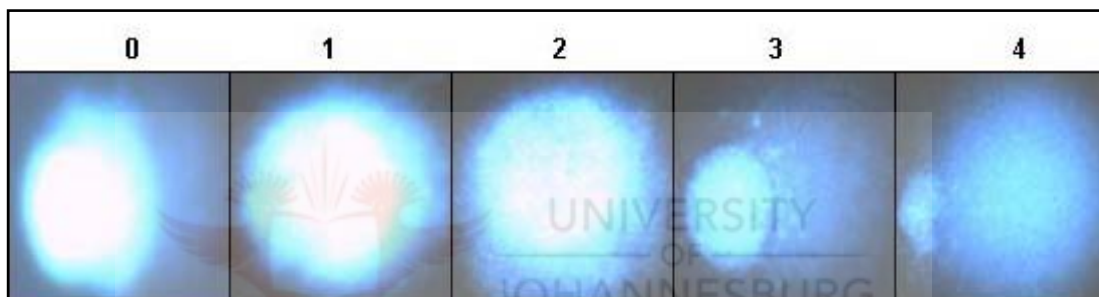


Figure 8 Classes of comets (0-4) stained with DAPI (1 μ g/ml). Images were visualised under the Olympus BH2-RFCA Epifluorescent microscope. Class 0 does not have a tail; class 1 has a short almost indistinguishable tail and a large head; class 2 has a big head and short tail; class 3 has a slightly bigger head than class 4 but shorter tail, while class 4 has the smallest head and the longest tail. Severe DNA damage is indicated by class 4 (400x magnification).

To quantify the amount of DNA damage, the number of comets allocated to each class was multiplied by the class number and added, thus giving an arbitrary unit. Arbitrary units ranged from 0 to 400; the sum for arbitrary units for each gel was calculated and the mean for each sample was then determined to find the DNA damage grade for each sample. An increase in arbitrary units indicates an increase in DNA damage.

3.7 Real Time Reverse Transcription PCR

Microarray and real time reverse transcription Polymerase Chain Reaction (real time RT-PCR) are amongst the several methods in which gene expression levels can be monitored. Microarray can be defined as a tool for monitoring gene expression levels for thousands of genes in parallel; it is typically a glass or polymer slide onto which DNA molecules are attached at fixed locations called spots or features. An array may contain many spots, each containing millions of identical DNA molecules (Causton *et al.*, 2003). Among the other names, this technology is referred to as DNA microarray, DNA array, Gene chips or DNA chips. On the other hand, real time RT-PCR refers to the process where the production of amplification products is directly monitored during each amplification cycle. This is different to the traditional or conventional PCR which measures the final endpoint products (Wang *et al.*, 2006). Real time RT-PCR can be used to monitor expression levels of one or more genes. The expression of one gene can be monitored using SYBR green, while if more genes are to be monitored labelled DNA probes are used. SYBR green dye intercalates with double stranded DNA and hence gives high signal of fluorescence when more double stranded DNA is bound (Wang *et al.*, 2006).

Reverse transcription PCR involves the use of complimentary deoxyribonucleic acid (cDNA), which is transcribed from ribonucleic acid (RNA), as a template for PCR. There are several kits on the market which can be used to extract RNA and synthesise cDNA. In this study a Fastlane cell cDNA synthesis kit (Southern Cross Biotechnology S.A., Qiagen 215011) which generates the first strand cDNA directly from cultured cells was used. With this kit RNA purification or RNase H digestion steps are not necessary, thus minimising pipetting tasks.

3.7.1 Primers

In this study, MPG was the gene of interest, beta Actin (ACTB), Glyceraldehyde 3 phosphate dehydrogenase (GAPDH) and Ubiquitin c (UBC) were selected as reference genes. The nucleotide sequences for these genes were obtained from GenBank using the following accession numbers: NM 002434 (MPG), NM 001101 (ACTB), NM 002046 (GAPDH) and NM 021009 (UBC), (Appendix C). The primer sequences were designed using Primer3 (<http://frodo.wi.mit.edu/cgi-bin/primer3/primer3-www.cgi>). Specificity and alignment of the primers were checked using the Basic local Alignment Search Tool (BLAST) on the National Centre for Biotechnology Information (NCBI) website (www.ncbi.nlm.nih.gov). The primer sets were then developed by Whitehead Scientific S.A. (Table 4).

Table 4 PCR primer sets and product sizes for gene of interest and reference genes.

GENE	PRIMER SEQUENCE	PRODUCT SIZE
MPG	Forward 5'-tggcacaggatgaagctgta-3' Reverse 5'-gtgtcctgctcagccactct-3'	181 bp
ACTB	Forward 5'-ggacttcgagcaagagatgg-3' Reverse 5'-agcactgtgttgccgtacag-3'	234 bp
GAPDH	Forward 5'-gagtcaacggatttggtcgt-3' Reverse 5'-ttgatttggagggatctcg-3'	238 bp
UBC	Forward 5'-ctttccagagagcggaacag-3' Reverse 5'-atcacagcgatccacaaaca-3'	175 bp

Upon receipt of the developed primers, they were dissolved in Tris EDTA (TE) buffer, pH 8.0 (Appendix B9.1) to make a stock solution of 100 μM . The reconstituted primers were stored at $-20\text{ }^{\circ}\text{C}$ in 20 μl aliquots to avoid repeated freeze thawing which would degrade them. The working primer concentration (10 μM) was made by diluting the stock solution 1:10 with PCR grade water (Celtic Molecular Diagnostic S.A., Boline, BIO-37080).

3.7.2 Ribonucleic acid (RNA) isolation

According to manufacturer's instructions, the kit comprises of 4 steps namely: removal of extracellular contaminants, cell lysis with RNA stabilisation, elimination of genomic DNA, and reverse transcription. Approximately 6×10^5 cells were irradiated with 5 or 16 J/cm^2 on day 1 and 4 and left to incubate for 1 or 24 h. After finding that MPG could not be detected, the project changed the irradiation frequency to irradiation on day 1 and isolated RNA at 0, 1, 3 or 8 h. Post irradiation cells were trypsinised and a cell count was performed, as described previously, and 5×10^3 cells were used in the real time RT-PCR reaction. Cells were mixed with 25 μl of wash buffer (FCW) to remove extracellular contaminants. The cell suspension was spun in a centrifuge (Harneus Fresco 17, Separation Scientific SA) at 2,200 rpm for 4 min and the supernatant discarded. Thereafter, 12.5 μl of lysis buffer (FCP) was added to the resuspended cell pellet and incubated for 10 min at room temperature to lyse the cells. This buffer stabilised cellular RNA and blocked inhibitors of reverse transcription. During the incubation, the following reagents were thawed at room temperature: quantiscript reverse transcriptase, quantiscript reverse transcriptase buffer, reverse transcriptase primer mix, genomic DNA wipe out buffer and RNase free water. Thereafter, quantiscript reverse transcriptase, quantiscript reverse transcriptase buffer and reverse transcriptase primer mix were stored on ice to avoid degeneration while the

other two reagents were left at room temperature. A mastermix for the common components of the genomic elimination was prepared by adding 2 μ l genomic DNA wipe out buffer and 8 μ l DNase/RNase free water per sample. A 5% more mastermix was prepared so that it was enough for the required tubes. Mastermixes are prepared so as to reduce pipetting errors and to achieve better reproducibility (Wang *et al.*, 2006). The mixture was gently mixed by inverting the tube six times and briefly centrifuged to collect the residual liquid from the sides of the tube (Figure A6). The mastermix was then stored on ice. The Fastlane cell lysate (12.5 μ l) for each group of cells was split into three equal biological samples (4 μ l each) into which the mastermix (10 μ l) was added (Table 5). The tubes were then incubated for 5 min at 42 °C and thereafter were immediately placed on ice to stop the reaction.

Table 5 Genomic DNA elimination.

COMPONENTS	SAMPLE TUBE (μ l)
Fastlane cell lysate	4
Mastermix	10
Total volume	14

3.7.3 cDNA synthesis

During incubation, the mastermix for the reverse transcription was made by adding 4 μ l quantiscript reverse transcriptase buffer and 1 μ l reverse transcriptase primer mix per sample. The mastermix was mixed by flicking, centrifuged briefly to collect the residual liquid from the sides of the tube and then stored on ice. From the mastermix, 5 μ l was drawn and added to tubes with 14 μ l Fastlane cell lysate. Thereafter, 1 μ l quantiscript reverse transcriptase or PCR grade water was added to the sample and no reverse

transcriptase (NRT) control tube respectively (Table 6). The mixture was vortexed and briefly centrifuged. The contents in the tube were incubated for 30 min at 42 °C to synthesise the first strand cDNA and then for 3 min at 95 °C to inactivate reverse transcriptase. The cDNA was then stored at -20 °C. The NRT tube was included in the reaction to serve as a negative control since the enzyme to transcribe RNA to cDNA was not added.

Table 6 Reverse transcription reaction.

COMPONENTS	SAMPLE TUBE (µl)	NRT TUBE (µl)
Fastlane cell lysate	14	14
Mastermix	5	5
Reverse transcriptase	1	-
PCR grade water	-	1
Total volume	20	20

NRT = no reverse transcriptase

cDNA quantification

The cDNA synthesis kit did not recommend quantification of cDNA prior to PCR. The manufacturers of the kit believe that after the PCR reaction, differences in gene expression (reference gene and gene of interest) would only be due to experimental conditions if the same volume of cDNA is added to the reactions. However, cDNA was quantified using a UV spectrophotometer (Thermospectronic) to determine average cDNA concentration per reaction. Each sample (2 µl) was diluted with 498 µl of Tris (Tris [hydroxymethyl] aminomethane) EDTA (TE) buffer, pH 8.0 and the spectrophotometer was zeroed with the same buffer at 260 nm. The absorption of DNA and RNA is maximum at 260 nm. Quartz cuvettes were used for reading the absorbance. The reading was multiplied by the dilution

factor (250) and then by the average extinction coefficient of 37 $\mu\text{g/ml}$ (de Mey *et al.*, 2006). The concentration was converted from $\mu\text{g/ml}$ to $\mu\text{g}/\mu\text{l}$ since it is easier to work with the latter than the former in PCR reactions. For calculation and concentration of samples see Appendix D.

3.7.4 PCR

Real time RT-PCR was set up using the cDNA which was stored at $-20\text{ }^{\circ}\text{C}$. PCR reactions were performed using the SensiMix™ dT PCR kit (Celtic Molecular Diagnostic S.A., Quantace, QT6T3-02). The kit contents and samples were thawed at room temperature and immediately stored on ice. All the reactions were performed on ice. Each experimental group had three biological samples. From each of the biological samples of the non irradiated N cells, 6 μl cDNA was drawn and pooled so that a standard curve could be made up of representative cDNA concentration. A 10 fold dilution series (1:10; 1:100; 1:1,000) was performed on 3 μl of the pooled cDNA. Undiluted and diluted cDNA was used to construct standard curves for each of the reference genes and gene of interest. Biological samples were also diluted 1:10 so that if the gene copy number was higher it would fall within the linear range of the standard curve and to minimise potentially interfering substances that inhibit PCR amplifications (Wang *et al.*, 2006).

The mastermix for the 25 μl PCR reaction was made by adding 12.5 μl sensimix, 9 μl PCR grade water and 0.5 μl SYBR green per sample. The mixture was gently mixed by flicking the bottom of the tube and briefly centrifuged to collect any residual liquid from the sides of the tube. PCR reaction components were then added to the respective tubes containing 2 μl template (Table 7). On average 300 ng of cDNA was added to each of the

sample tubes. PCR reactions were run in duplicate on each of the two biological samples for the experimental conditions, negative controls and for the standard curve dilutions. NRT and no template control (NTC) tubes were included to check if RNA samples, reagents in the reverse transcription or PCR mixes were contaminated with genomic DNA. A NTC sample also helps to determine if primers have formed primer dimers.

Table 7 PCR reaction components.

COMPONENTS	SAMPLE TUBE (µl)	NRT TUBE (µl)	NTC TUBE (µl)
Mastermix	22	22	22.0
Primer - Forward	0.5	0.5	0.5
Primer - Reverse	0.5	0.5	0.5
cDNA	2.0	-	-
NRT sample	-	2.0	-
PCR grade water	-	-	2.0
Total volume	25.0	25.0	25.0

NTC = No template control

PCR was carried out using the Corbet (Corbet Research, Australia) RotorGene 6000 series (Celtic Molecular Diagnostics S.A.) with SYBR green as a fluorescent marker (Figure A7). The thermocycler was programmed to commence PCR with incubation at 95 °C for 10 min to activate the Taq DNA polymerase, which is inactive at room temperature, and denature non specifically annealed primers to ensure highly specific amplifications. This was followed by 40 cycles at 95 °C for 5 s to denature the double stranded DNA, 60 °C for 15 s for primers to anneal to the template and 72 °C for 15 s for DNA synthesis. Amplicon extension was performed in 1 cycle at 72 °C for 10 min (Table 8).

Table 8 Three step PCR cycling program.

CYCLES	DURATION	TEMPERATURE (°C)
1	10 min	95
40	5 s	95
	15 s	60
	15 s	72
1	10 min	72

3.7.5 Melt curve analysis

A melt curve is used to distinguish specificity of an amplified product. Each double stranded DNA has its own specific melting temperature (T_m) depending on its base composition. All PCR products of a particular primer pair should have the same melting temperature, unless there is contamination, mispriming or primer dimer artefacts. Since SYBR green does not distinguish between different DNA samples, an important means of quality control is to check that all PCR products for a particular primer pair have a similar T_m . Thus, by measuring the T_m the DNA can be easily identified. At the melting point, the two strands of DNA separate and fluorescence rapidly decreases. The software plots the rate of change of relative fluorescence units (RFU) or derivatives of fluorescence over temperature (dF/dT) on the Y-axis versus temperature on the X-axis, and this peaks at the T_m .

After 40 cycles of real time RT-PCR amplification, the thermocycler performed a melt curve, which was set from 72 to 95 °C. The product was incubated at 72 °C for 90 s for pre-melt conditioning, followed by heating for 5 s in 1 °C increments, starting at 72 °C with fluorescence measured at each cycle.

3.7.6 Reference gene validation

Reference genes are used to normalise the gene of interest to correct for sample to sample variations such as cell number, RNA integrity or quantity or experimental treatment (Wang *et al.*, 2006; Gao *et al.*, 2008). ACTB, GAPDH and UBC were chosen as reference genes because they had been previously used in other studies (Gao *et al.*, 2008; Hosseini *et al.*, 2008; Vandesompele *et al.*, 2002). Since various factors can affect reference gene expression leading to false normalisation, the best solution to avoid this artefact is to study the expression profile of several potential reference genes and choose one which is least regulated. Having this in mind, three reference genes were studied prior to real time RT-PCR on the gene of interest.

3.7.7 REST program

REST, which is known as the relative expression software tool, is a stand alone software tool used to estimate the up or down regulation of gene expression. It is a relatively new program which statistically analyses the regulation of genes about 50,000 times (Pfaffl *et al.*, 2002). Data collected from the PCR reaction is fed into the program, whereby threshold cycle (C_t) values for the target gene and calibrator (control) gene are randomly compared and analysed. Results are also presented graphically via whisker box-plots which provide visual representation of variation for each gene and highlights potential issues such as distribution skew. In order to choose the least regulated reference gene, data (PCR efficiency, C_t values for controls and experimental samples) for each was fed into the program and analysed.

3.7.8 Gel electrophoresis

Once PCR reactions were complete, PCR products were run on a 2% agarose gel to confirm the presence of a single product of the appropriate molecular size. Thus, when the PCR reaction was in its 30th cycle, 1,500 ml of 1x TAE buffer was prepared from the stock solution (Appendix B9.2) and 75 µl of Ethidium bromide (10 mg/ml) was added to a final concentration of 0.5 µg/ml. Thereafter, 400 ml of the buffer was used to prepare a 2% agarose gel (Celtic Molecular Diagnostics S.A, Bioline, BIO-41026), which was poured into the casting tray and set in the refrigerator. The loading dye (Celtic Molecular Diagnostics S.A., Bioline, BIO-37045) was added to the samples and gently mixed, and then the mixture was loaded into the wells of the gel (Table 9). The dye makes samples dense, and hence they sink to the bottom of the well. During electrophoresis, the dye helps track samples. DNA hyperladder IV (580 ng) (Celtic Molecular Diagnostics S.A, Bioline, BIO-33058) was used to estimate the size of the PCR products. The remaining buffer was used for electrophoresis. The gel was run at 100 V for 1 h. Thereafter, the gel was scanned using a gel Bio Imaging System (Gene Genius, Syngene, Vacutec).

Table 9 Gel loading.

REAGENT	SAMPLE TUBE (µl)	NTC TUBE (µl)	MARKER (µl)
Loading dye (5x)	2.5	2.5	-
PCR product	10	10	-
Hyperladder IV	-	-	5

3.8 Statistical Analysis

Experiments were repeated six times ($n=6$), assays were performed in duplicate and the mean was used. Results were graphically presented and statistically analysed using Sigma Plot Version 8.0. A student t test and one-way ANOVA was performed to detect differences between the control and experiments, and as well as between experimental groups. Error bars were calculated using standard error. Results were considered to be statistically significant when $P \leq 0.05$. Statistical significance, compared to their respective control (0 J/cm^2) is shown in graphs as $P \leq 0.05$ (*), $P \leq 0.01$ (**) or $P \leq 0.001$ (***)).



CHAPTER 4 RESULTS

Normal (N) and wounded (W) human skin fibroblast cells were irradiated with 5 or 16 J/cm² on day 1 and 4 using a He-Ne laser (λ 632.8 nm). Cellular responses were assessed on day 4 at 1 or 24 h post irradiation. Cell morphology was assessed by light microscopy, cell viability by the Trypan blue exclusion test and ATP luminescent assay, cell proliferation by the XTT assay, DNA integrity by the comet assay and gene activation related to DNA repair (MPG) by real time RT-PCR. Non irradiated cells were used as controls.

4.1 Cell Morphology

The behaviour of N and W cells was observed using an inverted light microscope and digitally recorded at 1 or 24 h post irradiation on day 4. The number and intensity of colony formation, haptotaxis (direction) of the edge cells, number of fibroblasts present in the central scratch, and chemotaxis (movement or migration of cells across the central scratch) were evaluated to determine fibroblast activity (Rigau *et al.*, 1995).

There was no structural difference between irradiated and non irradiated N cells assessed at 1 or 24 h (Figure 9 a-f). Similarly, irradiated and non irradiated N and W cells showed typical morphology of long elongated cylindrical cells (Figure 9 and 10). Haptotaxis and cell migration was observed in all the wounded cultures but was more evident in cells irradiated with 5 J/cm² (Figure 10 c and d). The central scratch (CS) of non irradiated W cells showed incomplete closure at 1 or 24 h (Figure 10 a and b). There were

fewer cells in the CS of non irradiated cultures at 1 h compared to 24 h. Similarly, W cells irradiated with 16 J/cm^2 showed fewer cells in the CS at 1 h than at 24 h (Figure 10 e and f). In both cases the CS was about to close at 24 h due to the presence of more cells than at 1 h. W cells irradiated with 5 J/cm^2 showed complete wound closure at 1 and 24 h.

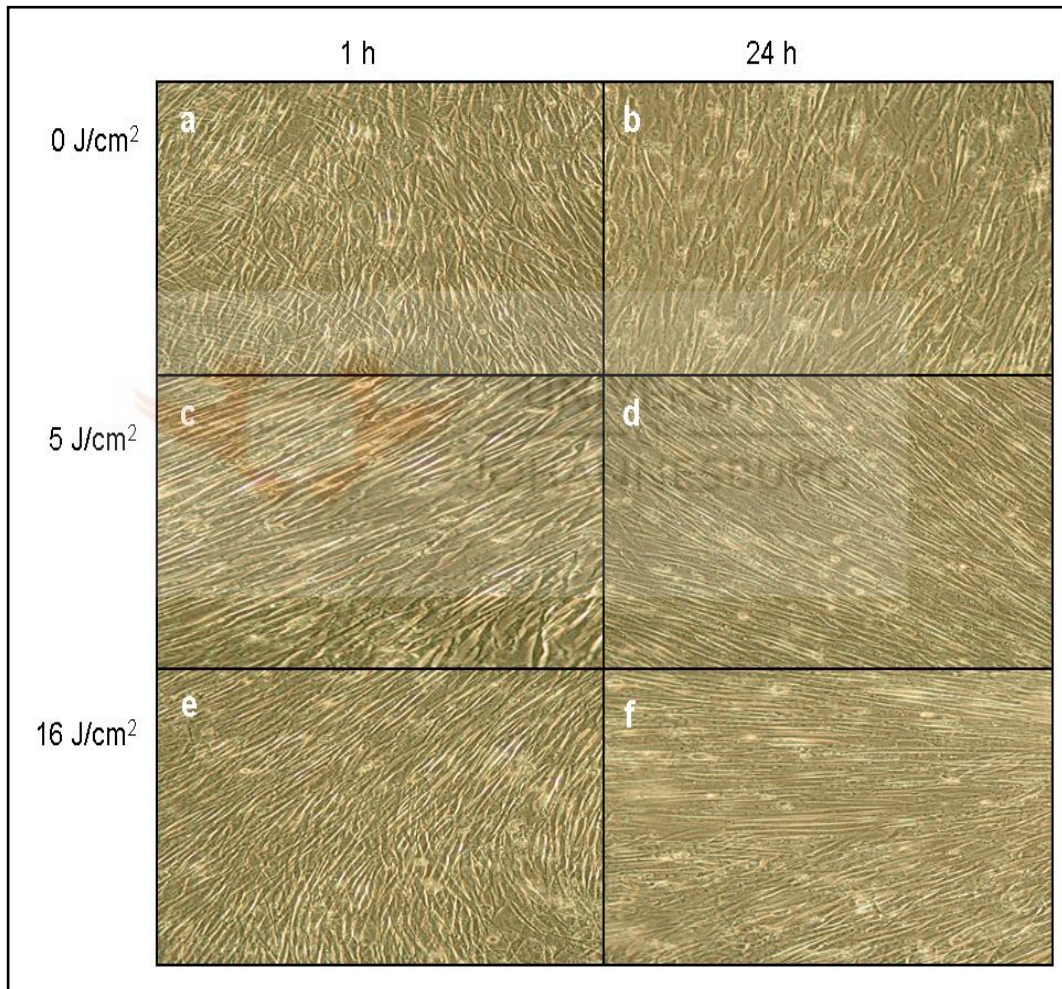


Figure 9 Micrograph of irradiated and non irradiated normal (N) WS1 cells. N WS1 cells are elongated and cylindrical in shape. WS1 cells were irradiated with 5 or 16 J/cm^2 on day 1 and 4 (c-f), while control cells were not irradiated (a and b). The behaviour of cells was digitally recorded at 1 or 24 h post irradiation on day 4. There was no structural difference between irradiated and non irradiated cells at 1 or 24 h (200x magnification).

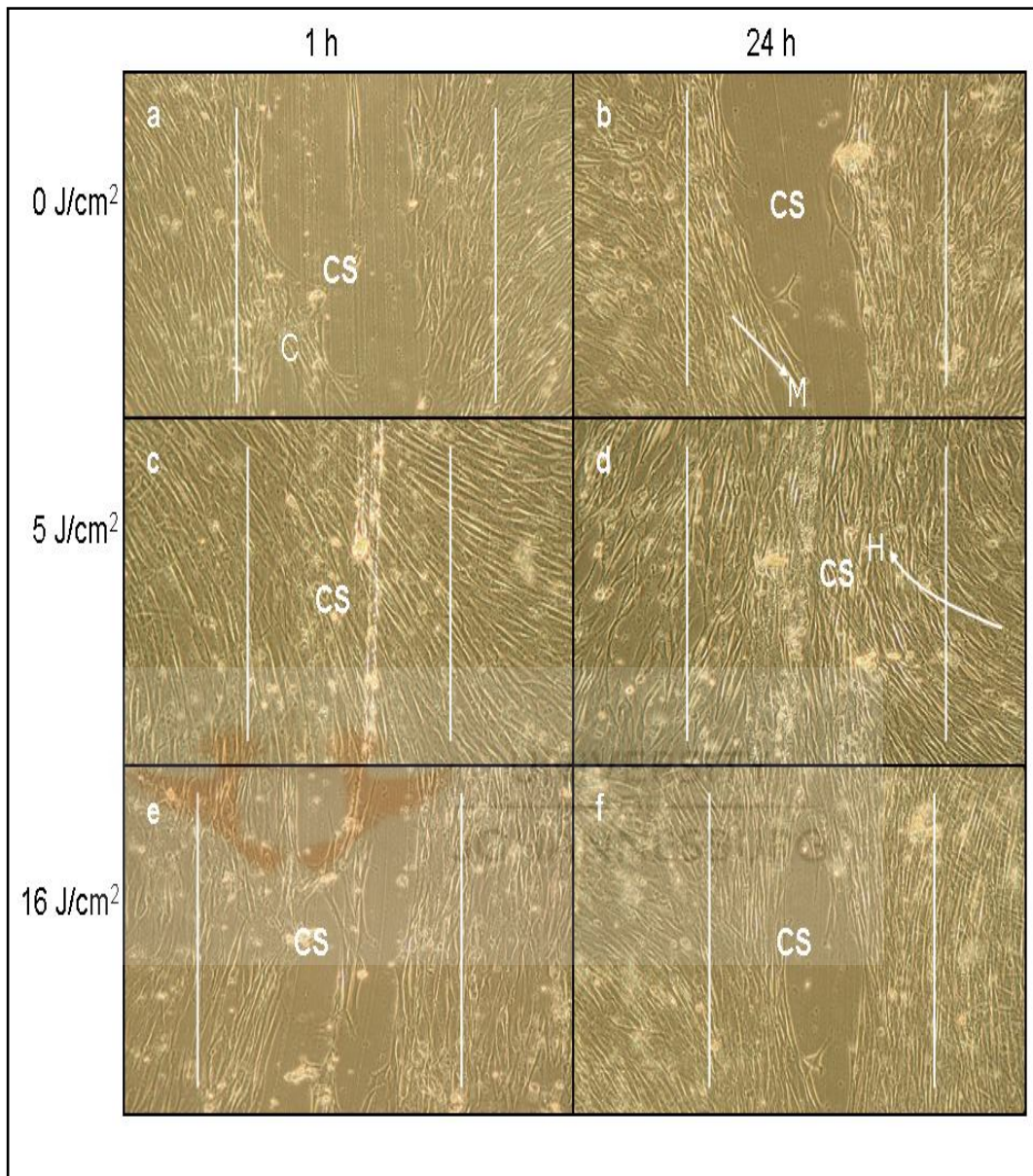


Figure 10 Micrograph of irradiated and non irradiated wounded (W) WS1 cells. A confluent monolayer of cells was scratched with a sterile 1 ml pipette to simulate a wound. Cells were irradiated at λ 632.8 nm using 5 or 16 J/cm² on day 1 and 4. The behaviour of cells was digitally recorded at 1 or 24 h post irradiation on day 4. Non irradiated cells were used as controls (a and b). The central scratch (CS) of cells irradiated with 16 J/cm² (e and f) and non irradiated cells showed incomplete closure at both 1 and 24 h, while cells irradiated with 5 J/cm² showed complete closure and more haptotaxis (H) at both 1 and 24 h (c and d). Non irradiated cells showed colony formation (C) and migration (M) along the CS in an attempt to close the wound (200x magnification).

4.2 Cell Viability

4.2.1 Trypan blue exclusion test

The Trypan blue exclusion test was used to assess the integrity of the cell membrane thus, cell viability (Table 10). Cells with intact membranes do not pick up the dye; only damaged membranes allow the dye to penetrate. Non irradiated cells (0 J/cm²) were used as controls. The total number of viable and non viable cells was calculated (Table 11).

Percent cell viability

Non irradiated N cells did not show any statistical difference in percentage cell viability when compared at 1 and 24 h ($P=0.5$), while N cells irradiated with 5 J/cm² showed an insignificant increase when compared at 1 and 24 h ($P=0.06$). N cells irradiated with 16 J/cm² did not show any significant difference when compared at 1 and 24 h ($P=0.6$). N cells irradiated with 5 or 16 J/cm² and left to incubate for 1 h showed an insignificant decrease compared to non irradiated N cells (1 h), ($P=0.07$ and $P=0.06$ respectively).

Table 10 Percent cell viability as determined by the Trypan blue exclusion test in normal (N) and wounded (W) WS1 cells. Cells irradiated with 5 or 16 J/cm² were compared with the respective controls (non irradiated cells), (0 J/cm²). The significance of results was indicated as follows: $P\leq 0.05$ (*), $P\leq 0.01$ (**) or $P\leq 0.001$ (***).

CELLS	0 J/cm ²	5 J/cm ²	16 J/cm ²
N (1 h)	96.9% ± 0.59	95.7% ± 1.1	95% ± 0.35
N (24 h)	97.5% ± 0.31	97% ± 0.18	95.4% ± 0.73
W (1 h)	97% ± 0.61	98.7% ± 0.17 *	94.4% ± 0.59 **
W (24 h)	97% ± 0.26	98% ± 0.1 **	94.9% ± 0.54 ***

± Standard error

Similar results were seen when cells were left to incubate for 24 h ($P=0.6$ and $P=0.09$ respectively). There was no significant difference between N cells irradiated at 5 or 16 J/cm² and left for 1 or 24 h ($P=0.6$ and $P=0.8$ respectively).

Non irradiated W cells did not show any statistical difference in cell viability when compared at 1 and 24 h ($P=0.4$), likewise W cells irradiated with 5 or 16 J/cm² did not show any significant difference ($P=0.7$ and $P=0.6$ respectively). W cells (1 h) irradiated with 5 J/cm² showed a significant increase compared to non irradiated W cells (1 h) ($P=0.05$), while irradiation with 16 J/cm² showed a significant decrease ($P=0.01$). Equivalent results were observed when W cells (24 h) irradiated with 5 or 16 J/cm² were compared with non irradiated W cells (24 h), ($P=0.01$ and $P<0.001$ respectively). At both 1 and 24 h, W cells irradiated with 5 J/cm² showed a significant increase in cell viability when compared to W cells irradiated with 16 J/cm², ($P<0.001$).

Comparison of non irradiated, W cells, N cells showed no differences at both 1 and 24 h ($P=0.6$ and $P=0.4$ respectively). W cells (1 h) irradiated with 5 J/cm² showed a significant increase when compared to N cells (1 h) irradiated with the same fluence ($P=0.005$), while the increase at 24 h was approaching statistical significance ($P=0.06$). W cells (1 h) irradiated with 16 J/cm² showed a significant decrease when compared to N cells (1 h) irradiated with the same fluence ($P=0.05$). On the other hand, there was no significant change at 24 h ($P=0.55$).

Cell number

Non irradiated N cells did not show any statistical difference in total number of viable cells when compared at 1 and 24 h ($P=0.28$), (Table 11). Similarly, there was no difference when irradiated with 5 or 16 J/cm² ($P=0.06$ and $P=0.79$ respectively). N cells (1 h) irradiated with 5 J/cm² showed an insignificant difference in cell number compared to N cells (1 h) irradiated with 0 or 16 J/cm² ($P=0.06$ and $P=0.13$ respectively). Equally, cells irradiated with 16 J/cm² showed an insignificant increase compared to non irradiated cells ($P=0.07$).

Table 11 Total number of viable and non viable cells as determined by the Trypan blue exclusion test. Significance of results was indicated by $P\leq 0.05$ (*), $P\leq 0.01$ () or $P\leq 0.001$ (**).**

CELLS	0 J/cm ²		5 J/cm ²		16 J/cm ²	
	VIABLE	NON VIABLE	VIABLE	NON VIABLE	VIABLE	NON VIABLE
N (1 h)	7.0x10 ⁵	1.2x10 ⁵	7.4x10 ⁵	1.0x10 ⁵	7.38x10 ⁵	1.1x10 ⁵
	± 1.3x10 ⁴	± 1.2x10 ³	± 8.6x10 ³	± 1.3x10 ³	± 8.2x10 ³	± 0.8x10 ³
N (24 h)	7.45x10 ⁵	1.3x10 ⁵	8.0x10 ⁵	1.15x10 ⁵	7.42x10 ⁵	1.2x10 ⁵
	± 1.8x10 ⁴	± 1.0x10 ³	± 2.7x10 ⁴	± 0.8x10 ³	± 1.2x10 ⁴	± 0.9x10 ³
W (1 h)	8.06x10 ⁵	1.6x10 ⁵	8.35x10 ⁵ *	1.5x10 ⁵	7.71x10 ⁵	1.7x10 ⁵
	± 7.8x10 ⁴	± 1.4x10 ³	± 9.9x10 ³	± 1.4x10 ³	± 2.2x10 ⁴	± 1.3x10 ³
W (24 h)	8.1x10 ⁵	1.5x10 ⁵	8.76x10 ⁵ **	1.47x10 ⁵	8.0x10 ⁵	1.76x10 ⁵
	± 1.1x10 ⁴	± 0.9x10 ³	± 2.7x10 ⁴	± 1.0x10 ³	± 5.8x10 ³	± 1.2x10 ³

± Standard error

Non irradiated W cells showed an insignificant difference in total viable cells when compared at 1 and 24 h ($P=0.77$). Similarly irradiation with 16 J/cm^2 did not cause any significant difference, while irradiation with 5 J/cm^2 caused a significant difference ($P=0.51$ and $P=0.003$ respectively). W cells (1 h) irradiated with 5 J/cm^2 showed a significant increase in viable cells compared to same cells irradiated with 0 or 16 J/cm^2 ($P=0.04$ and $P=0.02$ respectively), while W cells irradiated with 16 J/cm^2 showed an insignificant decrease compared to control cells (0 J/cm^2), ($P=0.08$). Similar results were observed when W cells (24 h) were irradiated with 5 or 16 J/cm^2 and compared to non irradiated cells ($P=0.01$ and $P=0.54$ respectively).

4.2.2 ATP luminescent assay

Results of cell viability as determined by ATP luminescence (Figure 11) showed that non irradiated N cells did not show any statistical difference in ATP when compared at 1 and 24 h ($P=0.56$). Similarly, N cells irradiated with 5 J/cm^2 did not show any significant change when compared at 1 and 24 h ($P=0.93$), while N cells irradiated with 16 J/cm^2 showed an insignificant increase at 1 h when compared to 24 h, ($P=0.17$). N cells (1 h) irradiated with 5 or 16 J/cm^2 showed an insignificant decrease compared to non irradiated N cells (1 h), ($P=0.9$ and $P=0.44$ respectively). Contrary, N cells (24 h) irradiated with 5 J/cm^2 showed an insignificant increase, while irradiation with 16 J/cm^2 showed an insignificant decrease compared to non irradiated N cells (24 h), ($P=0.76$ and $P=0.09$ respectively). N cells (1 h) irradiated with 5 J/cm^2 showed an insignificant decrease when compared to N cells (1 h) irradiated with 16 J/cm^2 ($P=0.71$), while an insignificant increase was observed when left to incubate for 24 h ($P=0.43$).

Non irradiated W cells did not show any statistical difference in ATP when compared at 1 and 24 h ($P=0.25$). Likewise, W cells irradiated with 5 or 16 J/cm² did not show any significant difference when compared at 1 and 24 h ($P=0.4$ and $P=0.1$ respectively). W cells (1 h) irradiated with 5 J/cm² showed a significant increase compared to non irradiated W cells (1 h), ($P=0.04$), while irradiation with 16 J/cm² showed a significant decrease ($P=0.02$). Equivalent results were observed when W cells were irradiated with 5 or 16 J/cm² and left for 24 h ($P=0.04$ and $P=0.003$ respectively). W cells (1 and 24 h) irradiated with 5 J/cm² showed a significant increase in ATP luminescence compared to cells irradiated with 16 J/cm² ($P=0.02$ and $P=0.001$ respectively).

Non irradiated W cells (1 h) showed no significant change in ATP compared to non irradiated N cells (1 h), ($P=0.55$), while non irradiated W cells (24 h) showed an insignificant increase compared to non irradiated N cells (24 h), ($P=0.3$). W cells (1 h) irradiated with 5 J/cm² showed a significant increase when compared to N cells (1 h) irradiated with the same fluence ($P=0.05$). On the other hand, W cells (24 h) irradiated with 5 J/cm² showed an insignificant increase compared to N cells (24 h) irradiated with the same fluence ($P=0.69$). W cells irradiated with 16 J/cm², and left to incubate for 1 or 24 h, showed an insignificant decrease compared to N cells irradiated with the same fluence ($P=0.21$ and $P=0.34$ respectively).

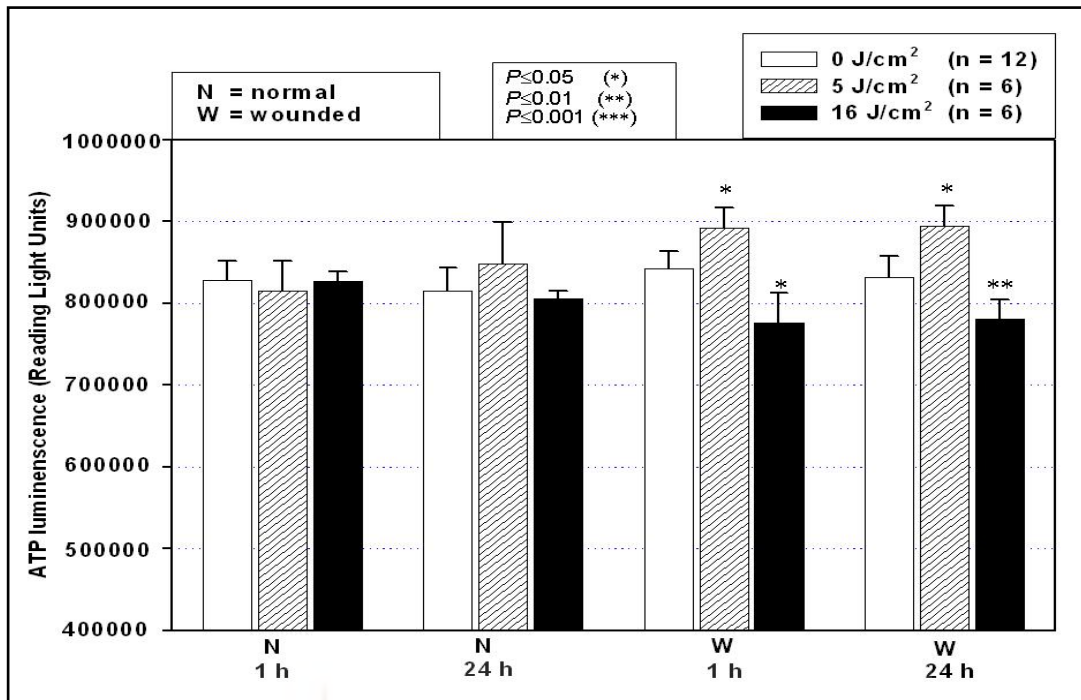


Figure 11 ATP luminescent assay graph. Normal (N) and wounded (W) WS1 cells were irradiated at λ 632.8 nm with a He-Ne laser using 5 or 16 J/cm² on day 1 and 4. ATP luminescence was assessed at 1 or 24 h post laser irradiation on day 4. Non irradiated cells (0 J/cm²) were used as controls. W cells non irradiated did not show any statistical difference in ATP compared to N cells non irradiated. W cells (1 h) irradiated with 5 J/cm² showed a significant increase compared to non irradiated W cells (1 h), while irradiation with 16 J/cm² showed a significant decrease. W cells (24 h) irradiated with 5 J/cm² also showed a significant increase in ATP when compared to non irradiated W cells (24 h), while irradiation with 16 J/cm² showed a significant decrease compared to non irradiated cells (24 h).

4.3 Cell Proliferation

Cell proliferation is one of the basic elements in the wound healing process, therefore its assessment is important (Koutiná *et al.*, 2003). Fibroblast cells proliferate under normal growth conditions. Mitochondrial succinate dehydrogenase in metabolically active cells cleaves XTT forming an orange formazan dye which is directly proportional to the number of proliferating cells.

Cell proliferation as determined by the XTT assay (Figure 12) demonstrated that non irradiated N cells did not show any statistical difference in cell proliferation when compared at 1 and 24 h ($P=0.08$). N cells irradiated with 5 J/cm^2 showed an insignificant difference when compared at 1 and 24 h ($P=0.07$). Similarly, N cells irradiated with 16 J/cm^2 did not show any significant difference ($P=0.06$). N cells (1 h) irradiated with 5 J/cm^2 showed an insignificant increase compared to non irradiated N cells (1 h), ($P=0.65$), while irradiation with 16 J/cm^2 showed an insignificant decrease ($P=0.08$). Equivalent results were observed when N cells (24 h) were irradiated with 5 or 16 J/cm^2 ($P=0.06$ and $P=0.94$ respectively). When cells were left to incubate for 1 h, N cells irradiated with 5 J/cm^2 showed an insignificant increase compared to N cells irradiated with 16 J/cm^2 ($P=0.32$). Equally, an insignificant increase was observed when the incubation period was changed to 24 h ($P=0.27$).



There was no significant change between 1 and 24 h in irradiated (5 and 16 J/cm^2) and non irradiated W cells ($P=0.7$, $P=0.41$ and $P=0.08$ respectively). W cells (1 and 24 h) irradiated with 5 J/cm^2 showed a significant increase compared to their respective controls ($P=0.01$ and $P<0.01$ respectively). Contrary, W cells (1 h) irradiated with 16 J/cm^2 showed a significant decrease compared to non irradiated W cells (1 h), ($P<0.01$), while the decrease at 24 h was insignificant ($P=0.52$). W cells (1 h) irradiated with 5 or 16 J/cm^2 showed a significant difference when compared to each other ($P<0.01$). Equally, the same observation was noted at 24 h ($P=0.01$).

Non irradiated W cells at 1 and 24 h showed an insignificant increase in cell proliferation compared to non irradiated N cells (1 and 24 h), ($P=0.48$ and $P=0.54$ respectively). W cells (1 h) irradiated with 5 J/cm^2 showed a

significant increase when compared to N cells (1 h) irradiated with the same fluence ($P=0.01$). The same significant increase in W cells irradiated with 5 J/cm² was seen when left to incubate for 24 h ($P=0.03$). W cells (1 h) irradiated with 16 J/cm² showed a significant decrease when compared to N cells (1 h) irradiated with the same fluence ($P=0.01$), while the decrease at 24 h was insignificant ($P=0.93$).

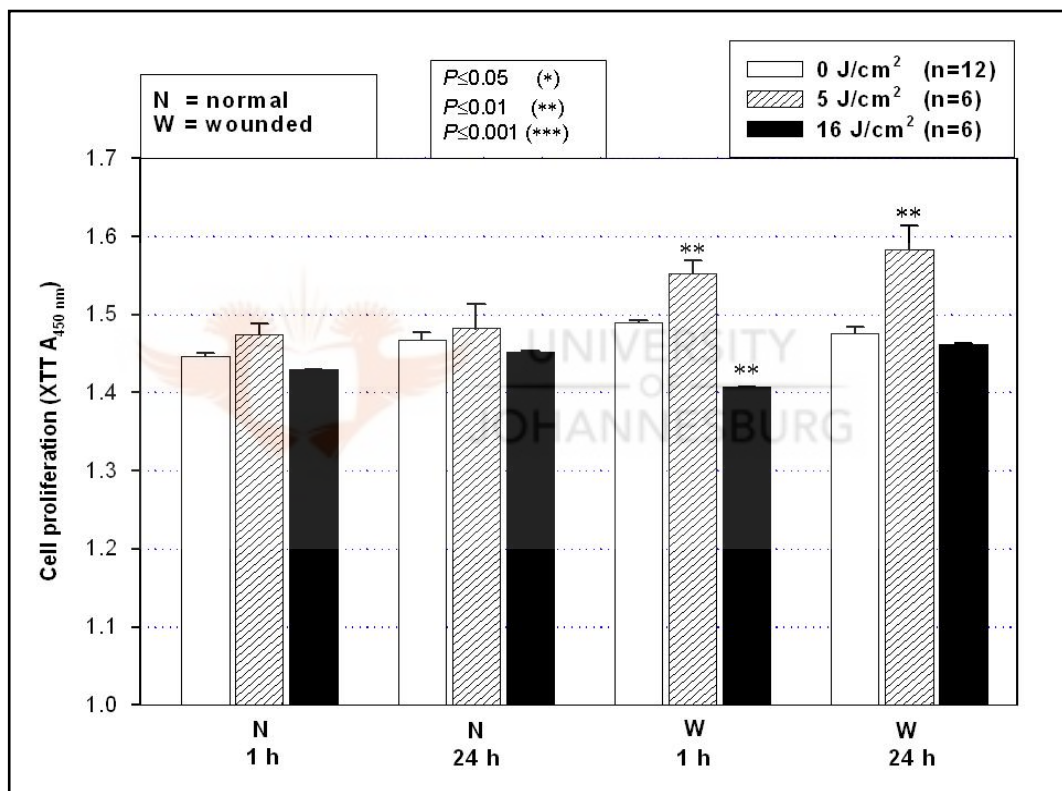


Figure 12 Cell proliferation as determined by XTT in normal (N) and wounded (W) cells. N and W WS1 cells were irradiated at λ 632.8 nm with a He-Ne laser using 5 or 16 J/cm² on day 1 and 4. Cell proliferation was assessed on day 4 at 1 or 24 h post irradiation. Non irradiated cells (0 J/cm²) were used as controls. W cells (1 and 24 h) irradiated with 5 J/cm² showed a significant increase compared to their respective controls. W cells (1 h) irradiated with 16 J/cm² showed a significant decrease compared to W cells (1 h) non irradiated. However, W cells (1 h) irradiated with 5 J/cm² showed a significant increase compared to N cells (1 h) irradiated with the same fluence ($P=0.01$). Though not significant, W cells irradiated with 16 J/cm² showed more proliferation at 24 h compared to 1 h.

HU at a final concentration of 5 mM has been used in many studies to inhibit proliferation while having no effect on other cell functions such as cell migration. The XTT assay was used to assess W cells treated with HU and irradiated with 5 J/cm² (Figure 13).

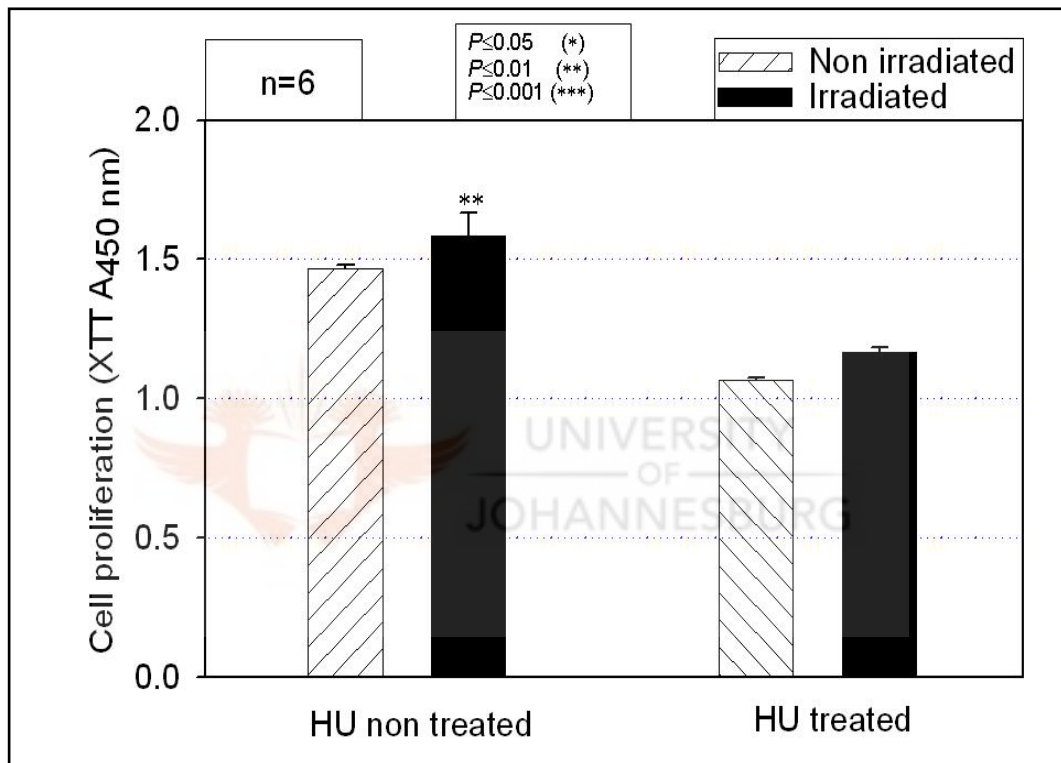


Figure 13 Hydroxyurea graph showing cell proliferation. The effect of phototherapy on 5 mM hydroxyurea (HU) treated cells (HU+) was assessed using the XTT assay. HU (+) cells showed a decrease in cell proliferation when compared to non treated cells (HU-). HU (-) irradiated cells showed a significant increase in cell proliferation compared to its respective control. Irradiated HU (+) cells showed a significant decrease in cell proliferation compared to irradiated HU (-) cells.

Non irradiated HU treated cells (HU+) showed a significant decrease in cell proliferation compared to non irradiated HU non treated cells (HU-), ($P=0.01$). Similarly, irradiated HU (+) cells showed a significant decrease in proliferation

compared to irradiated HU (-) cells, ($P=0.01$). Irradiated HU (+) cells showed an insignificant increase in cell proliferation compared to non irradiated HU (+) cells ($P=0.06$). Irradiated HU (-) cells showed a significant increase compared to non irradiated HU (-) cells, ($P=0.01$), (Zungu *et al.*, 2008).

4.4 Genetic Integrity

4.4.1 Alkaline comet assay

The alkaline comet assay was used to detect and quantify DNA damage. Comet assays which use enzymes have greater specificity and sensitivity compared to ordinary comet assays. Enzymes are used to detect lesion specific damage. For instance, Fpg detects and cleaves oxidised bases in DNA strands thereby creating additional strand breaks and hence produces an increase in arbitrary units. The alkaline comet assay with and without Fpg assessed DNA damage at 1 or 24 h post irradiation on day 4 (Figure 14). Non irradiated cells (0 J/cm^2) were used as controls and the comet assay without Fpg was used as a control for the comet assay with Fpg because the latter detects both strand breaks and oxidised bases.

Comet assay without Fpg

N cells irradiated with 0, 5 and 16 J/cm^2 did not show any significant change when incubated for 24 h and compared to incubation at 1 h ($P=0.68$, $P=0.34$ and $P=0.57$ respectively). N cells irradiated with 5 or 16 J/cm^2 and incubated post laser irradiation on day 4 for 1 h showed an insignificant increase in arbitrary units compared to non irradiated N cells (1 h), ($P=0.51$ and $P=0.18$ respectively). Equivalent results were observed when N cells (24 h) were irradiated with 5 or 16 J/cm^2 ($P=0.99$ and $P=0.34$ respectively). N cells (1 h)

irradiated with 5 J/cm² showed an insignificant decrease when compared to N cells (1 h) irradiated with 16 J/cm² ($P=0.43$). Likewise, an insignificant difference was observed when N cells (24 h) irradiated with 5 J/cm² was compared to N cells (24 h) irradiated with 16 J/cm² ($P=0.5$).

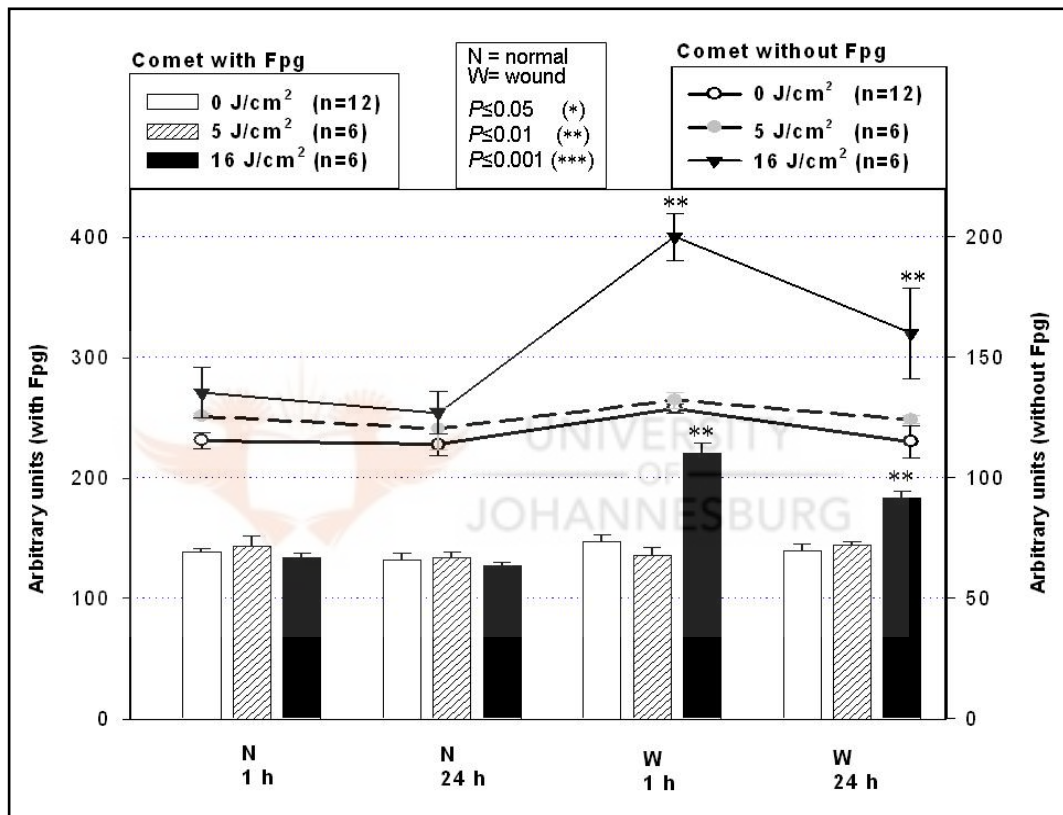


Figure 14 Comet assay with and without Fpg. Normal (N) and wounded (W) cells were irradiated at λ 632.8 nm with a He-Ne laser using 5 or 16 J/cm² on day 1 and 4. DNA damage was assessed at 1 or 24 h post irradiation on day 4 using the comet assay with and without Fpg. An increase in arbitrary units indicates an increase in DNA damage. Non irradiated cells (0 J/cm²) were used as controls. N cells irradiated with 5 or 16 J/cm² showed no significant change in DNA damage at 1 and 24 h when compared to their respective controls. W cells (1 and 24 h) irradiated with 16 J/cm² showed a significant increase in damage with and without Fpg compared to their respective controls. W cells irradiated with 16 J/cm² showed a significant increase in arbitrary units with Fpg when compared at 1 and 24 h ($P=0.02$), and similarly without Fpg ($P=0.04$).

Non irradiated W cells incubated for 24 h showed a decrease in DNA damage which was approaching statistical significance compared to the same cells incubated for 1 h ($P=0.06$). W cells irradiated with 5 J/cm^2 did not show any significant difference when 1 and 24 h incubation times were compared ($P=0.11$). Contrary, W cells irradiated with 16 J/cm^2 showed a significant difference ($P=0.04$) with a decrease at 24 h. W cells (1 and 24 h) irradiated with 5 J/cm^2 showed no significant change compared to their respective non irradiated W controls ($P=0.33$ and $P=0.36$ respectively), while irradiation with 16 J/cm^2 showed a significant increase on both repair times ($P<0.01$). W cells (1 h) irradiated with 5 or 16 J/cm^2 showed a significant difference when compared to each other ($P<0.01$), with cells irradiated with 5 J/cm^2 showing a decrease in DNA damage. Equally, the same observation was noted when W cells (24 h) irradiated with 5 or 16 J/cm^2 were compared ($P=0.02$).

Non irradiated W cells (1 h) showed an insignificant increase in DNA damage compared to non irradiated N cells (1 h), ($P=0.09$). Non irradiated W cells (24 h) showed no significant change compared to non irradiated N cells (24 h), ($P=0.46$). W cells (1 and 24 h) irradiated with 5 J/cm^2 showed an insignificant increase when compared to N cells (1 and 24 h) irradiated with the same fluence ($P=0.19$ and $P=0.52$ respectively). W cells (1 h) irradiated with 16 J/cm^2 showed a significant increase when compared to N cells (1 h) irradiated with the same fluence ($P<0.01$), while the increase at 24 h was approaching statistical significance ($P=0.06$).

Comet assay with Fpg

Non irradiated N cells did not show any statistical difference in DNA damage when compared at 1 and 24 h ($P=0.06$), (Figure 14). Similarly, N cells irradiated with 5 or 16 J/cm^2 showed insignificant changes when incubation

times (1 or 24 h) were compared ($P=0.09$ and $P=0.13$ respectively). N cells (1 h) irradiated with 5 J/cm^2 showed an insignificant increase in DNA damage compared to non irradiated N cells (1 h), ($P=0.11$). Contrary, irradiation with 16 J/cm^2 showed an insignificant decrease ($P=0.16$). Similar results were observed when N cells (24 h) were irradiated with 5 or 16 J/cm^2 and each compared with the respective control ($P=0.75$ and $P=0.27$ respectively). N cells (1 h) irradiated with 5 J/cm^2 showed an insignificant increase when compared to N cells (1 h) irradiated with 16 J/cm^2 ($P=0.06$). Equally, an insignificant difference was observed when N cells (24 h) irradiated with 5 J/cm^2 was compared to N cells (24 h) irradiated with 16 J/cm^2 ($P=0.21$).

Non irradiated W cells did not show any statistical difference when the different incubation times were compared ($P=0.2$). Similarly, W cells irradiated with 5 J/cm^2 did not show any significant difference ($P=0.12$), while W cells irradiated with 16 J/cm^2 and incubated for 24 h showed a significant decrease compared to incubation for 1 h ($P=0.02$). W cells (1 h) irradiated with 5 J/cm^2 showed an insignificant decrease compared to non irradiated W cells (1 h), ($P=0.32$), while irradiation with 16 J/cm^2 showed a significant increase ($P<0.01$). W cells (24 h) irradiated with 5 J/cm^2 showed an insignificant increase compared to non irradiated W cells (24 h), ($P=0.35$), while irradiation with 16 J/cm^2 showed a significant increase ($P<0.01$). W cells irradiated with 16 J/cm^2 and incubated for 1 or 24 h post irradiation showed a significant increase in oxidised DNA damage compared to the same cells irradiated with 5 J/cm^2 ($P<0.01$ and $P=0.01$ respectively).

When incubated for 1 h, the increase in DNA damage in non irradiated W cells was approaching statistical significance ($P=0.08$) compared to non irradiated N cells, while there was no significant change at 24 h ($P=0.11$). W

cells (1 h) irradiated with 5 J/cm² showed an insignificant decrease when compared to N cells (1 h) irradiated with the same fluence ($P=0.06$). W cells (24 h) irradiated with 5 J/cm² showed no significant change compared to N cells (24 h) irradiated with the same fluence ($P=0.09$). W cells (1 and 24 h) irradiated with 16 J/cm² showed a significant increase when compared to N cells (1 and 24 h) irradiated with the same fluence ($P<0.01$).

4.5 Real Time Reverse Transcription PCR

Real time RT-PCR was used to assess the up or down regulation of MPG in WS1 cells after exposure with a He-Ne laser at λ 632.8 nm. Zhang *et al.*, (2003) reported that when HS27 fibroblast cells were exposed to red light (λ 628 nm, 0.88 J/cm²) several genes were up regulated, including MPG.

4.5.1 Reference gene validation

Prior to the study of the regulation of MPG expression by irradiation with the validated reference gene, PCR results for the selected reference genes were analysed using the standard curve, melt curve and gel electrophoresis to check if they were influenced by wounding and irradiation, and if primers were of good quality. According to Wang *et al.*, (2006) a good primer set produces a single product, which is distinguished by a single melt peak in all the dilution series except NTC and produces a standard curve with acceptable correlation coefficient of R^2 (>0.995) and PCR efficiency ($\sim 100\%$). The R^2 value or R^2 value is the percentage of the data which is consistent with the statistical hypothesis that the given standards form a standard curve. Standard curves are used to quantify unknown samples. If the standard curve is generated from a sample of known abundance, the starting quantity of unknown

samples can be inferred from its C_t value relative to the standard curve. Even when the standard curve is generated from an abundant but unknown absolute quantity, the relative abundance of different unknown samples can be directly compared by calculating the position of their C_t values along the same standard curve.

Using data from serial dilutions of the standards, an arbitrary threshold was set and C_t values from all PCR samples were recorded. The insertion of a threshold allowed the generation of standard curves and corresponding correlation coefficient of R^2 and PCR efficiency for the respective reference genes ACTB, GAPDH and UBC (Figure 15, 16, and 17 respectively). The PCR efficiencies for ACTB, GAPDH and UBC were 94%, 82% and 97% respectively, with an R^2 value of 0.999, 0.995 and 0.895 respectively.

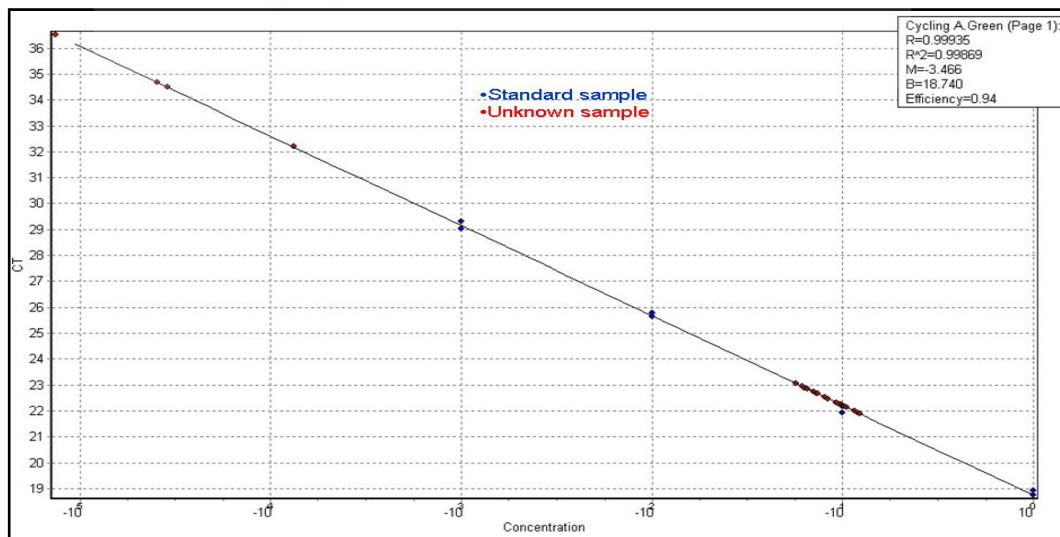


Figure 15 Standard curve for reference gene beta Actin (ACTB). The standard curve was generated from the C_t values of a 10 fold dilution series (1:10; 1:100; 1:1,000) of non irradiated N cells. Unknown samples were diluted 1:10 prior to the PCR run. The R^2 value or R^2 value is the percentage of data consistent with a statistical hypothesis that the given standards form a standard curve.

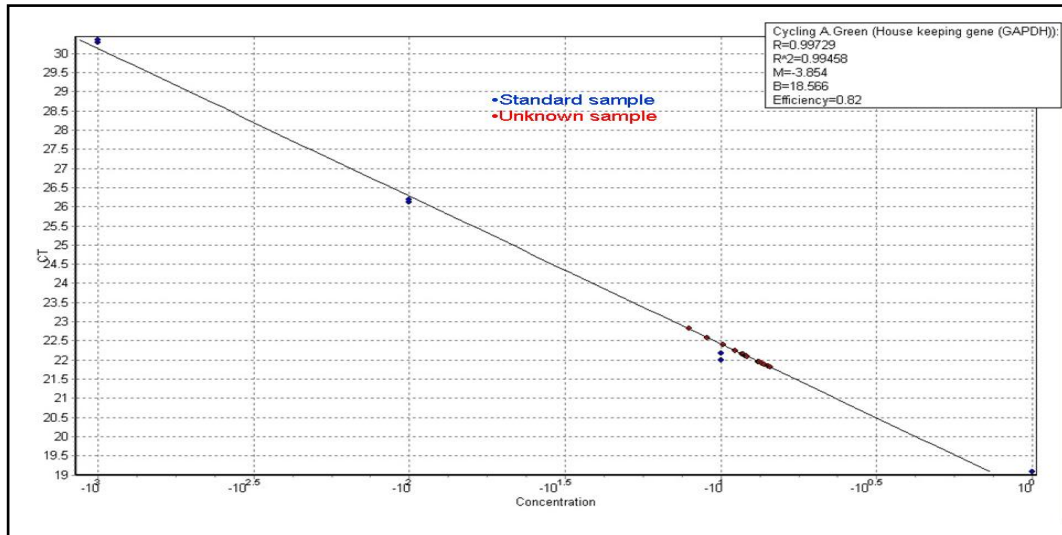


Figure 16 Standard curve for reference gene Glyceraldehyde 3 phosphate dehydrogenase (GAPDH). A 10 fold dilution series was made from pooled cDNA of non irradiated N samples (1:10; 1:100 and 1:1,000). All unknown samples were diluted 1:10 prior to the PCR run. R² is the percentage of data consistent with a statistical hypothesis that the given standards form a standard curve.

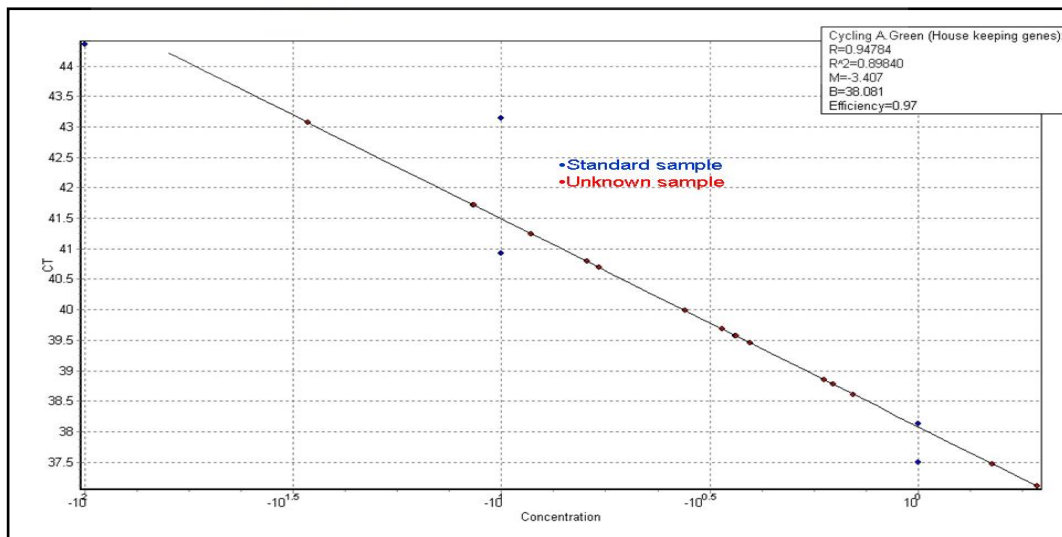
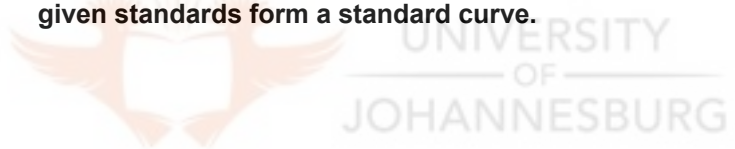


Figure 17 Standard curve for reference gene Ubiquitin c (UBC). A 10 fold dilution series (1:10; 1:100 and 1:1,000) was made from pooled cDNA of non irradiated N samples. All unknown samples were diluted 1:10 prior to the PCR run. R² is the percentage of data consistent with a statistical hypothesis that the given standards form a standard curve.

Melt curve analysis

In this study, the melt curve analysis for ACTB, GAPDH and UBC (Figure 18, 19 and 20 respectively), (Appendix E) showed that a single product was formed in each of the treatment conditions for the respective genes during the PCR run and was melted at a particular temperature (87.7 °C, 84.0 °C, and 88 °C respectively). However, one of the duplicates for NTC (blue-gray line) in the melt curve for ACTB appears to have had some genomic DNA contamination because the melt peak resembles those of the experimental samples.

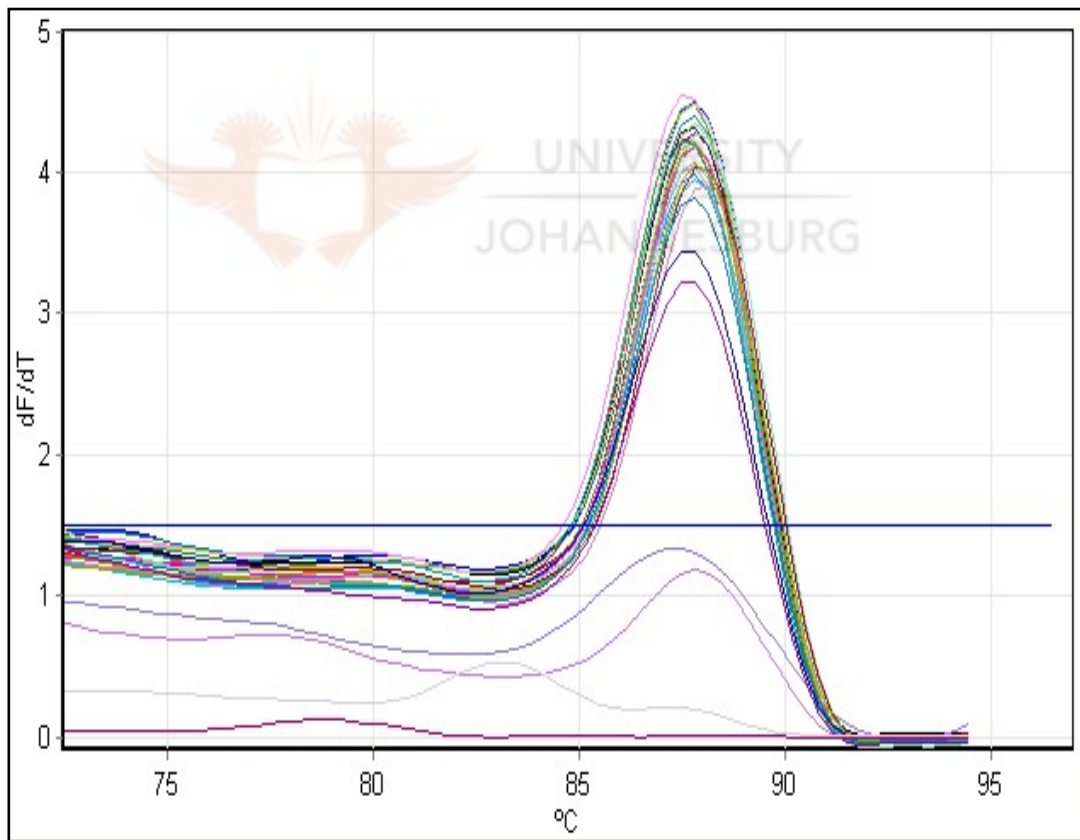


Figure 18 A melt curve analysis for ACTB PCR product. The formed product melted at 87.7 °C. The 4 lines below the threshold cycle are from the NTC samples.

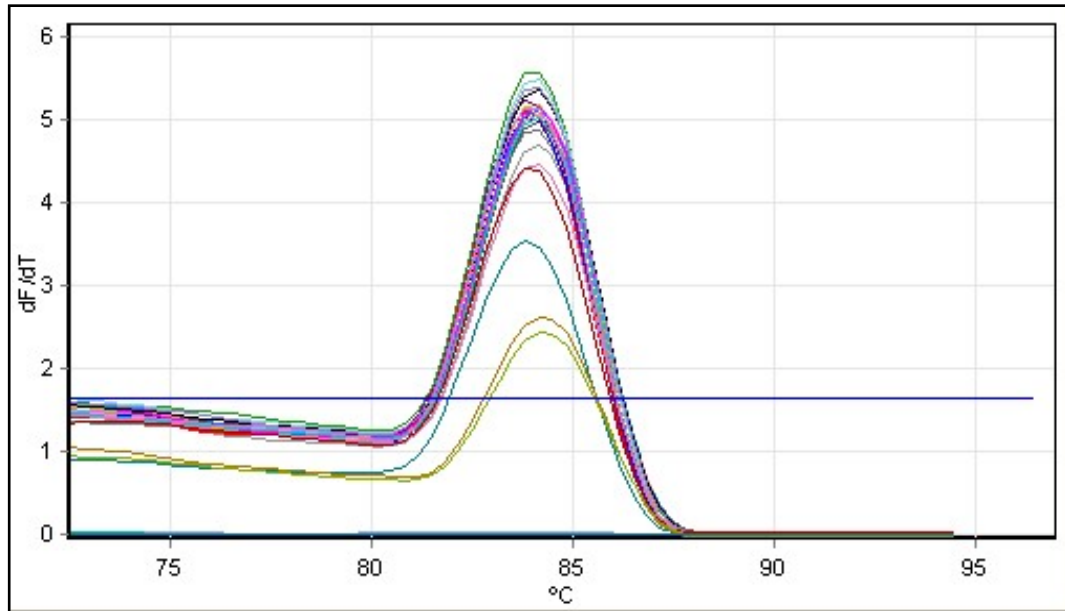


Figure 19 A melt curve analysis for GAPDH PCR product. The single PCR product melted at 84.0 °C. Products for NTC samples were not detected.

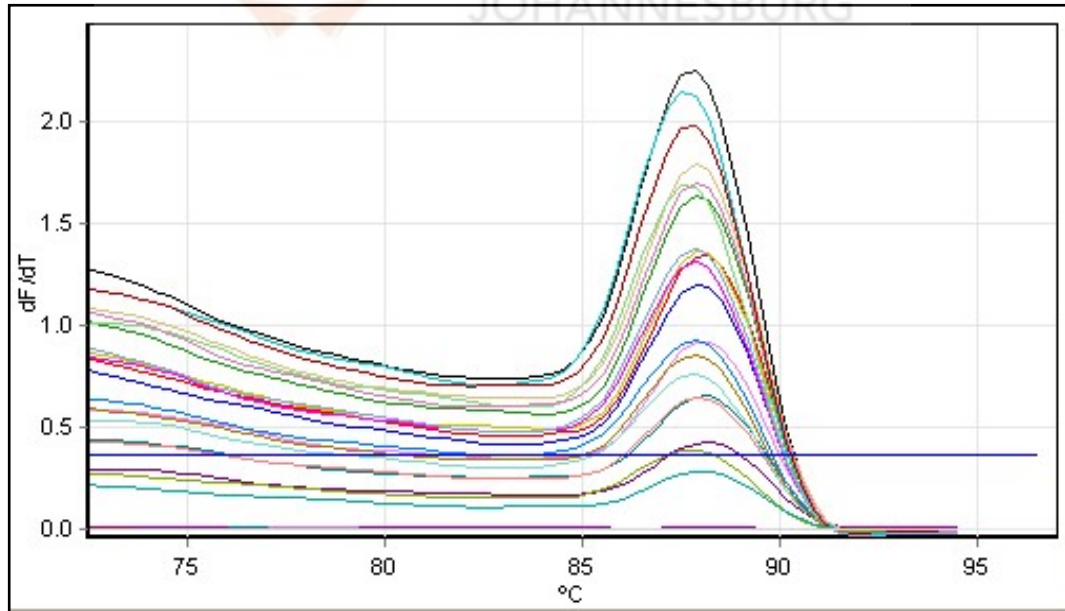


Figure 20 A melt curve analysis for UBC PCR product. A single PCR product was melted at 88 °C. The product was not detected in NTC samples and standard dilutions from 1:100 to 1:1,000.

Gel electrophoresis

Agarose gel electrophoresis, as another method of checking primer specificity, also showed a single PCR product of appropriate molecular size that was absent from the control (Figure 21). However, there is a faint band in lane 1 (NTC for ACTB) which appears to be contamination. This corresponds with the melt curve analysis. The photograph of the gel was taken by the Gene Genius (Syngene, Vacutec).

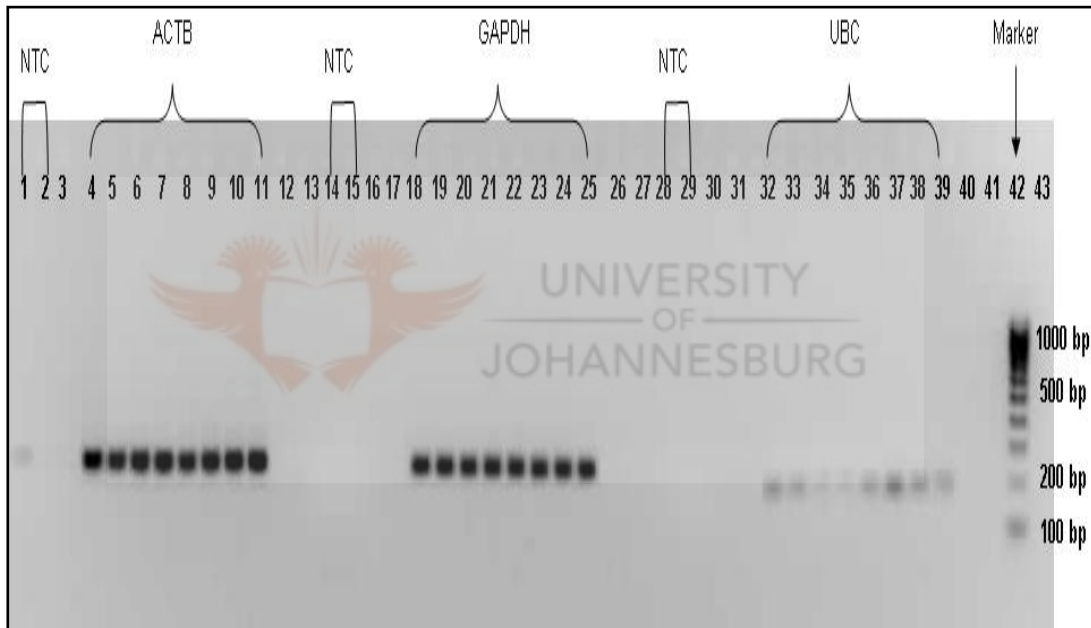


Figure 21 A 2% agarose gel was made to check PCR products of the reference genes. Beta Actin (ACTB), Glyceraldehyde 3 phosphate dehydrogenase (GAPDH) and Ubiquitin C (UBC) were the selected reference genes. ACTB showed a single product at 234 bp, GAPDH at 238 bp and UBC at 175 bp. Samples were loaded into the following lanes: ACTB; 1 and 2 (NTC), 4 and 5 (N non irradiated [N0]), 6 and 7 (W non irradiated [W0]), 8 and 9 (W irradiated with 5 J/cm² [W5]) and 10 and 11 (W irradiated with 16 J/cm² [W16]). GAPDH; 14 and 15 (NTC), 18 and 19 (N0), 20 and 21 (W0), 22 and 23 (W5) and 24 and 25 (W16). UBC; 28 and 29 (NTC), 32 and 33 (N0), 34 and 35 (W0), 36 and 37 (W5) and 38 and 39 (W16). Lane 42; DNA marker (580 ng).

REST program

A computer software tool (REST) was used to analyse the regulation of genes by providing statistics of their variability. The software randomly analyses genes and gives statistics in a table (Appendix E4) and graph form (Figure 22). Results from REST showed that ACTB in W cells non irradiated or irradiated with 5 or 16 J/cm² was no different to the N cells non irradiated ($P=0.095$, $P=0.055$, and $P=0.052$ respectively) (Figure 22). Similarly, the expression of UBC was not regulated by all the treatment conditions ($P=0.541$, $P=0.101$, and $P=0.481$ respectively). On the other hand, the expression of GAPDH in W cells irradiated with 16 J/cm² was significantly up regulated by a mean factor of 1.424 ($P=0.047$), while W cells non irradiated or irradiated by 5 J/cm² were not affected ($P=0.110$ and $P=0.574$ respectively).

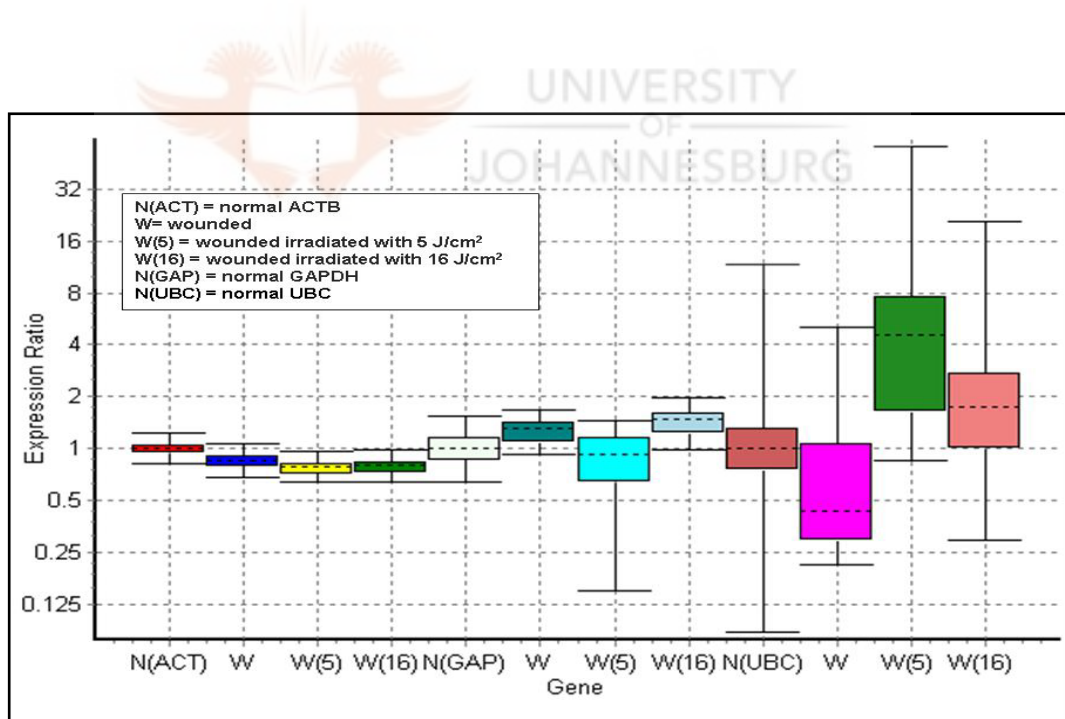


Figure 22 Relative gene expressions for ACTB, GAPDH and UBC. ACTB and UBC were least variable in their expression, while GAPDH was highly variable by irradiation with 16 J/cm².

4.5.2 MPG expression

Based on the results obtained from reference genes expression, ACTB was chosen as a gene with which to normalise the expression of MPG. It was the least variable and regulated gene amongst the three genes. Thus, the real time RT-PCR for MPG was run alongside ACTB, when W cells were irradiated with 5 J/cm^2 on day 1. These cells were left to incubate for 1 h post irradiation. The quantitative analysis of MPG showed that C_t values for W cells irradiated with 5 J/cm^2 were very close to those of the NTC samples (Appendix E5). The melt curve analysis showed that there was no specific MPG PCR product except for the reference gene, which is shown by a red line (ACTB), (Figure 23).

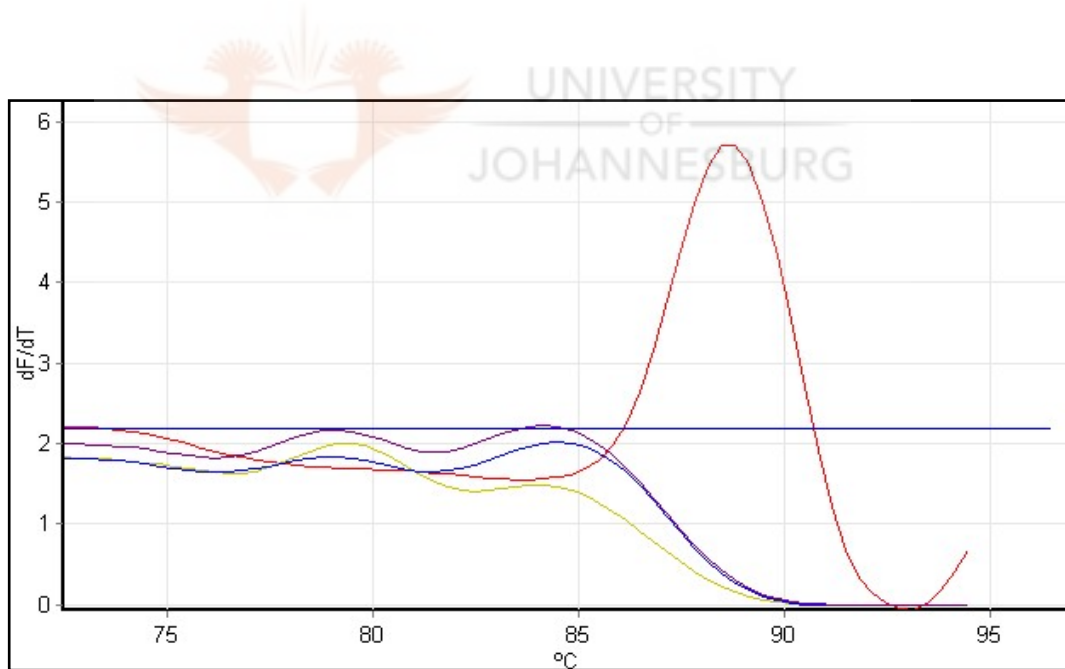


Figure 23 A melt curve analysis for MPG and ACTB PCR products. W cells were irradiated with 5 J/cm^2 and incubated for 1 h post irradiation. MPG and NTC melt peaks were formed at lower temperatures, and hence were non specific products. The ACTB PCR product was specific; it melted at $88.7 \text{ }^\circ\text{C}$.

Results from the agarose gel electrophoresis further confirmed results obtained from the melt curve analysis; MPG PCR product was not detected, while the expected ACTB PCR product was detected (Figure 24).

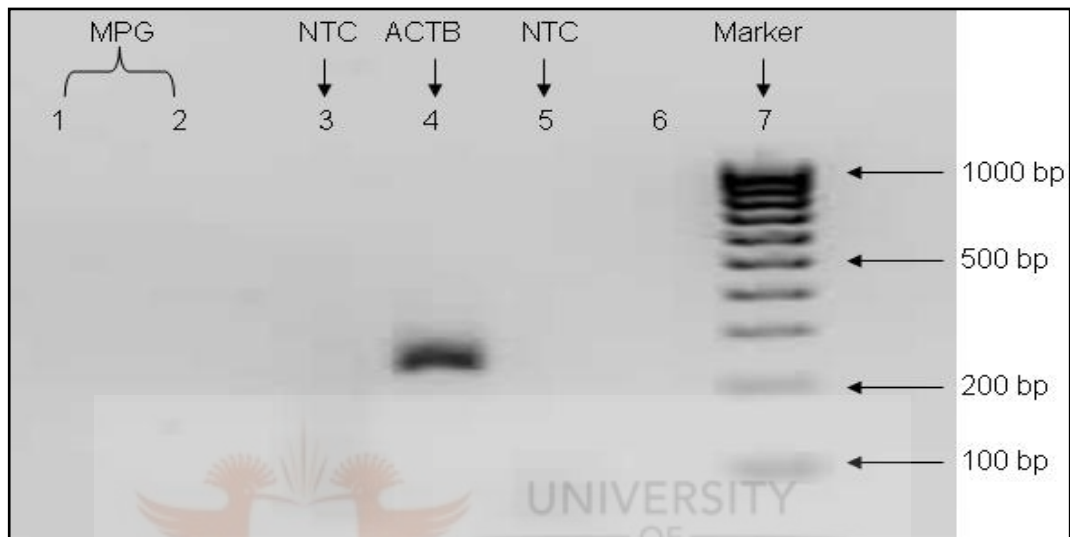


Figure 24 A 2% agarose gel for MPG and ACTB PCR products. W WS1 cells were irradiated with 5 J/cm² and incubated for 1 h post irradiation. Equal volume of PCR products (10 µl) was loaded, except the DNA marker (5 µl). RNA was extracted and transcribed by a Fastlane cell cDNA synthesis kit. Lane 1 and 2 = MPG products, lane 3 = NTC for MPG, lane 4 = ACTB PCR product, lane 5 = NTC for ACTB and 7 = DNA marker (580 ng).

Since MPG expression was not detected in W cells irradiated with 5 J/cm², it was decided to irradiate the cells with a higher fluence (16 J/cm²) so that more damage could be caused, and hence induce the expression of the gene. In addition, MPG expression was also monitored in MCF 7 cells (breast cancer cells) because reports indicate that these cells express more MPG than WS1 cells (Cerdeira *et al.*, 1998; Bouziane *et al.*, 2000). This cell line was to act as a positive control. MCF 7 cells were then analysed alongside WS1 W cells which were left to incubate at 0, 3 or 8 h post irradiation; MCF 7 cells were not irradiated.

When the expression of MPG in W cells irradiated on day 1 with 16 J/cm^2 and in MCF 7 cells was analysed at 0 h, it was observed that the C_t values for these cells were not different to the values of NRT and NTC samples (Appendix E6). The MPG melt curve (Figure 25) and gel electrophoresis (Figure 26) analysis showed that the PCR products melted at lower temperatures and thus they were not the expected products while the gel did not detect any PCR product.

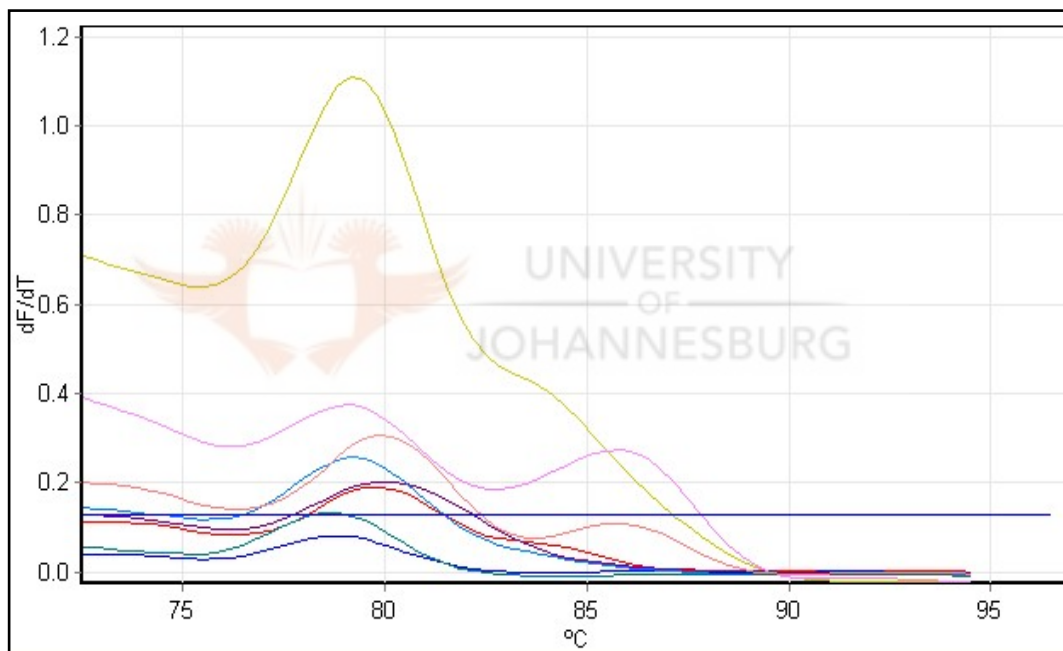


Figure 25 A melt curve analysis for MPG PCR products at 0 h incubation post irradiation. W WS1 cells were irradiated with 16 J/cm^2 on 1 day, while MCF 7 cells were not irradiated. No specific MPG PCR melt peaks were detected in W WS1 cells, MCF 7 cells, NRT and NTC samples; all peaks melted at temperatures lower than the specific PCR product.

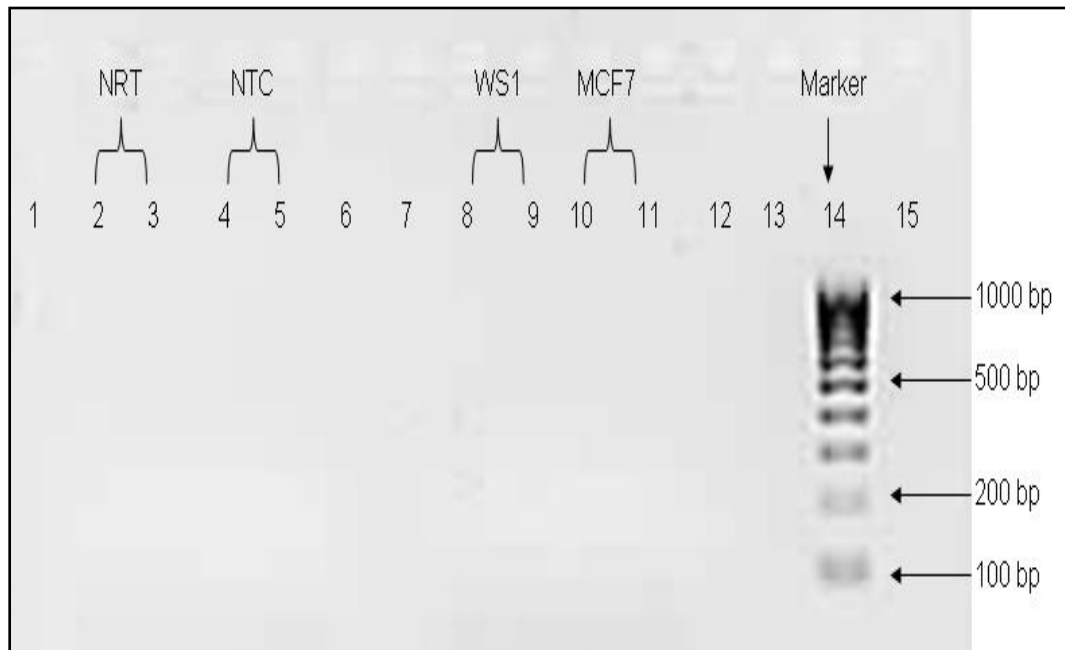


Figure 26 A 2% agarose gel for MPG PCR products 0 h incubation post irradiation. W WS1 cells were irradiated with 16 J/cm² on day 1, while MCF 7 cells were not irradiated. RNA was extracted and transcribed by a Fastlane cell cDNA synthesis kit. Equal volume of PCR products (10 µl) was loaded, except the DNA marker (5 µl). MPG PCR products were not detected in all the samples. Lane 2 and 3 = NRT, lane 4 and 5 = NTC, lane 8 and 9 = W WS1 cells, lane 10 and 11 = MCF 7 cells, and 14 = DNA marker (580 ng).

The PCR result for W WS1 cells irradiated on day 1 with 16 J/cm² and incubated for 3 h prior to RNA extraction and transcription to cDNA, showed that the C_t values for MPG in WS1 and MCF 7 cells were not different to values for NRT samples (Appendix E7). The melt curve analysis did not detect any specific MPG PCR product as all the peaks melted at temperatures lower than the specific MPG PCR product (90.7 °C), (Figure 27). The agarose gel electrophoresis did not detect any PCR product (Figure 28).

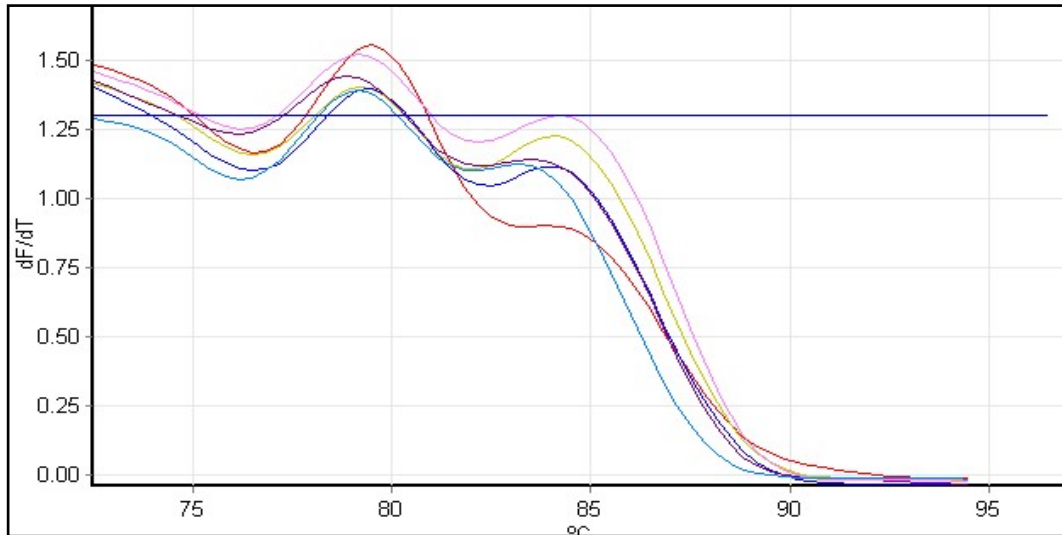


Figure 27 A melt curve analysis for MPG PCR products at 3 h incubation post irradiation. W WS1 cells were irradiated with 16 J/cm^2 on day 1, while MCF 7 cells were not irradiated. Non specific PCR product was formed which melted at $79.2 \text{ }^\circ\text{C}$.



Figure 28 A 2% agarose gel for MPG PCR products 3 h incubation post irradiation. W WS1 cells were irradiated with 16 J/cm^2 on day 1, while MCF 7 cells were not irradiated. RNA was extracted and transcribed by a Fastlane cell cDNA synthesis kit. Equal volume of PCR products ($10 \mu\text{l}$) were loaded into labelled lanes except the DNA marker ($5 \mu\text{l}$). MPG PCR products were not detected in all lanes. Lane 1 and 2 = NRT, lane 3 and 4 = W WS1 cells, lane 5 and 6 = MCF 7 cells, and 7 = DNA marker (580 ng).

The quantitative results for W WS1 cells irradiated with 16 J/cm^2 and incubated for 8 h post irradiation, showed that C_t values for MPG in WS1 and MCF 7 cells were not different to the values of NRT samples; the C_t value for MPG in WS1 cells was less by 2 cycles, while in MCF 7 cells by 0.5 cycles (Appendix E8). The melt curve analysis showed that a non specific product was formed and melted at 81°C (Figure 29). Agarose gel electrophoresis showed that MPG PCR product was not formed (Figure 30). Zhang *et al.*, (2003) detected MPG 8 h post irradiation. It was because of this observation that it was decided to use 8 h incubation post irradiation.

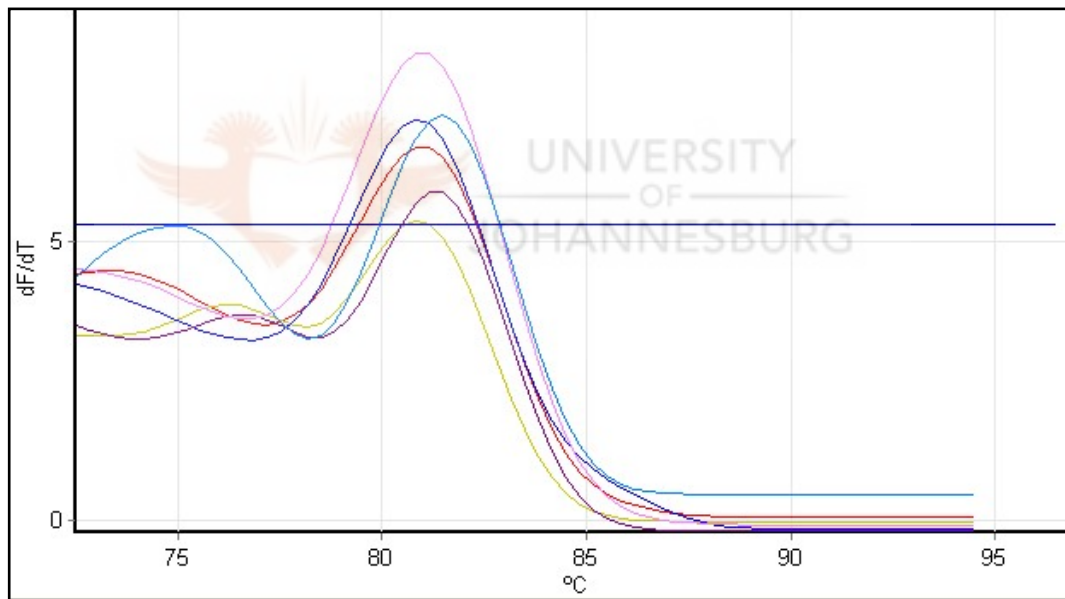


Figure 29 A melt curve analysis for MPG PCR product at 8 h incubation post irradiation. A non specific PCR product was formed. W WS1 cells were irradiated with 16 J/cm^2 on day 1, while MCF 7 cells were not irradiated.

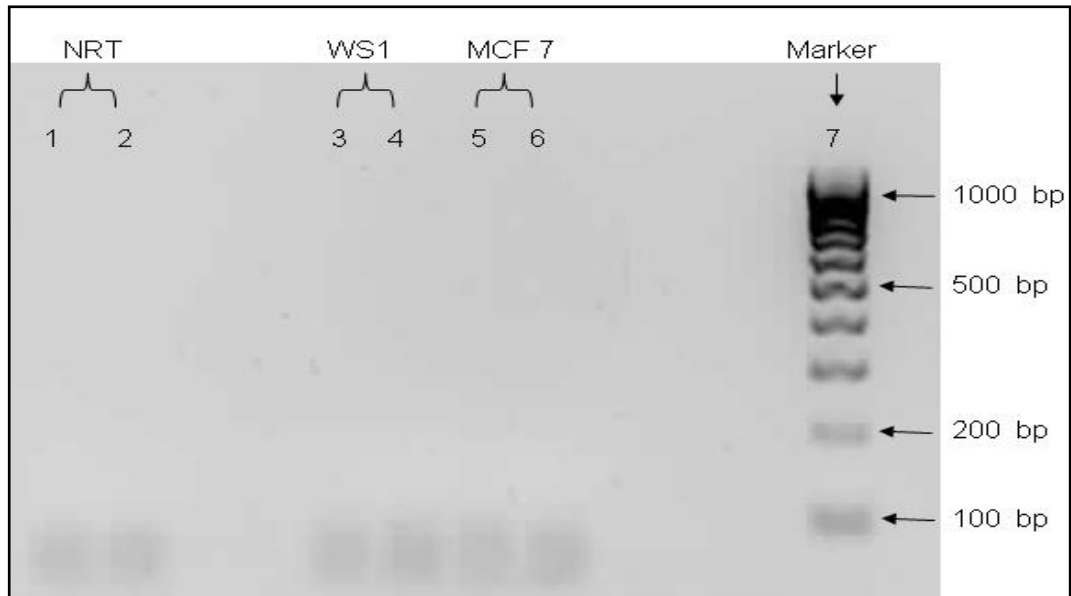


Figure 30 A 2% agarose gel for MPG PCR products 8 h incubation post irradiation. W WS1 cells were irradiated with 16 J/cm^2 on day 1. MCF 7 cells were not irradiated. RNA was extracted and transcribed by a Fastlane cell cDNA synthesis kit. Equal volume of PCR products ($10 \mu\text{l}$) were loaded into labelled lanes except the DNA marker ($5 \mu\text{l}$). MPG PCR products were not detected in all lanes. Lane 1 and 2 = NRT, lane 3 and 4 = W WS1 cells, lane 5 and 6 = MCF 7 cells, and 7 = DNA marker (580 ng).

CHAPTER 5 DISCUSSION AND CONCLUSION

Phototherapy has been proven worldwide to enhance proliferation and migration of biological cells. However, these cellular responses seem to confuse scientists as to whether wound healing is due to cell proliferation or migration or both. Thus, prior to the study to determine the effect of phototherapy on DNA damage and gene activation related to DNA repair in WS1 human skin cells, a mini project was performed to determine whether *in vitro* wound closure was due to migration or proliferation or both (Zungu *et al.*, 2008). Cell proliferation was arrested using hydroxyurea (HU) so that cell migration could be assessed properly. HU is a known antiproliferative drug. The desired effects of HU are known to be dependent on cell type, concentration and stage of the cell cycle at the time of use (Rocha *et al.*, 1984; Schrell *et al.*, 1997). Fibach *et al.*, (1993) observed that high a concentration of HU could ablate cells and this meant that concentration was an important factor when using HU.

W WS1 cells, with or without HU (5 mM) were irradiated with 5 J/cm² using a He-Ne laser on day 1 and 4. Cell morphology, viability and proliferation were assessed 24 h post irradiation on day 4. The study showed that there was a decrease in cell number in HU treated cells, however, there was no apparent cytotoxicity as evidenced by cell morphology and the Trypan blue exclusion test (Zungu *et al.*, 2008). This finding was in agreement with what Hamuro *et al.*, (2002) observed, when 5 mM HU was used to inhibit cell proliferation; it was found that HU arrested cell proliferation in human aortic endothelial cells (HAECs) without detectable cytotoxicity. This suggested that 5 mM HU was able to inhibit proliferation through its cytostatic effect without damaging the viability of W cells. There was also a significant decrease in ATP which could

be attributed to the inhibition of ribonucleotide reductase which is responsible for DNA synthesis. This might have resulted in the depletion of intracellular deoxyadenosine triphosphate (dATP). The decrease in ATP might also have been due to a decrease in cell number as a direct result of the antiproliferative effect of HU and not due to a decrease in cell viability or induction of apoptosis. The decrease in cell number also directly correlated with the results of the XTT assay, which showed a significant decrease in the formazan dye in HU treated cells compared to non treated cells (Zungu *et al.*, 2008).

Skog *et al.*, (1987) observed that HU concentrations of between 3 and 6 mM applied to mouse S49 T-lymphoma and human CEM T-lymphoblastoid cells resulted in cytotoxicity that led to irreparable DNA lesions and chromosomal fragmentation. This finding was different to the observation made in this study and that of Hamuro *et al.*, (2002). Cai *et al.*, (2000) observed that 2 mM of HU completely inhibited proliferation and had limited effect on cell migration. Other authors have found that HU exhibited antiproliferative and cytotoxic effects on HeLa cells in a fluence dependent manner. These authors noted that the response of HeLa cells to HU differed, depending on the growth phase of cells. For instance when non confluent (proliferating) cultures of HeLa cells were treated with 100 ng/ml of HU, a significant antiproliferative effect was observed. However, when confluent (non proliferating) HeLa cells were treated with the same concentration, 20% cell death was observed (Akça and Özeş, 2001).

The above mentioned observations led to the speculation that HU mainly affected DNA synthesis, thereby interfering with the growth of proliferating cells, and that HU has direct cytotoxic effects on non proliferating cells. This

study showed enhanced cell migration and an insignificant increase in cell proliferation. The enhanced cell migration was attributed to laser irradiation which was absent in the study by Cai *et al.*, (2000), and correlates with the findings of Hamuro *et al.*, (2002) in terms of non cytotoxicity, and with Akça and Özeş, (2001) in terms of HU antiproliferative effect in proliferating cells (Zungu *et al.*, 2008).

According to Hayashi *et al.*, (2003), the role of apoptosis in the anticancer activity was not clear. Induction of apoptosis might occur in only some types of cells, such as those of the haematopoietic lineage. Linke *et al.*, (1996) proposed that HU, which was dependent on concentration, through a p53 dependent effect, leads to reversible cell quiescence (arrest above G₁), most probably due to depletion of deoxyribonucleotide triphosphates (dNTPs) and non senescence like irreversible cell arrest. In this study apoptosis could not be ruled out since the Trypan blue exclusion test might not be sensitive enough to detect apoptosis in its early stages. However, other researchers have found that HU causes apoptosis, while others did not at similar concentrations (Cai *et al.*, 2000; Hayashi *et al.*, 2003). At the same time, irradiation is known to down regulate genes involved in apoptosis (Zhang *et al.*, 2003).

Morphologically, HU treated cells appeared normal and were still able to migrate towards the central scratch. There was a decrease in the number of cells in the central scratch, corresponding with a decrease in cell proliferation as determined by the XTT and ATP assay results (Zungu *et al.*, 2008). Thus, HU inhibited cell proliferation. This correlates with the findings of Schrell *et al.*, (1997) that HU has an antiproliferative effect on cells. The few cells across the central scratch of the non irradiated cells could be explained as due to a

lack of stimuli required to stimulate an increase in the rate of cell migration when compared with cells irradiated with 5 J/cm^2 . This was in agreement with findings in the literature, where phototherapy had been shown to stimulate cell proliferation and migration (Hawkins and Abrahamse, 2005; Hopkins *et al.*, 2004; Houreld and Abrahamse, 2007). Proliferation in the treated non irradiated and irradiated cells was limited by HU; the presence of more cells in the central scratch of the treated irradiated cells was due to migration as a result of irradiation at 5 J/cm^2 .

The slight increase in cell viability, as determined by the Trypan blue exclusion test, in irradiated and HU treated and non treated cells was due to the stimulatory effect of using a correct fluence (5 J/cm^2) and λ (632.8 nm). HU at 5 mM was not toxic to cells; cells were able to normalise despite receiving three stressors, namely wounding, irradiation and HU treatment.

The number of cells remained relatively constant, when proliferation was blocked by HU as evidenced by the Trypan blue cell count (Zungu *et al.*, 2008). Treated cells were limited in their response to the injury due to the inhibition of cell proliferation. Thus, the presence of cells in the central scratch could only be attributed to migration, as the effect of cell number or proliferation could be excluded. Few cells had migrated to the central scratch of the non irradiated HU treated cells, while more cells were observed in the central scratch of the irradiated treated cells. Thus, the presence of more cells in the central scratch is due to laser irradiation stimulation on migration.


Thereafter, the main project looked at cell morphology, viability, proliferation and DNA damage as a source of baseline data in the study of gene expression. WS1 cells were irradiated with 5 or 16 J/cm² using a He-Ne laser (λ 632.8 nm) on day 1 and 4; responses were measured 1 or 24 h post irradiation on day 4. Morphologically N cells irradiated with 0, 5 or 16 J/cm² did not show any structural differences at either 1 or 24 h incubation. This was also true for other parameters such as cell viability, proliferation and DNA damage; they did not show any significant differences when compared at 1 or 24 h. This observation is in agreement with Karu *et al.*, (2003) who demonstrated that laser irradiation on non stressed cells does not alter their biological behaviour because the physiological activity of the cells is at the maximum, hence there is nothing to stimulate. On the other hand, irradiation of W cells with 5 J/cm² showed that it was able to stimulate cellular viability, proliferation and migration, and hence complete wound closure was observed. The total number of viable cells increased significantly at both 1 and 24 h compared to the respective controls.

The importance of ATP in a cell cannot be overemphasised because it provides readily available energy to the cells. Cells that lack ATP, depending on severity, result in decreased cellular function. In extreme cases, energy depletion leads to a calcium influx and activation of apoptotic and necrotic processes (Streeter *et al.*, 2004). Coulter (2003) stated that an increase in ATP encourages cell proliferation and since wound healing requires new cells, increased ATP indicates enhanced wound healing. In this study, increased levels of ATP was noted in cells irradiated with 5 J/cm². This might have increased the biological activity of the cells and hence stimulated proliferation and migration of the cells. This could be the explanation why there was complete wound closure in cells irradiated with 5 J/cm². This observation is in agreement with the comet assay results which showed that

irradiation of cells with 5 J/cm^2 did not cause significant damage. Hawkins and Abrahamse (2007a) observed that W cells irradiated with 5 J/cm^2 in the dark using a He-Ne laser at λ of 632.8 nm showed an increase in ATP viability.

Irradiation using a higher fluence of 16 J/cm^2 showed a decrease in cell migration, viability and proliferation. W cells irradiated with 16 J/cm^2 showed incomplete wound closure at both 1 and 24 h. There was also a decrease in percentage viability and ATP in these cells. Furthermore, W cells irradiated with 16 J/cm^2 , showed a higher number of non viable cells than cells irradiated with 5 J/cm^2 . These results concur with those of the comet assay which showed more DNA damage with irradiation using 16 J/cm^2 . This fluence appears to be too high to stimulate the behaviour of cells. Karu (1988) observed that high fluences cause destruction of photoreceptors which is accompanied by growth inhibition and cell lethality. A decrease in ATP production cannot support life for the reason that biological activities depend on ATP which provide energy to the cells. Simunovic (2000) observed that cells' biological activities correlate with the amount of ATP in the cells. This means that when cells have less ATP their biological activities are also reduced as evidenced in W cells non irradiated or irradiated with 16 J/cm^2 . Other researchers have also demonstrated that irradiation with fluences higher than 10 J/cm^2 damages DNA (Hourelid and Abrahamse, 2008). The behaviour of the two fluences used in this study can be explained well using the Arndt-Schultz law which states that small fluences stimulate biological activity while higher fluences inhibit (Sommer *et al.*, 2001). Therefore, it can be deduced that laser irradiation at 5 J/cm^2 definitely promotes wound closure *in vitro*.

Contrary, the failure of non irradiated W cells to close the wound at both 1 and 24 h, could mean that there was possibly nothing more, apart from the wound, to stimulate the biological activity of the cells. However, it was noted that an incubation period of 24 h post irradiation had an effect on these cells. For instance, non irradiated W cells left to incubate for 24 h had more cells in the central scratch compared to cells incubated for 1 h. The difference in the observation could be attributed to cell proliferation and migration as they had more time. For cells that were irradiated with 16 J/cm^2 , the difference would be ascribed to DNA repair. More DNA was repaired at 24 h compared to 1 h and hence more cells were able to multiply (proliferate) and migrate. Thus, the total number of cells was increased at 24 h than at 1 h, supporting what other studies found (Hawkins and Abrahamse, 2007b; Kreisler *et al.*, 2003). If cells were left longer than 24 h, the damage could be completely repaired.



The hypothesis for using Fpg in the modified comet assay and assessment of MPG expression was that the oxidised bases formed by irradiation would be repaired by MPG. Previous studies showed that irradiation of W cells with 16 J/cm^2 caused more DNA damage compared to irradiation with 5 J/cm^2 (Hawkins and Abrahamse, 2006; Houreld and Abrahamse, 2008). With this in mind, it was thought that irradiation of cells with 16 J/cm^2 would cause more DNA damage, and hence up regulate MPG expression. Since the damage in the form of oxidised bases would be excised and repaired by MPG using the BER pathway, Fpg would detect insignificant damage in terms of arbitrary units compared to the conventional comet assay. This view was supported by the comet assay results in this study and has been alluded to below. Though insignificant, the modified comet assay detected more arbitrary units compared to the conventional comet assay.

The modified comet assay showed that it was more sensitive than the conventional comet assay. This was manifested by the higher number of arbitrary units in the former assay than in the later. It can be explained that the modified comet assay detected and cleaved oxidised bases in addition to single strand breaks, which the conventional comet assay detected. Therefore, it could be said that the additional strand breaks could be attributed to irradiation with 16 J/cm^2 , however care must be taken in this interpretation since Fpg is multifunctional; it is not specific to oxidised bases due to irradiation only.

According to literature oxidised bases are caused due to several factors, namely: ROS, laser irradiation and diseases just to mention a few (Dale and Park, 2004). ROS is also known to induce SSBs (Takao and Yasui, 2005). Molecular oxygen is consumed during respiration in mitochondria and thereby converted to ROS as byproducts. It is known that continued irradiation increases production of ROS possibly due to an increase in cellular metabolism and so increases the rate of their scavenging (Lubart *et al.*, 2006). If there is dysfunction, there is increased ROS leakage and hence an increase in oxidative DNA damage. Therefore, it can be postulated that with a higher irradiation fluence of 16 J/cm^2 more oxidised bases would be formed as this would disrupt the normal biochemical functions of cells, while irradiation with 5 J/cm^2 would produce an insignificant number of oxidised bases as this fluence has been proven to be stimulatory and not DNA damaging. This rationale was proved by the comet assay, where more damage was observed in W cells irradiated with 16 J/cm^2 compared to irradiation with 5 J/cm^2 .

Real time RT-PCR has been described as the most sensitive method for measuring low abundance mRNA. It was used in this study to assess the expression of MPG, which is a DNA repair gene. Reference genes were validated in order to select the least regulated gene to be used for normalisation of the gene of interest (MPG). Most researchers have recommended validation of reference genes prior to the study of the gene of interest (Dheda *et al.*, 2004). Most reference genes are affected by the experimental conditions. If they are not validated, false regulation of the gene of interest may be observed since the variable expression might be that of the reference gene and not the gene of interest (Dheda *et al.*, 2004). The issue of reference genes need not be generalised because experimental models are different and should be looked at as per individual experiment.

This study found that ACTB was the least regulated gene and that its expression levels were consistent. It produced an acceptable PCR efficiency of 94% and R^2 of 0.999. However, GAPDH primers produced a low PCR efficiency (82%), while UBC produced a low R^2 (0.898). Wang *et al.*, (2006) recommends an R^2 of more than 0.995 and a PCR efficiency of between 90 and 100%. If the R^2 value is low, the given standards do not easily fit into a line of best fit and thus, if used, the results obtained may not be reliable. PCR efficiency threshold is used to exclude samples with noise from the analysis. Wang *et al.*, (2006) observed that ACTB, as a reference gene, was highly regulated. Similarly, Wilson *et al.*, (2003) demonstrated that it was regulated by 2.5 fold with Argon laser irradiation, possibly because an ablative laser was used, whereas this study used a He-Ne laser which is non photothermic.

After observing that MPG expression could not be detected when W cells were irradiated with 5 J/cm^2 , it was decided to irradiate W cells with 16 J/cm^2 and alter incubation periods to 0, 3, or 8 h. A breast cancer cell line, MCF 7, was included as a positive control. Cerda *et al.*, (1998) found that MPG protein was increased approximately 3 to 6 fold in these cells as compared to normal cells. Zhang *et al.*, (2003) detected MPG when cells were left to incubate for 8 h post irradiation. Holt *et al.*, (2000) observed that most DNA inducible proteins increase between 2 and 8 h after exposure to damage. Thus, MPG expression was explored at the different incubation periods so as to increase chances of its detection. However, its expression was not detected. The C_t values of MPG in W and MCF 7 cells were similar to the negative control values. This meant that MPG was not present for amplification during the PCR. There should be a difference of 5 C_t values between a negative and positive expression. The absence of MPG expression was confirmed by the 2% agarose gel electrophoresis, which also did not detect the MPG PCR product.

The comet assay showed that W cells irradiated with 16 J/cm^2 had more DNA damage compared to W cells irradiated with 5 J/cm^2 and non irradiated cells. However, the degree of damage became less when cells were left to incubate for 24 h post irradiation. It is apparent that DNA repair took place. MPG, which is one of the main DNA glycosylases involved in BER of the altered or abnormal bases, was not detected in WS1 or MCF 7 cells. Possibly the altered bases produced may not have been specific for MPG, and hence an alternative repair mechanism was induced and repaired the damage. In this case, it might be that MPG was not induced and hence the failure to be detected. Other studies established that when glycosylase genes were disrupted they showed either mild or no effect in mice (Engelward *et al.*, 1997). However, it was observed in these studies that

DNA repair took place suggesting that cells frontline defences have back up systems. It has also been observed that a number of DNA glycosylases have overlapping substrate specificity (Takao and Yasui, 2005). So, it appears that an unexpected number of DNA glycosylases may participate in the maintenance of the genome integrity from oxidative DNA lesions in mammalian cells. All these arguments augment the idea that DNA damage which was observed in W cells irradiated with 16 J/cm^2 , was repaired by alternative pathways apart from MPG since it was not expressed.

Reports indicate that on the basis of substrate specificity, there are two classes of DNA glycosylase in mammals namely; uracil DNA glycosylase (UDG) and MPG. UDG exclusively acts on uracil in DNA (Krokan *et al.*, 1997), while MPG excises oxidised purines. It might be that the altered bases were of the uracil type, and hence UDG might have repaired the damage. Secondly, the DNA damage might have been repaired by the human Nth homologue (NTH) protein which is known to excise oxidised bases. Surprisingly, this protein is localised in the same chromosomal region as MPG. Human oxoguanine DNA glycosylase 1 (hOGG1) has also been implicated in the repair of the most mutagenic lesion, 8-oxoG of which MPG also repairs. However, according to literature, MPG is inferior to hOGG1 in the excision of this lesion.

It has been recently discovered that MPG is a low copy gene and is poorly expressed in cells *in vitro* (Adhikari *et al.*, 2008). It appears that the low copy number of MPG creates a healthy balance between base excision and repair. MPG overexpression has been shown to increase the normally slow rate excision of 7 methylguanine, leading to the accumulation of the toxic repair intermediates (Rinne *et al.*, 2005). Due to this, its expression is highly

controlled. Most studies have also demonstrated that MPG expression is cell cycle dependent and is known to increase by 2.5 to 3.5 fold in synchronised cells. It increases during the G₁ phase and decreases after mitosis. In studies where it was detected, cells were cultured in serum free medium for 14 days to ensure that cells were synchronised in gap 0 (G₀). After 14 days at 0 h, approximately 95% of the cells were in the G₀ phase. Expression of MPG mRNA increased 10 to 20 h after the addition of serum (Bouziane *et al.*, 2000).

FBS provides serum response factors to cells and thus, contributes to mitogen stimulated transcriptional induction of many immediate early genes during the G₀ to G₁ cell cycle transition and is also essential for cell cycle progression (Schratt *et al.*, 2001). Thus, the absence of serum in the medium slows down proliferation and cell cycle progression. Lau and Nathans (1985) speculated that time of accumulation of particular mRNA appeared to be an ordered expression of genes that comprised a genetic program for growth, so a disruption to a single gene might affect others. Even though Zhang *et al.*, (2003) observed an increase in cell proliferation when 5% FBS was used during cell cultures, it is possible that cell cycle progression was slowed and hence many cells were maintained in the G₁ phase. This could be the possible reason they detected MPG expression.

In contrast, in this study 10% FBS was supplemented to the media so cells might have been actively proliferating and progressing to the next cell cycle, which according to literature, slows down MPG expression after mitosis. It would, therefore, be possible that during the assessment of MPG expression, most cells had just passed through mitosis in which case MPG expression was low. The proportion of W WS1 or MCF 7 cells in the G₁

phase at the various time intervals might have been so few that MPG was undetectable. The other intriguing observation is that magnesium ions are said to inhibit MPG activity by abrogating its substrate binding and decreases the active enzyme concentration (Adhikari *et al.*, 2008). MEM, the media which was used in this study, contained Magnesium sulphate (200 mg/L) at a higher concentration than the other media (Dulbecco's Modified Eagle Medium [D-MEM] and Roswell Park Memorial Institute medium 1460 [RPMI]) which was used by the others authors who detected its expression. It might be possible that the high concentration of magnesium ions in the media down regulated MPG expression.

It was also noted that Zhang *et al.*, (2003) used a fluence of 0.88 J/cm^2 at λ of 628 nm to detect MPG expression through microarray. The fluence and wavelength used might have been ideal to induce MPG expression. On the other hand, 5 or 16 J/cm^2 , which was used in this study, might have been too much and therefore damaged the sensor protein for MPG expression. It might be that MPG does not need a high fluence to be induced. In summary, the effects of irradiation on cells are mediated by many factors such as fluence, duration of exposure, cell culture conditions, and wavelength. These parameters can greatly vary results. For instance, Zhang *et al.*, (2003) used a very short duration of exposure every day for 3 days. The effect this kind of irradiation might have on cells would possibly be different to cells irradiated once or after 3 days with a higher fluence.

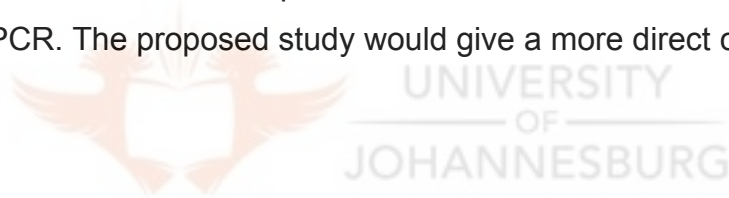
Most studies both *in vivo* and *in vitro*, in which MPG expression has been investigated, have used Southern blot, Western blot or Northern blot. If any, very few studies have used real time RT-PCR to study MPG expression. It is difficult to exactly compare with what other studies have found because

gene expression and protein expression are relatively different. DNA repair genes are induced at specific times and do not remain elevated for long periods. Therefore, to detect their expression timing must be correct and accurate. Furthermore, more cells and hence more protein is used in Western blots, whereas only 5×10^3 cells were used in this study (according to manufacturer's recommendations).

Few reports are available with regards to the use of He-Ne laser irradiation in the study of MPG expression. Many *in vivo* studies have induced MPG expression by the use of alkylating chemicals as DNA damaging agents (Holt *et al.*, 2000). Laser irradiation has been shown to be beneficial in many areas. Therefore, in this study, it is possible that irradiation switched off MPG expression since its molecular biomodulation is not well known. These observations might help to explain why MPG was not detected in W cells grown for 4 days and analysed at 1 or 24 h or grown for 1 day and analysed at 0, 1, 3 or 8 h.

In conclusion, this project has demonstrated that irradiation of W cells with 5 J/cm^2 increases ATP, cell proliferation and migration which was evidenced by cell morphology for both the mini and main project. Irradiation of cells with higher fluences such as 16 J/cm^2 is damaging to DNA and inhibitory to cell proliferation and migration. MPG expression was not detected possibly due to differences in cell culture conditions, fluence and duration of exposures.

Therefore, this project would like to propose further investigations on DNA repair genes like human NTH and other genes, which are not cell cycle dependent to suit the project design of growing cells. For instance, it would be necessary to look at DNA repair genes, which encode proteins for both glycosylases and AP lyases because these have both activities to remove the substrate bases and incise the phosphodiester backbone. This would be more sensitive in inducing the DNA repair gene as it would be affected by both activities and hence would be up regulated. Smith *et al.*, (2006) demonstrated that hOGG1 was more specific to excise oxidised bases than Fpg. Fpg recognises oxidised bases including alkylation damage. It would be important in the follow up study to the current one to use hOGG1 in the modified comet assay to assess the type of DNA damage caused by irradiation. Thereafter, the expression of hOGG1 can be assessed with real time RT-PCR. The proposed study would give a more direct comparison.



REFERENCES

Abrahamse, H., Hawkins, D. and Houreld, N. (2006) Effect of wavelength and fluence on morphology, cellular and genetic integrity of diabetic wounded human skin fibroblasts. In: Hamblin, M.R., Waynant, R.W. and Anders, J. (eds), *Proceedings of SPIE*, **6140**: 140060-73

Adhikari, S., Manthena, P.V., Üren, A. and Roy, R. (2008) Expression, purification and characterisation of codon optimised human *N*-methylpurine DNA glycosylase from *Escherichia coli*, *Protein expression and purification*, **58**(2): 257-262

Akça, H. and Özeş, O.N. (2001) Hydroxyurea induces p53 accumulation and apoptosis in human carcinoma cells, *Turk J Biol*, **26**: 145-150

Allendorf, J.D., Bessler, M., Huang, J., Kayton, M.L., Laird, D., Nowygrod, R. and Treat, M.R. (1997) Helium Neon laser irradiation at fluences of 1, 2 and 4 J/cm² failed to accelerate wound healing as assessed by both wound contracture rate and tensile strength, *Lasers in Surgery and Medicine*, **20**(3): 340-345

Andreoli, C., Leopardi, P., Rossi, S. and Crebelli, R. (1999) Processing of DNA damage induced by hydrogen peroxide and methyl methanesulfonate in human lymphocytes: Analysis by alkaline single cell gel electrophoresis and cytogenetic methods, *Mutagenesis*, **14**(2): 497-503

Atabey, A., Karademir, S., Atabey, N. and Barutçu, A. (1995) The effects of the Helium Neon laser on wound healing in rabbits and on human skin fibroblasts *in vitro*, *European Journal of Plastic Surgery*, **18**: 99-102

Azevedo, L.H., Eduardo, F.P., Moreira, M.S., Eduardo, C.P. and Marques, M.M. (2006) A pilot study: Influence of different power densities of LILT on cultured human fibroblast growth, *Lasers in Medical Science*, **21**: 86-89

Basford, J.R. (1989) Low energy laser therapy: Controversies and new research findings, *Lasers in Surgery and Medicine*, **9**: 1-5

Berdal, K.G., Johansen, R.F. and Seeberg, E. (1998) Release of normal bases from intact DNA by a native DNA repair enzyme, *Embo Journal*, **17**(2): 363-367

Blainey, P.C., Oijen, A.M., Barnejee, A., Verdine, G.L. and Xie, X.S. (2006) A base excision DNA repair protein finds intrahelical lesion bases by fast sliding in contact with DNA, *PNAS*, **103**(15): 5752-5757

Bouziane, M., Miao, F., Bates, S.E., Somsouk, L., Sang, B.C., Denissenko, M. and O'Connor, T.R. (2000) Promoter structure and cell cycle dependent expression of the human methylpurine DNA glycosylase gene, *Mutation Research*, **461**(1): 15-29

Buschini, A., Giordan, F., de Albuquerque, C.N., Pellacani, C., Pelosi, G., Rossi, C., Araújo, T.M., Zucchi, D. and Poli, P. (2007) Trypanocidal nitroimidazole derivatives: Relationships among chemical structure and genotoxic activity, *Biochemical Pharmacology*, **73**: 1537-1547

Cai, G., Lian, J., Shapiro, S.S. and Beacham, D.A. (2000) Evaluation of endothelial cells migration with a novel in vitro assay system, *Methods Cell Sci*, **22**: 107-114

Calvin, M. (1998) Cutaneous wound repair, *Wounds*, **10**(1): 12-32

Carnevali, C.M., Soares, C.P., Zangaro, R.A., Pinheiro, A.L. and Silva, A.S. (2003) Laser light prevents apoptosis in CHO K-1 cell line, *Clinical Laser Medicine and Surgery*, **21**(4): 193-196

Carroll, L. and Humphreys, T.R. (2006) Laser-tissue interactions, *Clinic in Dermatology*, **24**: 2-7

Causton, H.C., Quackenbush, J. and Brazma, A. (2003) *A beginner's Guide: Microarray/Gene expression data analysis*. Blackwell Publishing, United Kingdom, pp. 1, 2, 4

Cerda, S.R., Turk, P.W., Thor, A.D. and Weitzman, S.A. (1998) Altered expression of the DNA repair protein, N-methylpurine DNA glycosylase (MPG), in breast cancer, *FEBS letters*, **431**: 12-18

Clark, R.A.F. (1996) Wound Repair. Overview and general considerations. In: Clark, R.A.F. (ed) *The molecular and cellular biology of wound repair*. 2nd edition. Plenum Publishing Corporation, New York, USA, pp. 4

Collins, A.R., Duthie, S.J. and Dobson, V.L. (1993) Accelerated paper: Direct enzymatic detection of endogenous oxidative base damage in human lymphocyte DNA, *Carcinogenesis*, **14**(9): 1733-1735

Collins, A.R., Dušinská, M., Gedik, C.M. and Štětina, R. (1996) Oxidative damage to DNA: Do we have a reliable biomarker? *Environmental Health Perspectives*, **104**(3): 465-469

Collins, A.R. (2000) Measurement of oxidative DNA damage using the comet assay. In: Lunec, J. and Griffiths, H.R. (eds) *A practical approach: Measuring in vivo oxidative DNA damage*. John Wiley and Sons Ltd, England, pp. 83-94

Collins, A.R., Dušinská, M. and Horská, A. (2001) Detection of alkylation damage in human lymphocyte DNA with the comet assay, *Acta Biochimica Polonica*, **48**(3): 611-614

Conlan, M.J., Rapley, J.W. and Cobb, C.M. (1996) Biostimulation of wound healing by low energy laser irradiation, *Journal of Clinical Periodontal*, **23**: 492-496

Coulter, A.H. (2003) Let there be light and healing, *Alternative and Complimentary Therapies*, **9**(6): 322-326

Croteau, D.L. and Bohr, V.A. (1997) Minireview: Repair of oxidative damage to nuclear and mitochondria DNA in mammalian cells, *The Journal of Biological Chemistry*, **272**(41): 25409-25412

Csele, M. (2004) Lasing Processes. *Fundamentals of light sources and lasers*. 1st edition, John Wiley and Sons, USA, pp. 84-85

Dale, J.W. and Park, S.F. (2004) Mutation and variation. *Molecular genetics of bacteria*. 4th edition, John Wiley and Sons, England, pp. 54-55

Damante, C.A., Greggi, S.L.A., Sant'ana, A.C.P. and Passanezi, E. (2004) Clinical evaluation of low intensity laser (GAALAS) on wound healing after gingivoplasty in humans, *Journal of Applied Oral Science*, **12**(2): 133-136

de Bont, R. and Larebeke, N. (2004) A review of quantitative data: Endogenous DNA damage in humans, *Mutagenesis*, **19**(30): 169-185

de Mey, M., Lequeux, G., Maertens, J., de Maeseneire, S., Soetaert, W. and Vandamme, E. (2006) Comparison of DNA and RNA quantification methods suitable for parameter estimation in metabolic modeling of microorganisms, *Analytical Chemistry*, **383**(2): 198-203

Demir, H., Yaray, S., Kirnap, M. and Yaray, K. (2004) Comparison of the effects of laser and ultrasound treatments on experimental wound healing in rats, *Journal of Rehabilitation Research and Development*, **41**(5): 721-728

Diegelmann, R.F. and Evans, M.C. (2004) An overview of acute, fibrotic and delayed healing: Wound healing, *Frontiers in Biosciences*, **9**: 283-289

Dušinská, M. and Collins, A. (1996) Detection of oxidised purines and UV-induced photoproducts in DNA of single cells by inclusion of lesion specific enzymes in the comet assay, *Alternatives to Laboratory Animals*, **24**(3): 405-411

Dyson, M. (1991) Cellular and sub-cellular aspects of low level laser therapy (LLLT). *Progress in Laser therapy. Selected papers from October 1990 ILTA Congress*. Wiley and Sons Inc, New York and Brisbane, pp. 221-222

Engelward, B.P., Weeda, G., Wyatt, M.D., Broekhof, J.L.M., de Wit, J., Donker, I., Allan, J.M., Gold, B., Hoeijmakers, J.H.J. and Samson, L.D. (1997) Base excision repair deficient mice lacking the Aag alkyladenine DNA glycosylase, *Proc. Natl. Acad. Sci. USA* **94** 1308-13092

Ennis, W.J., Lee, C., and Meneses, P. (2007) A biochemical approach to wound healing through the use of modalities, *Clinics in Dermatology*, **25**(1): 63-72

Enwemeka, C.S. (2004) Therapeutic light, *Interdisciplinary Journal of Rehabilitation*, **January/February**: 1-10

Fan, J. and Wilson, D.M. (2005) Protein-protein interactions and posttranslational modifications in mammalian base excision repair, *Free Radical Biology and Medicine*, **38**(9): 1121-1138

Fibach, E., Burke, L.P., Schechter, A.N., Noguchi, C.T. and Rodger, G.P. (1993) Hydroxyurea increases foetal haemoglobin in cultured erythroid cells derived from normal individuals and patients with sickle cell anaemia or β -thalassemia, *Blood*, **81**: 1630-1635

Fishel, M.L., Seo, Y.R., Smith, M.L. and Kelly, M.R. (2003) Imbalancing the DNA base excision repair pathway in the mitochondria; targeting and overexpressing *N*-methylpurine DNA glycosylase in mitochondria leads to enhanced cell killing, *Cancer Research*, **63**: 603-615

Flemming, K. and Cullum, N. (2000) Laser therapy for venous leg ulcers, *Cochrane Database of Systemic Reviews*, **2**: CD0011182

Friedberg, E.C., Walker, G.C. and Siede, W. (1995) Editorial: Out of the shadows and into the light. The emergency of DNA repair, *Trends in Biochemical Science*, **20**(10): 381

Friedberg, E.C. (2003) DNA damage and repair, *Nature*, **421**(6921): 436-440

Gao, Q., Wang, X.Y., Fan, J., Qiu, S.J., Zhou, J., Shi, Y.H., Xiao, Y.S., Xu, Y., Huang, X.W. and Sun, J. (2008) Selection of reference genes for real time PCR in human hepatocellular carcinoma tissues, *J Cancer Res Clin Oncol*, **DOI**: 10.1007/s00432-008-0369-3

Gál, P., Vindinský, B., Toporcer, T., Mokrý, M., Mozeš, Š., Longauer, F. and Sabo, J. (2006) Histological assessment of the effect of irradiation on skin wound healing in rats, *Photomedicine and Laser Surgery*, **24**(4): 480-488

Goode, E.L., Ulrich, C.M. and Potter, J.D. (2002) Polymorphism in DNA repair genes and associations with cancer risk, *Cancer Epidemiology, Biomarkers and Prevention*, **11**(12): 1513-1530

Gregory, R. (1998) Laser physics and physiology, *Clinics in Plastic Surgery*, **25**(1): 89-93

Greulich, K.O. (2003) Low level laser therapy (LLLT) – Does it damage DNA? *Clinixperience*, **63**: 1-2

Hall, G., Anneroth, G., Schennings, T., Zetterqvist, L. and Ryden, H. (1994) Effect of low level laser irradiation on wound healing: An experimental study in rats, *Sweden Dental Journal*, **18**(1-2): 29-34

Hamuro, M., Polan, J., Natarajan, M. and Mohan, S. (2002) High glucose induced nuclear factor kappa B mediated inhibition of endothelial cell migration, *Atherosclerosis*, **16**(2): 277-287

Hartley, A. (2004) New York Manhattan Physical Therapy, *Advanced Online Editions for Directors in Rehabilitation*, **13**(1): 43

Hayashi, M., Hamasu, T., Endoh, D., Shimojima, R. and Okui, T. (2003) Inhibition of replication induces non apoptotic cell death in fibroblast cell lines derived from LEC rats, *J Vet Med Sci*, **65**: 249-254

Hawkins, D. and Abrahamse, H. (2005) Biological effects of Helium Neon laser irradiation on normal and wounded fibroblasts, *Photomedicine and Laser Surgery*, **23**(3): 251-259

Hawkins, D. and Abrahamse, H. (2006) Effect of multiple exposures of low level laser therapy on the cellular responses of wounded human skin fibroblasts, *Photomedicine and Laser Surgery*, **24**(6): 705-714

Hawkins, D. and Abrahamse, H. (2007a) Changes in cell viability of wounded fibroblasts following laser irradiation in broad spectrum or infrared light, *Laser Chemistry*, DOI: 10.1155/2007/71039

Hawkins, D. and Abrahamse, H. (2007b) How long after laser application should cellular responses be measured to determine the laser effect? *Journal of Laser Applications*, **19**(2): 74-83

Holt, S., Roy, G., Mitra, S., Upton, P.B., Bogdanffy, M.S. and Swenberg, J.A. (2000) Deficiency of N methylpurine DNA glycosylase expression in nonparenchymal cells, the target cell for vinyl chloride and vinyl fluoride, *Mutation Research*, **460**: 105-115

Hopkins, J.T., McLoda, T.A., Seegmiller, J.G. and Baxter, G.D. (2004) A triple blind, sham controlled study: Low level laser therapy facilitates superficial wound healing in humans, *J Athl Train*, **39**: 223-229

Hosseini, S.M., Herd, S., Vincent, A.L. and Héon, E. (2008) Genetic analysis of chromosome 20-related posterior polymorphous corneal dystrophy: Genetic heterogeneity and exclusion of three candidate genes, *Molecular Vision*, **14**: 71-80

Hourel, N.N. and Abrahamse, H. (2007) *In vitro* exposure of wounded diabetic fibroblast cells to a Helium Neon laser at 5 J/cm² and 16 J/cm², *Photomed Laser Surgery*, **25**: 78-84

Hourel, N.N. and Abrahamse, H. (2008) Laser light influences cellular viability and proliferation in diabetic wounded fibroblast cells in a dose and wavelength dependent manner, *Lasers in Medical Science*, **23**(1): 11-18

Itoh, T. and Linn, S. (2005) The fate of p21^{CDKN1A} in cells surviving UV-irradiation, *DNA Repair*, **4**: 1457-1462

Iyer, V.R., Eisen, M.B., Ross, D.T., Schuler, G., Moore, T., Lee, J.C.F., Trent, J.M., Staudt, L.M., Hudson Jr., J., Boguski, M.S., Lashkari, D., Shalon, D., Botstein, D. and Brown, P.O. (1999) The transcriptional program in the response of human fibroblasts to serum, *Science*, **283**: 83-87

Kai, C.K.Y. (2002) History of phototherapy and photochemotherapy: Bulletin for Medical Practitioners, *National Skin Centre*, **13**(2): 1-3

Karu, T. (1988) Molecular mechanism of the therapeutic effects of low intensity laser irradiation, *Lasers in Life Sciences*, **2**(1): 53-74

Karu, T. (1990) Yearly review: Effects of visible radiation on cultured cells, *Photochemistry and Photobiology*, **52**(6): 1089-1098

Karu, T. (2003) Low power laser therapy. *Biomedical Photonic Handbook*, Chapter 48, CRC Press LLC, Russia, pp. 1-25

King, P.R. (1989) A review: Low level laser therapy, *Lasers in Medical Science*, **4**: 141-150

Kopera, D., Kokoi, R., Berger, C. and Haas, J. (2005) Does the use of low level laser influence wound healing in chronic venous leg ulcers? *Journal of Wound Care*, **14**(8): 391-394

Koutin, M., Janisch, R. and Veselsk, R. (2003) Effect of low power laser irradiation on cell proliferation, *Scripta Medica (BRNO)*, **76**(3): 163-172

Kreisler, M., Christoffers, A.B., Willershausen, B. and d'Hoodt, B. (2003) An *in vitro* study: Effects of low level GaAlAs laser irradiation on the proliferation rate of human periodontal ligament fibroblast, *Journal of Clinical Periodontal*, **30**(4): 353-358

Krokan, H.E., Standal, R. and Slupphaug, G. (1997) Review article: DNA glycosylases in the base excision of DNA, *Biochem J*, **325**: 1-16

Kujawa, J., Zavodnik, B., Lapshina, A., Labieniec, M. and Bryszewska, M. (2004) Cell survival, DNA, and protein damage in B14 cells under low intensity near infrared (810 nm) laser irradiation, *Photomedicine Laser Surgery*, **22**(6): 504-508

Lau, L.F. and Nathan, D. (1985) Identification of a set of genes expressed during the G₀/G₁ transition of cultured mouse cells, *Embo Journal*, **4**(12): 3145-3151

Lazarus, G.S., Cooper, D.M., Knighton, D.R., Margolis, D.J., Pecoraro, R.E., Rodeheaver, G. and Robson, M.C. (1994) Definitions and guidelines for assessment of wounds and evaluation of healing, *Archives of Dermatology*, **130**(4): 489-493

Lewis, E., Rogachev, B., Shaked, G. and Douvdevani, A. (2001) The *in vitro* effects of ketamine at large concentrations can be attributed to a non specific cytostatic effect, *Anesthesia and Analgesia*, **92**: 927-929

Lindahl, T. and Wood, R.D. (1999) A review of quality control by DNA repair: Frontiers in Cell Biology, *Science*, **286**: 1897-1905

Linke, S.P., Clarkin, K.C., di Leonard, A., Tsou, A. and Wahl, G.M. (1996) A reversible, p53 dependent G₀/G₁ cell cycle arrest induced by ribonucleotide depletion in the absence of detectable DNA damage, *Gene Dev*, **10**: 934-947

Livneh, Z. (2001) Minireview: DNA damage control by novel DNA polymerases. Translesion replication and mutagenesis, *Journal of Biological Chemistry*, **276**(28): 25639-25642

Lubart, R., Lavi, R., Friedman, H. and Rochkind, H. (2006) Photochemistry and photobiology of light absorption by living cells, *Photomedicine and Laser Surgery*, **24**(2): 179-185

Maher, R.L., Vallur, A.C., Feller, J.A. and Bloom, L.B. (2007) Slow base excision by human alkyl adenine DNA glycosylase limits the rate of formation of AP sites and AP endonuclease 1 does not stimulate base excision, *DNA Repair*, **6**: 71-81

Martin, A.M., Kulski, J.K., Witt, C., Pontarotti, P. and Christiansen, F.T. (2002) Review: Leukocyte Ig-like receptor complex (LRC) in mice and men, *Trends in Immunology*, **23**(2): 81-88

Matic, M., Lazetic, B., Poljacki, M., Duran, V. and Ivkov-Simic, M. (2003) Low level laser irradiation and its effect on repair processes in the skin, *Med Pregl*, **56**: 137-141

Mbene, A.B., Zungu, I.L., Hawkins, D.H., Houreld, N.N. and Abrahamse, H. (2006) Adaptive response after 632.8 nm laser irradiation decreases cellular damage in diabetic wounded fibroblast cells, *Medical Technology South Africa*, **20**(1): 21-24

Mester, E., Spiry, T., Szende, B. and Tota, J.G. (1971) Effects of laser rays on wound healing, *The American Journal of Surgery*, **122**: 532-535

Mester, E., Mester, A.F. and Mester, A. (1985) The biomedical effects of laser application, *Lasers in Surgery and Medicine*, **5**(1): 31-39

Mester, A.F., Snow, J.B. and Shaman, P. (1991) Photochemical effects of laser irradiation on neuritic outgrowth of olfactory neuroepithelial explants, *Otolaryngol Head Neck Surg*, **105**: 449-456

Møller, P., Knudsen, L.E., Loft, S. and Wallin, H. (2000) Review: The comet assay as a rapid test in biomonitoring occupational exposure to DNA damaging agents and effect of confounding factors, *Cancer Epidemiology, Biomarkers and Prevention*, **9**: 1005-1015

Olsen, A.K., Bjørtarf, H., Wiger, R., Holme, J.A., Seeberg, E.C., Bjorås, M. and Brunborg, G. (2001) Highly efficient base excision repair (BER) in human and rat male germ cells, *Nucleic Acids Research*, **29**(8): 1781-1790

Papillion, P., Valiulis, J., Cunningham, M., Simolke, E., Veillon, D., Mukherjee, D. and Ogden, A. (2004) Health management publications, *Wounds*, **16**(12): 355-358

Peng, S.L. (2004) Short analytical review: Transcriptional factors in the pathogenesis of autoimmunity, *Clinical Immunology*, **110**: 112-123

Pfaffl, M.W., Horgan, G.W. and Dempfle, L. (2002) Relative expression software tool (REST©) for group-wise comparison and statistical analysis of relative expression results in real time PCR, *Nucleic Acids Research*, **30**(9): 1-10

Pullar, C.E., Grahn, J.C., Liu, W. and Isseroff, R.R. (2006) β 2-Adrenergic receptor activation delays wound healing, *The FASEB Journal*, **20**: 76-86

Ridder, L., Verbeke, M. and Thierens, H. (1988) Biological effects of low intensity Helium Neon and Gallium-Arsenide laser irradiation on embryonic chick heart fragments *in vitro*, *Lasers in Medical Science*, **4**: 97-102

Rigau, J., Sun, C.H., Trelles, M.A. and Berns, M.W. (1995) Effects of 633 nm laser on the behaviour and morphology of primary fibroblast culture. In: Karu, T. and Young, A. (eds) *Effects of low power light on biological systems. Progress in Biomedical Optics Barcelona, Spain*, pp. 32-42

Rinne, M.L., He, Y., Pachkowski, B.F., Nakamura, J. and Kelly, M.R. (2005) *N*-methylpurine DNA glycosylase overexpression increases alkylation sensitivity by rapidly removing non toxic 7 methylguanine adducts, *Nucleic Acids Research*, **33**(9): 2859-2867

Rinnie, M., Caldwell, D. and Kelley, M.R. (2004) Transient Adenoviral N-methylpurine DNA glycosylase overexpression imparts chemotherapeutic sensitivity to human breast cancer cells, *Molecular Cancer Therapeutics*, **3**(8): 955-967

Riss, T., Moravec, R., Beck, M., Hannah, R., Wilson, K. and Swanson, R. (2002) A viable solution for cytotoxic screening; "CellTiter-Glo™ luminescent cell viability assay: Fast, sensitive and flexible", *Promega Notes*, **81**: 2-5

Rocha, B., Larsson, E.L. and Freitas, A.A. (1994) Effect of hydroxyurea on concanavalin-A-induced T-cell proliferation: Depletion of T-cell growth factor reactive and producing T lymphocytes, *Scand J Immunol*, **19**: 315-321

Ronen, A. and Glickman, B.W. (2001) Human DNA repair genes, *Environmental and Molecular Mutagenesis*, **37**(3): 241-283

Roy, G., Roy, R. and Mitra, S. (1997) Quantitative reverse transcriptase polymerase chain reaction for measuring the N-methylpurine DNA glycosylase mRNA level in rodent cells, *Analytical Biochemistry*, **246**: 45-51

Ruttan, C.C. and Glickman, B.W. (2002) Coding variants in human double strand break DNA repair genes, *Mutation Research*, **509**(1-2): 175-200

Samson, L., Derfler, B., Boosalis, M. and Call, K. (1991) Genetics: Cloning and characterisation of a 3-methyladenine DNA glycosylase cDNA from human cells whose gene maps to chromosome 16, *Proc. Natl. Acad. Sci. USA*, **88**: 9127-9131

Sancar, A., Lindsey-Boltz, L.A., Ünsal-Kaçmaz, K. and Linn, S. (2004) Molecular mechanisms of mammalian DNA repair and the DNA damage check points, *Annual Review Biochemistry*, **73**: 39-85

Sarkar, R., Meinberg, E.G., Stanley, J.C., Gordon, D. and Webb, C.R. (1996) Nitric oxide reversibly inhibits the migration of cultured vascular smooth muscle cells, *Circulation Research*, **78**: 225-230

Saygun, I., Karacay, S., Serdar, M., Ural, A.U., Sencimen, M. and Kurtis, B. (2008) Effects of laser irradiation on the release of basic fibroblast growth factor (bFGF), insulin like growth factor 1 (IGF-1), and receptor of IGF-1 (IGFBP3) from gingival fibroblasts, *Lasers in Medical Science*, **23**(2): 211-215

Schindl, A., Schindl, M., Pernerstorfer-Schön, H. and Schindl, L. (2000) A review: Low intensity laser therapy, *Journal of Investigative Medicine*, **48**(5): 312-26

Schratt, G., Weinhold, B., Lundberg, A.S., Schuck, S., Berger, J., Schwarz, H., Weinberg, R.A., Rüther, U. and Nordheim, A. (2001) Serum response factor is required for immediate early gene activation yet is dispensable for proliferation of embryonic stem cells, *Molecular and Cellular Biology*, **21**(8): 2933-2943

Schrell, U.M.H., Ritting, M.G., Anders, M., Kiesewetter, F., Marschalek, R., Koch, U.H. and Fahlbusch, R. (1997) Hydroxyurea for treatment of unresectable and recurrent meningiomas. Inhibition of primary human meningioma cells in culture and in meningioma transplants by induction of the apoptotic pathway, *J Neurosurg*, **86**: 845-852

Seeberg, E., Eide, L. and Bjorås, M. (1995) The base excision repair pathway, *Trends Biochemistry Science*, **20**: 391-397

Senese, S., Zaragoza, K., Minardi, S., Muradore, I., Ronzoni, S., Passafaro, A., Bernard, L., Draetta, G.F., Alcaly, M., Seisar, C. and Chiocca, S. (2007) Role of Histone deacetylase 1 in human tumour cell proliferation, *Molecular and Cellular Biology*, **27**(13): 4784-4795

Sidorenko, V.S., Nevinsky, G.A. and Zharkov, D.O. (2008) Specificity of stimulation of human 8 oxoguanine DNA glycosylase by AP endonuclease, *Biochemical and Biophysical Research Communications*, **368**: 175-179

Siegman, A.E. (1986) An introduction to lasers. In: Clark, J. (ed) *Lasers* publisher USA, pp. 62

Simunovic, Z. (2000) Lasers in Medicine and Dentistry Basic Science and Up-To-Date. *Clinical Application of Energy Level Laser Therapy*, Croatia and Switzerland, pp. 279-280

Singer, A.J. and Clark, R.A.F. (1999) Mechanism of disease: Cutaneous wound healing, *New England Journal of Medicine*, **341**(10): 738-746

Skog, S., Tribukait, B., Wallstrom, B. and Ericksson, S. (1987) Hydroxyurea induced cell death as related to cell cycle in mouse and human T-lymphoma cells, *Cancer Res*, **47**: 6490-6493

Smith, C.C., O'Donovan, M.R. and Martin, E.A. (2006) hOGG1 recognises oxidative damage using the comet assay with greater specificity than Fpg or Endo III, *Mutagenesis*, **21**(3): 185-190

Soet, J.S. (2005) Light wave of the future, *Interdisciplinary Journal of the Rehabilitation*, **January/February**: 1-13

Sohn, T.J., Kim, N.K., An, H.J., Ko, J.J., Hahn, T.R., Oh, D., Lee, S.G., Roy, R., Cha, K.Y. and Oh, Y.K. (2001) Gene amplification and expression of the DNA repair enzyme, N-methylpurine DNA glycosylase (MPG) in HPV infected cervical neoplasias, *Anticancer Research*, **21**: 2405-2412

Sommer, A.P., Pinheiro, A.L.B., Mester, A.R., Franke, R.P. and Whelan, H.T. (2001) Biostimulatory windows in low intensity laser activation: Lasers, scanners, and NASA's light emitting diode array system, *Journal of Clinical Medicine and Surgery*, **19**(1): 29-33

Steen, W.M. (2003) Background and general applications. In: O'Neill, B., Li, L. and Akhter, R. (eds) *Laser material processing*. 3rd edition, London, pp.52

Streeter, J., Taboada, L. and Oron, U. (2004) Mechanisms of action of light therapy for stroke and acute myocardial infarction, *Mitochondrion*, **4**: 569-576

Takac, S., Stojanovic, S. and Muhi, B. (1998) Types of medical lasers, *Medicinski Pregled*, **51**(3-4): 146-50

Takao, M. and Yasui, A. (2005) DNA repair initiated by glycosylases in the nucleus and mitochondria of mammalian cells; how our cells respond to a flood of oxidative DNA damage, *Journal of Dermatological Science Supplement*, **1**: 9-19

Tunér, J. and Hode, L. (2002) *Laser therapy-clinical practice and scientific background*, Prima Books, AB Grängesberg, Sweden, pp. 8, 49

Vandesompele, J., de Preter, K., Pattyn, F., Poppe, B., Roy, N., de Paepe, A. and Speleman, F. (2002) Research: Accurate normalisation of real time quantitative RT-PCR data by geometric averaging of multiple internal control genes, *Genome Biology*, **3**(7): 1-11

van Houten, B., Croteau, D.L., Vecchia, M.J.D., Wang, H. and Kisker, C. (2005) "Close-fitting sleeves": DNA damage recognition by the UvrABC nuclease system, *Mutation Research*, **577**(1-2): 92-117

Vincky, E.M., Cagnie, B.J., Cornelissen, M.J., Declercq, H.A. and Cambier, D.C. (2003) Increased fibroblast proliferation induced by light emitting diode and low power laser irradiation, *Lasers in Medical Science*, **18**: 95-99

Wang, Y., Zhu, W. and Levy, D.E. (2006) Nuclear and cytoplasmic mRNA quantification by SYBR green based real time RT-PCR, *Methods*, **39**(4): 356-362

Wang, A., Robertson, J.L., Holladay, S.D., Tennant, A.H., Lengi, A.J., Ahmed, S.A., Huckle, W.R. and Kligerman, A.D. (2007) Measurement of DNA damage in rat urinary bladder transitional cells: Improved selective harvest of transitional cells and detailed comet assay protocols, *Mutation Research*, **634**: 51-59

Whelan, H.T., Buchmann, E.V., Dhokalia, A., Kane, M.P., Whelan, N.T., Wong-Riley, M.T.T., Eells, J.T., Gould, L.J., Hammamieh, R., Das, R. and Jett, M. (2003) Effect of NASA light emitting diode irradiation on molecular changes for wound healing in diabetic mice, *Clinical Laser Medicine and Surgery*, **21**(2): 67-74

Williams, J.Z. and Barbul, A. (2003) Nutrition and wound healing, *Surgical Clinics North America*, **83**(3): 193-197

Wilson, A.S., Hobbs, B.G., Shen, W.Y., Speed, T.P., Schmidt, U., Begley, C.G. and Rackoczy, P.E. (2003) Argon laser photocoagulation induced modification of gene expression in the retina, *Invest Ophthalmol Vis Sci*, **14**: 1426-1434

Wood, R. (1994) DNA Repair. In: Kendrew, J. and Lawrence, E. (eds) *The encyclopedia of molecular biology*, 1st edition, Blackwell Science, Oxford, pp. 277-281

Yabro, J.W., Kennedy, B.J. and Barnum, C.P. (1965) Hydroxyurea inhibition of DNA synthesis in Ascites tumour, *Proceedings of the National Academy of Sciences*, **53**: 1033-1035

Yarrow, J.C., Perlman, Z.E., Westhod, N.J. and Mitchison, T.J. (2004) A high-throughput cell migration assay using scratch wound healing, a comparison image-based readout methods, *BMC Biotechnology*, **4**(21): 1-9

Yilmaz, N., Comelekoglu, U., Aktas, S., Coskun, B. and Bagis, S. (2006) Effect of low energy Gallium Arsenide (GaAS, 904 nm) laser irradiation on wound healing in rat skin, *Wounds*, **18**(11): 323-328

Yu, H.S., Chang, K.L., Yu, C.L., Chen, J.W. and Chen, G.S. (1996) Low energy Helium Neon laser irradiation stimulates interleukin 1 α and interleukin 8 release from cultured human keratinocytes, *Journal of Investigative Dermatology*, **107**: 593 -96

Yu, H.S., Wu, C.S., Yu, C.L., Kao, Y.H. and Chiou, H.M. (2003) Helium Neon laser irradiation stimulates migration and proliferation in melanocytes and induces repigmentation in segmental vitiligo, *Journal of Investigative Dermatology*, **120**: 56-63

Zhang, Y., Song, S., Fong, C.C., Tsang, C.H., Yang, Z. and Yang, M. (2003) cDNA microarray analysis of gene expression profiles in human fibroblast cells irradiated with red light, *Journal of Investigative Dermatology*, **120**(5): 849-857

Zheng, J., Jin, H., Xingang, L., Yuquan, J., Wei, Z. and Daru, L. (2006) Expression analyses of 27 DNA repair genes in astrocytoma by Taqman low density array, *Neuroscience Letters*, **409**: 112-117

Zungu, I., Mbene, A., Houreld, N., Hawkins, D. and Abrahamse, H. (2008) Phototherapy promotes cell migration in the presence of hydroxyurea, *Lasers in Medical Science*, **DOI**: 10.1007/s10103-007-0533-z

MATERIALS AND METHODS

A1 Flow Diagram

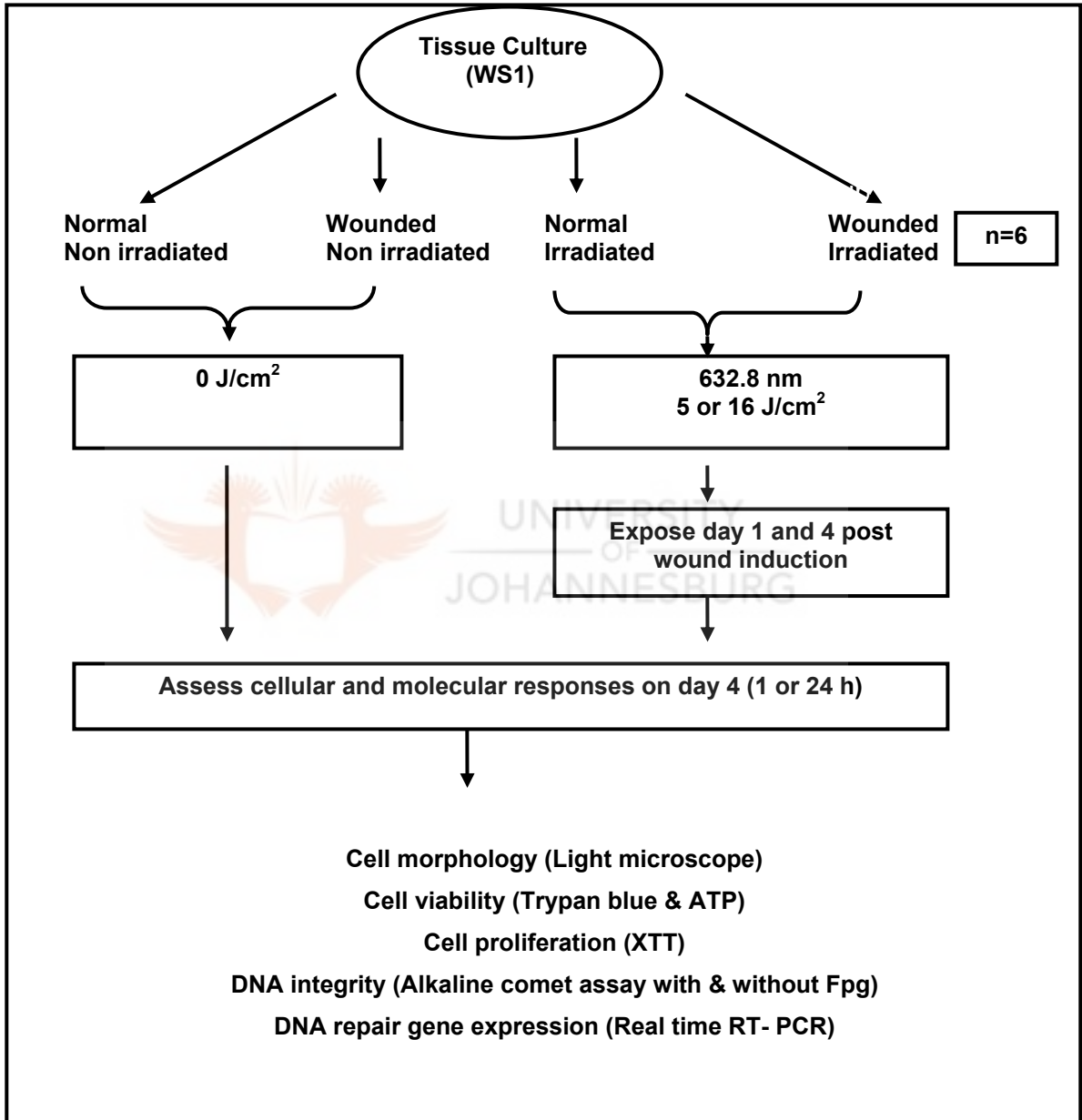


Figure A1 Flow diagram of normal (N) and wounded (W) WS1 cells irradiated with a He-Ne laser (λ 632.8 nm) on day 1 and 4. Cellular responses were measured 1 or 24 h post irradiation on day 4. Non irradiated cells were used as controls.

A2 Equipment Used



Figure A2 An incubator in which cells were grown at 37 °C in 5% CO₂ and 85% humidity.



Figure A3 A centrifuge (DIGICEN-R, INSTRULAB S.A) used to spin cell culture suspensions at 2,200 rpm for 4 min.



Figure A4 An inverted light microscope used to study cell morphology, check contamination and confluence of cells in the 75 cm² culture flasks and 3.4 cm diameter culture dishes. The microscope has a camera attached for digitally recording photographs.



Figure A5 A fluorescent microscope used to score comet assay slides stained with DAPI.



Figure A6 A centrifuge used to spin samples during RNA and cDNA synthesis. This centrifuge has both rpm and gravitation functions.



Figure A7 The RotorGene thermocycler which was used for the real time RT-PCR. It has a hardware for high resolution melts (HRM) which characterises samples based on sequence length, GC content and complementarity.

APPENDIX B

MEDIA, SOLUTIONS AND CALCULATIONS

B1 Cell Line Description

ATCC catalogue number	CRL-1502
Cell line designation	WS1
Organism	<i>Homo sapiens</i> (human)
Tissue	Normal skin fibroblast
Age/stage	12 weeks gestation
Gender	Female
Ethnicity	Black
Morphology	Fibroblast
Depositors	R.J. Hay
Growth properties	Adherent
Comments	WS1 cells are restricted to 67 population doublings

B2 Composition of Complete Media

Minimum essential medium (MEM), (INV/32360-026)	43 ml
10% Foetal bovine serum (FBS), (INV/10108-165)	5 ml
2 mM L-glutamine (INV/25030-024)	1 ml
1 mM Sodium pyruvate (INV/11360-039)	0.5 ml
1% Pen-strep fungizone (INV/17-745E)	0.5 ml
0.1 mM Non essential amino acid (NEAA), (INV/11140-053)	0.5 ml
Complete media prepared for 1 week, labelled and stored in the refrigerator at 4 – 6 °C	

B3 0.25% Trypsin in HBSS

Hanks balanced salt solution (HBSS), (INV/14170-088)	45 ml
2.5% Trypsin (INV/ 15090-046)	5 ml
Label and store at 4 – 6 °C	

B4 3% EDTA (Ethylenediaminetetracetic acid)

EDTA (Merck S.A., A2236020EM)	1.8 g
Distilled water	100 ml

Aliquot in 5 ml tubes, autoclave at 121 °C for 15 min or filter sterilise using a 0.2 µm syringe filter. Label and store at 4 - 6 °C

Working solution of 0.25% Trypsin and 0.03% EDTA
Add 100 µl stock 3% EDTA to 9.9 ml of Trypsin in HBSS

B5 Calculation of Cell Number and Seeding of Culture Dishes (Plates)

Cells/ml = average number of viable cells/square X dilution factor X 10^{4*}

Total number of viable cells = viable cells/ml X total volume (ml)

* Factor to convert number of cells to per ml

6 x 10⁵ cells in 3 ml media is seeded into 3.4 cm diameter culture plates. To determine the number of culture plates and number of cells per plate the following calculations were used:

$$\text{Number of plates} = \frac{\text{Total viable cells}}{6 \times 10^5 \text{ cells}}$$

$$\text{Volume of cells to add} = \frac{\text{Total volume (ml)}}{\text{Number of plates}}$$

Make up to 3 ml with complete media

Example 1: If the total cell count was $4.09 \times 10^6/5$ ml, the number of plates to be made would be

$$\frac{4.09 \times 10^6 \text{ cells}}{6 \times 10^5 \text{ cells}} = 6.817 \text{ plates}$$

Therefore, theoretically among the 6.817 plates, each would get:

$$\frac{5 \text{ ml}}{6.817} = 0.733 \text{ ml of the total cell suspension in 5 ml.}$$

This would translate to 5.99594×10^5 cells/culture plate. Practically 6 plates would be made. The volume of complete medium to be added to each plate would be: $3.0 - 0.733 \text{ ml} = 2.267 \text{ ml}$

Example 2: After harvesting cells from small culture plates, cells are resuspended in 500 μ l HBSS. The total number of

(a) cells would be:

average number of cells/square X dilution factor X 10^4 X 0.5 ml.

(b) the total number of viable cells would be:

average number of viable cells/square X dilution factor X 10^4 X 0.5 ml.

B6 ATP Assay

CellTiter-Glo[®] Luminescent Cell Viability Assay (Promega S.A., G7571)

Aliquot 500 μ l buffer into eppendorfs. Label and store at -20°C .

Weigh 0.0035 g of substrate and store in labelled eppendorfs at -20°C .

Working solution

Dissolve 0.0035 g of substrate into the thawed buffer.

B7 XTT Assay

Thaw XTT labelling reagent (Sodium 3' - [1 - {phenylaminocarbonyl} - 3, 4 - tetrazolium] - bis [4 - methoxy - 6 -nitro] benzene sulfonic acid hydrate) and coupling reagent (PMS [N-methyl dibenzopyrazine methyl sulphate]) (Roche S.A., 11 465 015 001).

Aliquot the thawed reagents into labelled 1.5 ml and 30 µl eppendorfs respectively. Protect from light and store at -80 °C

Working solution

Thaw and add 1.5 ml of XTT labelling reagent to 30 µl coupling reagent. This is enough for 30 tests. Working reagent should be used fresh.

B8 Comet Assay Solutions



B8.1 Phosphate buffered saline (PBS), 1% standard agarose and slide preparation

PBS – dry powder (Sigma-Aldrich S.A., P3744)

The pre-weighed contents of PBS were dissolved in distilled water in a one litre labelled bottle. The solution was autoclaved and stored at 4 – 6 °C.

1% standard agarose

Agarose (Celtic Molecular Diagnostics S.A., Bioline, BIO-41025) 0.8 g

PBS 80 ml

Slides

Cleaned slides were dipped into 1% standard agarose set at 37 °C and let to dry at room temperature over night.

B8.2 1% Low melting point agarose (LMP)

1g LMP agarose (Sigma-Aldrich S.A., A-9414)	0.8g
PBS	80 ml

B8.3 Lysis solution

2.5 M NaCl (Merck S.A., 5822320 EM)	146.1 g/L
0.1 M EDTA	37.2 g/L
10 mM Tris base (Sigma-Aldrich S.A., T-6066)	1.21 g/L

Dissolve in 0.8 L of distilled water, immediately add 35 ml of NaOH to ensure that NaCl, EDTA and Tris dissolve. Add drop wise to pH 10.0 and raise volume to 1 L. Label and autoclave the solution. Store at 4 – 6 °C. Add 1 ml Triton X - 100 per 100 ml of lysis solution immediately before use.

B8.4 Electrophoresis solution

0.3 M NaOH (Merck S.A., 5823200 EM)	12 g/L
1 mM EDTA	0.372 g/L

Add distilled water up to 1 litre. Label, autoclave and store at 4 – 6 °C.

B8.5 Neutralisation buffer

0.4 M Tris base (Tris [hydroxymethyl]aminomethane)	48.44 g/L
--	-----------

Dissolve in 0.8 L of distilled water, pH to 7.5 with concentrated HCl then make up volume to 1 L with distilled water.

Label, autoclave and store at 4 – 6 °C.

B8.6 Sodium hydroxide (NaOH) solution (10 M)

10 M NaOH	200 g
-----------	-------

Dissolve 200 g of NaOH in distilled water to a final volume of 500 ml. Label and autoclave the solution; crystals dissolve during autoclaving. Store the solution at 4 – 6 °C.

B8.7 Enzyme reaction buffer

40 mM HEPES (N-[2-Hydroxyethyl] piperazine-N'-[2-ethane-sulfonic acid]), (Sigma-Aldrich S.A., H-7006)	10.412 g/L
0.1 M KCl (Merck S.A., AB004936.500)	7.455 g/L
0.5 mM EDTA	0.1861 g/L
0.2 mg/ml Bovine Serum Albumin (AEC-Amersham S.A., RPN 412)	0.2 g/L
pH 8.0 with KOH	
Stock 1 M KOH	56.11g/L

BSA was filter sterilised and added after autoclaving so as not to denature the protein. The reaction buffer was aliquoted into labeled 500 ml bottles and stored at -20 °C.

B8.8 Formamido pyrimidine glycosylase (Fpg)

Fpg (Sigma-Aldrich S.A., F-3174); 10 µg/ml stock (1 ml) in enzyme buffer stored at -20 °C. Add 2 µl of the stock to 598 µl of enzyme buffer (1:300). Aliquot 30 µl into 20 tubes and store at -20 °C.

Working solution

Add 270 µl enzyme reaction buffer to 30 µl aliquoted tubes (1:10 dilution). Therefore, final dilution was 1:3,000.

B8.9 4'6-diamidine-2-phenylindol dihydrochloride (DAPI)

Store DAPI (Sigma-Aldrich S.A., D-9564) at room temperature upon receipt and protect from light. To prepare 1 mg/ml stock DAPI, 10 mg DAPI dissolved in 10 ml of sterile distilled water. Protect from light, label and store at -20 °C.

Working solution (1 µg/ml)

Dilute 1 µl of 1 mg/ml DAPI with 999 µl of PBS. Aliquot into labelled 500 µl eppendorfs wrapped in a foil and stored at -20 °C and used within 6 months.

B9 Real Time RT-PCR Solutions

B9.1 Tris-EDTA (TE) buffer, pH 8.0

0.01 M Tris 0.606 g/L

0.001 M EDTA 0.372 g/L

Dissolve in about 600 ml of distilled water. Adjust pH with 5 M HCl (Sigma-Aldrich S.A., H-1111CCO2500) to pH 8.0. Allow the solution to cool to room temperature before making the final pH adjustments. Adjust final volume to one litre with distilled water. Label, autoclave and store at room temperature.

B9.2 50x Tris acetate EDTA (TAE) buffer

4 M Tris base 242 g/L

0.025 M EDTA 9.3 g/L

17.4 M Glacial acetic acid (Merck S.A., 1021020LC) 57.1 ml

Dissolve Tris and EDTA in 600 ml of distilled water and add 57.1 ml glacial acetic acid. Adjust the pH of the solution to pH 8.0 and make up the volume with distilled water to 1 litre. Label, autoclave and store at room temperature.

Working solution (1x TAE buffer)

For 1 litre, mix 20 ml of 50x TAE buffer with 980 ml of sterile distilled water.

APPENDIX D

CALCULATION AND CONCENTRATION OF cDNA

Samples were diluted in Tris EDTA buffer, pH 8.0 and the same buffer was used to zero the UV spectrophotometer at 260 nm using the quartz cuvettes. The average extinction coefficient of single stranded DNA at 260 nm is 37 $\mu\text{g/ml}$. Thus, using a 1 cm path length 1 unit of absorbance at 260 (A_{260}) = 37 $\mu\text{g/ml}$ single stranded DNA. The final concentration was divided by 1000 to convert to $\mu\text{g}/\mu\text{l}$.

Table D1 Average concentration of cDNA

EXPERIMENTAL SAMPLE	BIOLOGICAL SAMPLE	A_{260}	DILUTION FACTOR	EXTINCTION COEFFICIENT	CONCENTRATION ($\mu\text{g}/\mu\text{l}$)
N	1	0.145	250	37	1.3
	2	0.156	250	37	1.4
	Average				1.4
W	1	0.160	250	37	1.5
	2	0.159	250	37	1.5
	Average				1.5
W5	1	0.169	250	37	1.6
	2	0.178	250	37	1.6
	Average				1.6
W16	1	0.155	250	37	1.4
	2	0.180	250	37	1.7
	Average				1.6

N = normal; W = wounded; W5 = wounded irradiated with 5 J/cm^2 ; W16 = wounded irradiated with 16 J/cm^2 .

On average the concentration of cDNA was 1.5 $\mu\text{g}/\mu\text{l}$ (1500 $\text{ng}/\mu\text{l}$). Samples were diluted 1:10 prior to PCR reaction therefore cDNA concentration after dilution was 150 $\text{ng}/\mu\text{l}$. Since 2 μl of cDNA was used per PCR reaction that means total cDNA concentration was 300 ng per reaction.

APPENDIX E

REAL TIME RT-PCR RESULTS

E1 Melt Report for ACTB



14 Hilly Street Mortlake NSW 2137 Australia
T + 61 2 9736 1320
F + 61 2 9736 1364
W www.corbettlifescience.com

Experiment Information

Run Name	Expression ACTB
Run Start	2008/03/13 10:31:11 AM
Run Finish	2008/03/13 11:44:19 AM
Operator	Alwin
Notes	Expression of house keeping gene (ACTB)
Run On Software Version	Rotor-Gene 1.7.75
Run Signature	The Run Signature is valid.
Gain Green	5.

Melt Information

Digital Filter	Light
Imported Analysis Settings	
Sample Page	Page 1
Temp. Threshold	0°C
Threshold	1.95948

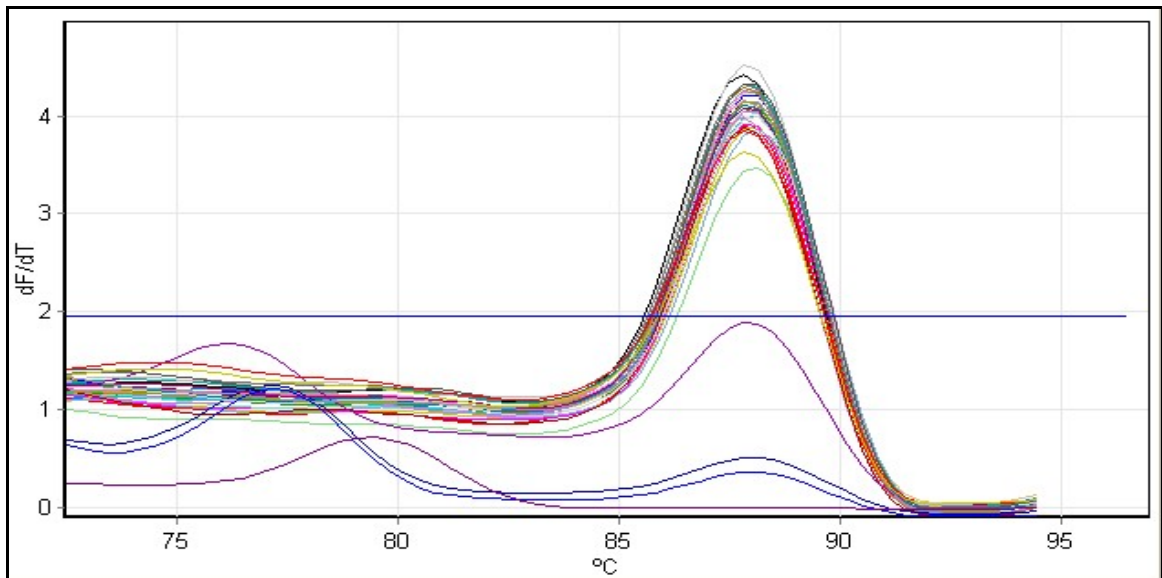
Messages

Message
























Profile

Cycle	Cycle Point
Hold @ 95°C, 10 min 0 sec	
Cycling (40 repeats)	Step 1 @ 95°C, hold 5 sec
	Step 2 @ 60°C, hold 15 sec
	Step 3 @ 72°C, hold 15 sec, acquiring to Cycling A([Green][1][1])
Melt (72-95°C) , hold sec on the 1st step, hold 5 sec on next steps, Melt A([Green][1][1])	

Melt data for Melt A. Green



No.	Colour	Name	Genotype	Peak 1
1	Red	Normal (0J) 1 1 :10 ACTB		88.0
2	Yellow	Normal (0J) 1 1 :10 ACTB		88.0
3	Blue	Normal (0J) 2 1 :10 ACTB		88.0
4	Purple	Normal (0J) 2 1 :10 ACTB		88.0
5	Pink	Normal (0J) 3 1 :10 ACTB		88.0
6	Light Blue	Normal (0J) 3 1 :10 ACTB		88.0
7	Teal	Wounded (0J) 1 1 :10 ACTB		88.0
8	Light Red	Wounded (0J) 1 1 :10 ACTB		88.0
9	Green	Wounded (0J) 2 1 :10 ACTB		88.0
10	Magenta	Wounded (0J) 2 1 :10 ACTB		88.0
11	Black	Wounded (0J) 3 1 :10 ACTB		87.8
12	Cyan	Wounded (0J) 3 1 :10 ACTB		88.0

No.	Colour	Name	Genotype	Peak 1
13		Wounded (5J) 1 1 :10 ACTB		88.0
14		Wounded (5J) 1 1 :10 ACTB		88.0
15		Wounded (5J) 2 1 :10 ACTB		88.0
16		Wounded (5J) 2 1 :10 ACTB		88.2
17		Wounded (5J) 3 1 :10 ACTB		88.0
18		Wounded (5J) 3 1 :10 ACTB		88.0
19		Wounded (16J) 1 1 :10 ACTB		87.8
20		Wounded (16J) 1 1 :10 ACTB		88.0
21		Wounded (16J) 2 1 :10 ACTB		88.0
22		Wounded (16J) 2 1 :10 ACTB		88.0
23		Wounded (16J) 3 1 :10 ACTB		88.0
24		Wounded (16J) 3 1 :10 ACTB		88.0
25		Water		
26		Water		
27		Undiluted		88.0
28		Undiluted		88.0
29		Standard 1:10		88.0
30		Standard 1.10		88.0
31		Standard 1:100		88.0
32		Standard 1:100		88.0
33		Standard 1:1000		88.0
34		Standard 1:1000		88.0
35		Water		
36		Water		

Bin Name	Temperature	Sample No.	Sample Name	Peak
----------	-------------	------------	-------------	------



**Quality
Endorsed
Company**
ISO 9001 Lic 21313
SAI Global

This report generated by Rotor-Gene 6000 Series Software 1.7 (Build 75)
 Copyright ©2000-2006 Corbett Research, a Division of Corbett Life Science. All rights reserved.
 ISO 9001:2000 (Reg. No. QEC21313)



E2 Melt Report for GAPDH



14 Hilly Street Mortlake NSW 2137 Australia
 T + 61 2 9736 1320
 F + 61 2 9736 1364
 W www.corbettlifescience.com

Experiment Information

Run Name	Run 2008-03-07 Reference genes GAPDH
Run Start	3/7/2008 10:02:35 AM
Run Finish	3/7/2008 11:15:32 AM
Operator	Alwin
Notes	Reference genes (GAPDH)
Run On Software Version	Rotor-Gene 1.7.75
Run Signature	The Run Signature is valid.
Gain Green	5.

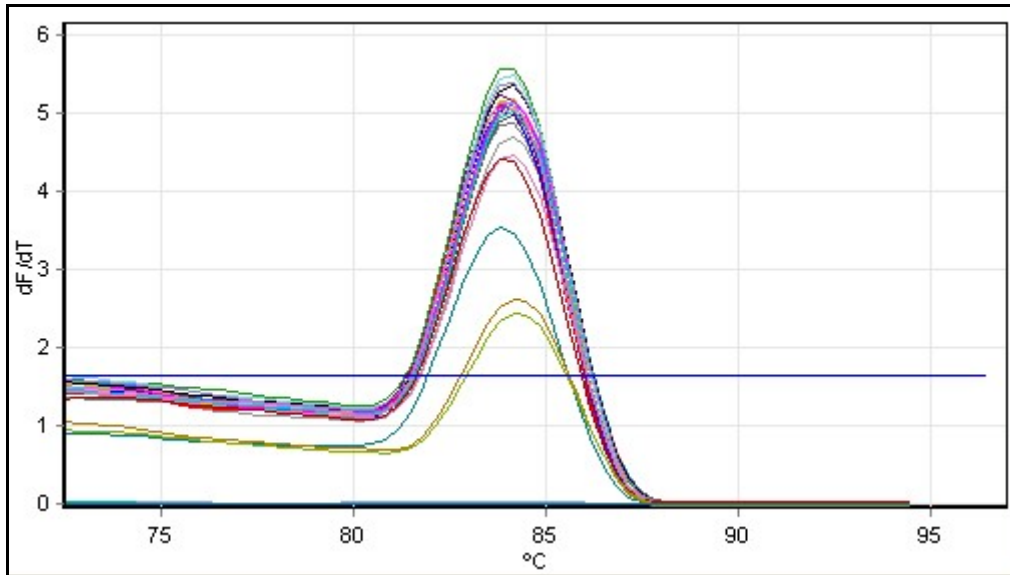
Melt Information

Digital Filter	Light
Imported Analysis Settings	
Sample Page	Reference gene (GAPDH)
Temp. Threshold	0°C
Threshold	1.62928













Profile

Cycle	Cycle Point
Hold @ 95°C, 10 min 0 sec	
Cycling (40 repeats)	Step 1 @ 95°C, hold 5 sec
	Step 2 @ 60°C, hold 15 sec
	Step 3 @ 72°C, hold 15 sec, acquiring to Cycling A([Green][1][1])
Melt (72-95°C) , hold sec on the 1st step, hold 5 sec on next steps, Melt A([Green][1][1])	

Melt data for Melt A. Green



No.	Colour	Name	Genotype	Peak 1
29	Grey	Normal sample (0J) 1 1:10		84.0
30	Grey	Normal sample (0J) 1 1:10		84.0
31	Dark Grey	Normal sample (0J) 2 1:10		84.0
32	Black	Normal sample (0J) 2 1:10		84.0
33	Red	Wounded sample (0J) 1 1:10		84.0
34	Yellow	Wounded sample (0J) 1 1:10		84.0
35	Blue	Wounded sample (0J) 2 1:10		84.0
36	Purple	Wounded sample (0J) 2 1:10		84.0
37	Pink	Wounded sample (5J) 1 1:10		84.2
38	Light Blue	Wounded sample (5J) 1 1:10		84.2
39	Teal	Wounded sample (5J) 2 1:10		83.8
40	Light Red	Wounded sample (5J) 2 1:10		84.2
41	Green	Wounded sample (16J) 1 1:10		84.0
42	Magenta	Wounded sample (16J) 1 1:10		84.0
43	Black	Wounded sample (16J) 2 1:10		84.0
44	Cyan	Wounded sample (16J) 2 1:10		84.0

No.	Colour	Name	Genotype	Peak 1
45		Water		
46		Water		
47		Undiluted std		84.0
48		Undiluted std		
49		Std 1:10		84.0
50		Std 1:10		84.0
51		Std 1:100		84.0
52		Std 1:100		84.0
53		Std 1:1000		84.3
54		Std 1:1000		84.3
55		Water		
56		Water		

Bin Name Temperature Sample No. Sample Name Peak



™ This report generated by Rotor-Gene 6000 Series Software 1.7 (Build 75)
 Copyright ©2000-2006 Corbett Research, a Division of Corbett Life Science.
 All rights reserved.
 ISO 9001:2000 (Reg. No. QEC21313)



E3 Melt Report for UBC



14 Hilly Street Mortlake NSW 2137 Australia
T + 61 2 9736 1320
F + 61 2 9736 1364
W www.corbettlifescience.com

Experiment Information

Run Name	Alwin (Reference gene (UBC) 2008-03-07
Run Start	3/7/2008 2:18:21 PM
Run Finish	3/7/2008 3:31:39 PM
Operator	Alwin
Notes	Reference gene (UBC)
Run On Software Version	Rotor-Gene 1.7.75
Run Signature	The Run Signature is valid.
Gain Green	5.

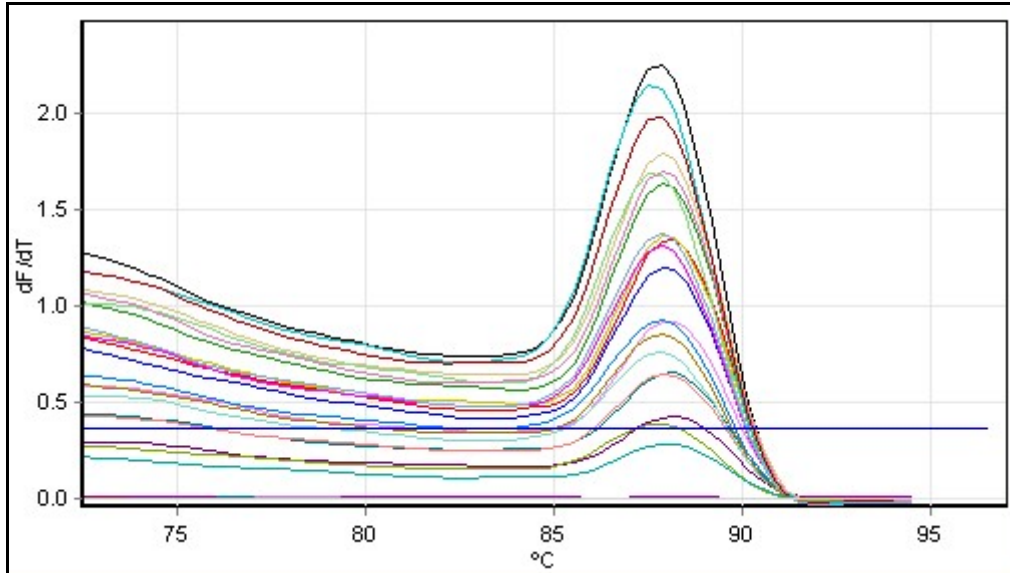
Melt Information

Digital Filter	Light
Imported Analysis Settings	
Sample Page	Reference gene
Temp. Threshold	0°C
Threshold	0.36554











Profile

Cycle	Cycle Point
Hold @ 95°C, 10 min 0 sec	
Cycling (45 repeats)	Step 1 @ 95°C, hold 5 sec
	Step 2 @ 60°C, hold 15 sec
	Step 3 @ 72°C, hold 15 sec, acquiring to Cycling A([Green][1][1])
Melt (72-95°C) , hold sec on the 1st step, hold 5 sec on next steps, Melt A([Green][1][1])	

Melt data for Melt A. Green



No.	Colour	Name	Genotype	Peak 1	Peak 2
1	Red	Normal (0J) 1 1:10		88.0	
2	Yellow	Normal (0J) 1 1:10		88.0	
3	Blue	Normal (0J) 2 1:10		88.0	
4	Purple	Normal (0J) 2 1:10		88.0	
5	Pink	Wounded (0J) 1 1:10		88.0	
6	Light Blue	Wounded (0J) 1 1:10		87.8	
7	Teal	Wounded (0J) 2 1:10		88.0	
8	Light Red	Wounded (0J) 2 1:10		88.0	
9	Green	Wounded (5J) 1 1:10		88.0	
10	Magenta	Wounded (5J) 1 1:10		87.8	
11	Black	Wounded (5J) 2 1:10		87.7	
12	Cyan	Wounded (5J) 2 1:10		87.5	
13	Olive	Wounded (16J) 1 1:10		87.8	
14	Light Green	Wounded (16J) 1 1:10		87.7	
15	Light Cyan	Wounded (16J) 2 1:10		87.8	
16	Light Blue	Wounded (16J) 2 1:10		87.8	
17	Light Purple	Water			
18	Light Purple	Water			

No.	Colour	Name	Genotype	Peak 1	Peak 2
19		Undiluted		88.0	
20		Undiluted		83.5	87.7
21		Std 1:10		87.8	
22		Std 1:10		87.7	
23		Std 1:100			
24		Std 1:100			
25		Std 1:1000			
26		Std 1:1000			
27		Water			
28		Water			

Bin Name Temperature Sample No. Sample Name Peak



**Quality
Endorsed
Company**
ISO 9001 Lic 21313
SAI Global

This report generated by Rotor-Gene 6000 Series Software 1.7 (Build 75)
Copyright ©2000-2006 Corbett Research, a Division of Corbett Life Science. All rights reserved.
ISO 9001:2000 (Reg. No. QEC21313)

UNIVERSITY
OF
JOHANNESBURG

E4 Relative Expression Report for Reference Genes

Notes

Relative expression of the 3 reference genes (ACTB, GAPDH and UBC)

Assay Parameters

Parameter	Value
Iterations	50000
Normalisation Factor	1.00

Gene	Reaction Efficiency	Expression	Std Error	95% C.I.	P(HI)	Results
ACTB						
N	94%	1.000	0.9 - 1.11	0.8 - 1.2	1.000	
W		0.851	0.8 - 0.9	0.7 - 1.0	0.095	
W5		0.773	0.7 - 0.8	0.6 - 1.0	0.055	
W16		0.798	0.7 - 0.9	0.6 - 1.0	0.052	
GAPDH						
N	82%	1.000	0.7 - 1.3	0.6 - 1.5	1.000	
W		1.256	1.0 - 1.5	0.9 - 1.6	0.110	
W5		0.691	0.2 - 1.2	0.1 - 1.4	0.574	
W16		1.424	1.1 - 1.8	1.0 - 1.9	0.047	UP
UBC						
N	97%	1.000	0.3 - 5.5	0.1 - 11	1.000	
W		0.620	0.2 - 2.5	0.2 - 4.9	0.541	
W5		4.574	1.3 - 14	0.8 - 52	0.101	
W16		1.940	0.6 - 8.0	0.3 - 19	0.481	

N = Normal non irradiated; W = Wounded non irradiated; W5 = Wounded irradiated with 5 J/cm²; W16 = Wounded irradiated with 16 J/cm²; P(HI) = Probability of alternate hypothesis that difference between sample and control groups is due only to chance.

Interpretation

N(ACT) sample group is not different to control group. P(H1)=1.000

W sample group is not different to control group. P(H1)=0.095

W(5) sample group is not different to control group. P(H1)=0.055

W(16) sample group is not different to control group. P(H1)=0.052

N(GAP) sample group is not different to control group. P(H1)=1.000

W sample group is not different to control group. P(H1)=0.110

W(5) sample group is not different to control group. P(H1)=0.574

W(16) is UP-regulated in sample group (in comparison to control group) by a mean factor of 1.424 (S.E. range is 1.139 - 1.862).

W(16) sample group is different to control group. $P(H1)=0.047$

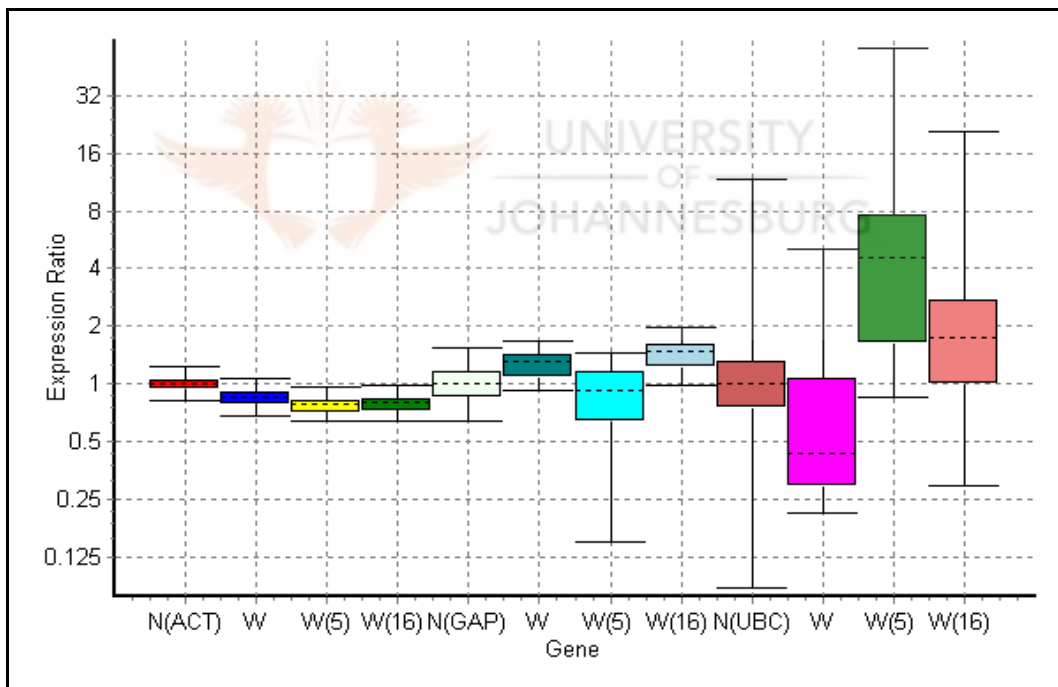
N(UBC) sample group is not different to control group. $P(H1)=1.000$

W sample group is not different to control group. $P(H1)=0.541$

W(5) sample group is not different to control group. $P(H1)=0.101$

W(16) sample group is not different to control group. $P(H1)=0.481$

Boxes represent the interquartile range, or the middle 50% of observations. The dotted line represents the median gene expression. Whiskers represent the minimum and maximum observations.



Report produced by REST 2005 V1.9.12
© Corbett Research, 2005

E5 MPG Expression in W Cells Irradiated With 5 J/cm² 1 h Incubation Post Irradiation

Quantitation Report



14 Hilly Street Mortlake NSW 2137 Australia
T + 61 2 9736 1320
F + 61 2 9736 1364
W www.corbettlifescience.com

Experiment Information

Run Name	Alwin 2008-02-14 (1)
Run Start	2008/02/14 10:47:13 AM
Run Finish	2008/02/14 11:52:54 AM
Operator	Alwin
Notes	14/02/08
Run On Software Version	Rotor-Gene 1.7.75
Run Signature	The Run Signature is valid.
Gain Green	5.

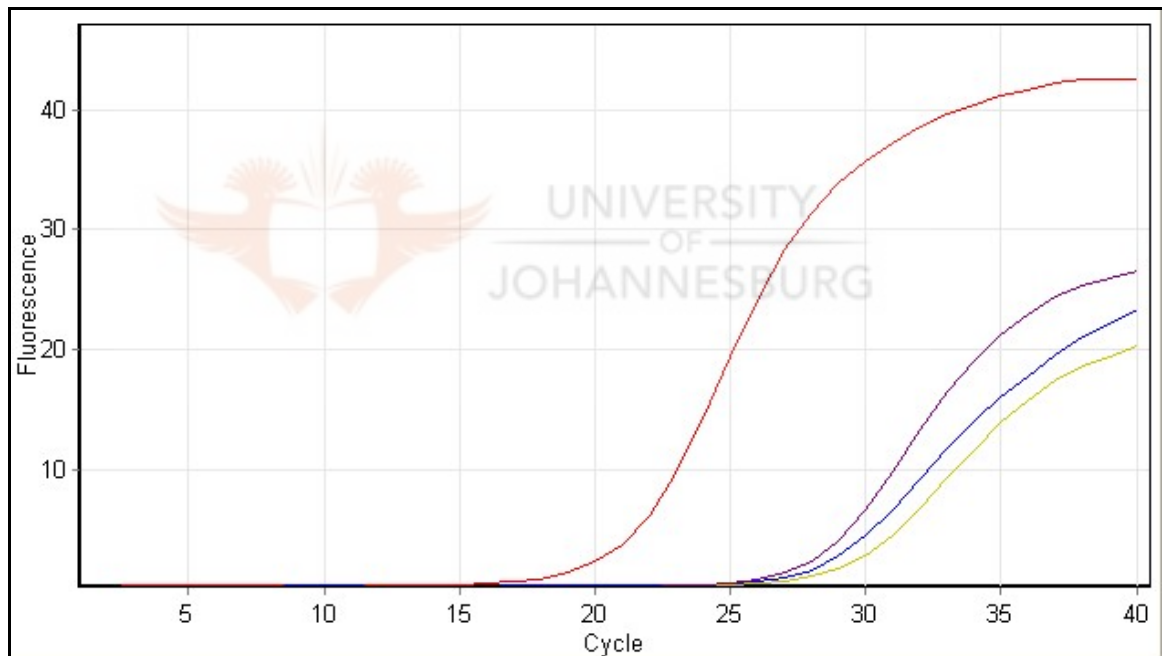
Quantitation Information

Threshold	0.01103
Left Threshold	1.000
Standard Curve Imported	No
Standard Curve (1)	N/A
Standard Curve (2)	N/A
Start normalising from cycle	1
Noise Slope Correction	No
No Template Control Threshold	0%
Reaction Efficiency Threshold	Disabled
Normalisation Method	Dynamic Tube Normalisation
Digital Filter	Light
Sample Page	Page 1
Imported Analysis Settings	

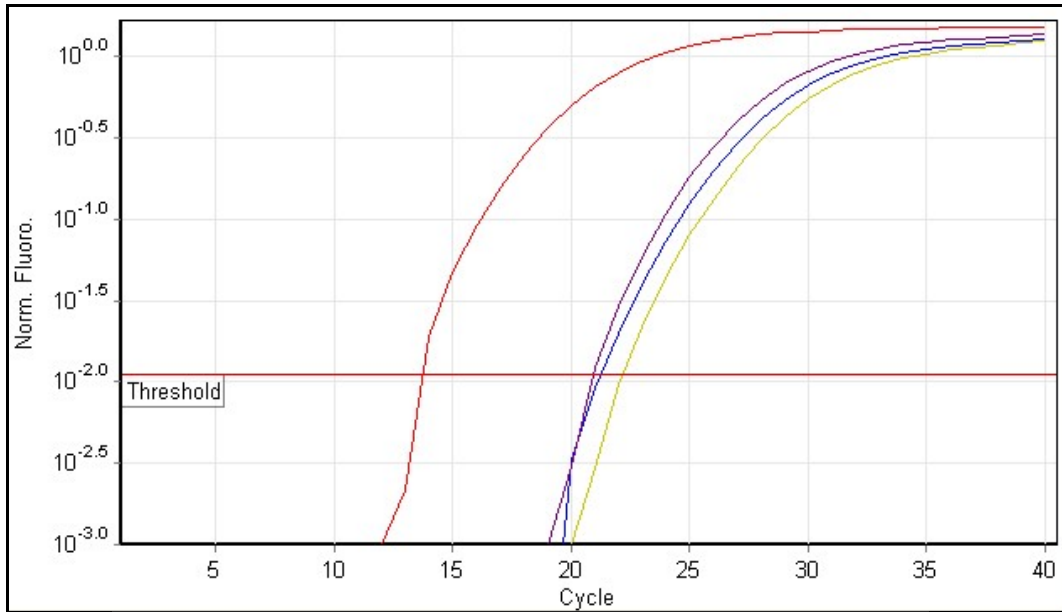
Profile

Cycle	Cycle Point
Hold @ 95°C, 10 min	
Cycling (40 repeats)	Step 1 @ 95°C, hold 5 s
	Step 2 @ 60°C, hold 15 s
	Step 3 @ 72°C, hold 15 s, acquiring to Cycling A([Green][1][1])
Melt (72-95°C) , hold on the 1st step, hold 5 s on next steps, Melt A ([Green][1][1])	






Raw Data For Cycling A. Green



Quantitation data for Cycling A. Green



Threshold cycles (C_t) for ACTB and MPG in W WS1 cells irradiated with 5 J/cm^2 and left to incubate 1 h post irradiation.

No.	Colour	Type		C_t
1		W cells	ACTB	13.60
2		W cells	NTC	21.2
3		W cells	MPG	22.15
4		W cells	MPG	21.22
5		W cells	NTC	20.88



This report generated by Rotor-Gene 6000 Series Software 1.7 (Build 75)
 Copyright ©2000-2006 Corbett Research, a Division of Corbett Life Science. All rights reserved.
 ISO 9001:2000 (Reg. No. QEC21313)

E6 MPG Expression in W Cells Irradiated With 16 J/cm² 0 h Incubation Post Irradiation

Quantitation Report



14 Hilly Street Mortlake NSW 2137 Australia
 T + 61 2 9736 1320
 F + 61 2 9736 1364
 W www.corbettlifescience.com

Experiment Information

Run Name	Expression of MPG in WS1 or MCF7 cells 2008-04-18 (1)
Run Start	2008/04/18 11:54:56 AM
Run Finish	2008/04/18 01:06:41 PM
Operator	Alwin
Notes	Expression of MPG in WS1 (W cells irradiated with 16 J/cm ²) or MCF 7 cells 0 h post irradiation
Run On Software Version	Rotor-Gene 1.7.75
Run Signature	The Run Signature is valid.
Gain Green	5.

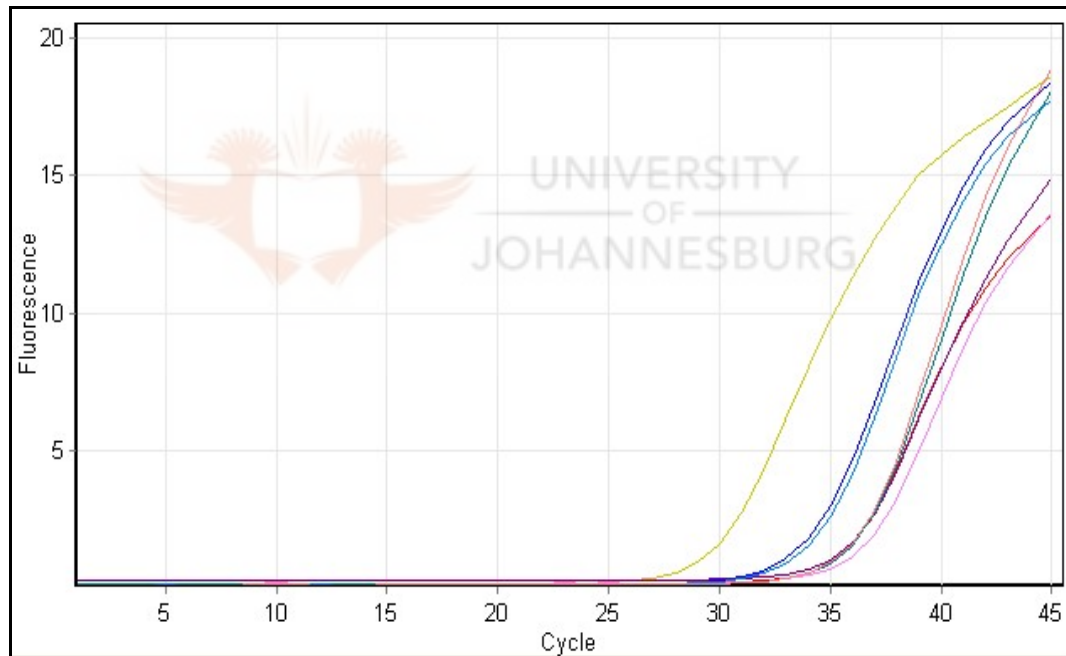
Quantitation Information

Threshold	0.01609
Left Threshold	1.000
Standard Curve Imported	No
Standard Curve (1)	N/A
Standard Curve (2)	N/A
Start normalising from cycle	1
Noise Slope Correction	No
No Template Control Threshold	0%
Reaction Efficiency Threshold	Disabled
Normalisation Method	Dynamic Tube Normalisation
Digital Filter	Light
Sample Page	Page 1
Imported Analysis Settings	

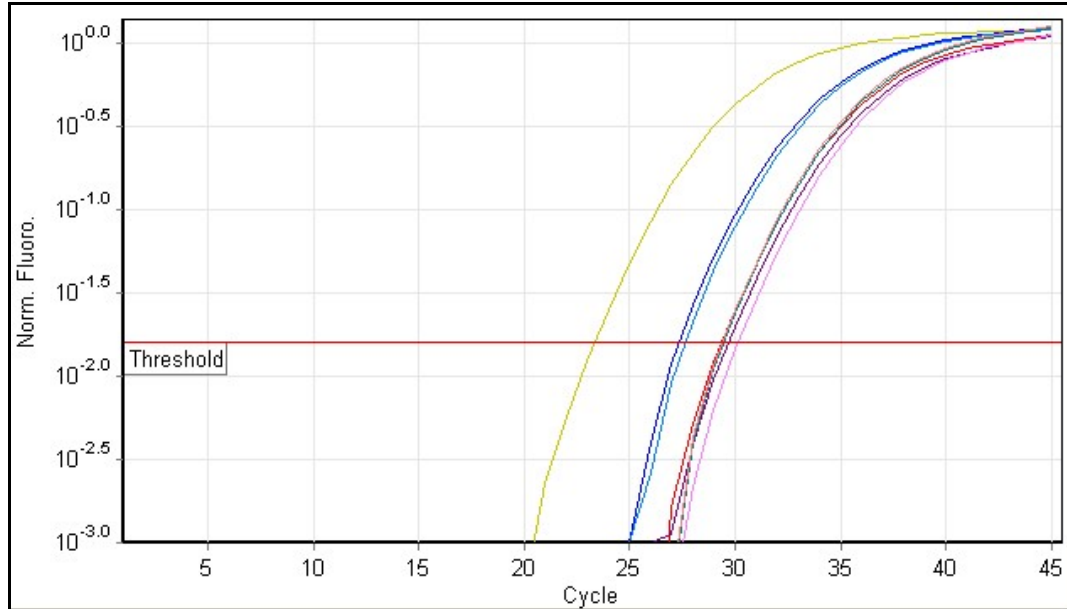
Profile

Cycle	Cycle point
Hold @ 95°C, 10 min	
Cycling (45 repeats)	Step 1 @ 95°C, hold 5 s
	Step 2 @ 60°C, hold 15 s
	Step 3 @ 72°C, hold 15 s, acquiring to Cycling A ([Green][1][1])
Melt (72-95°C) , hold on the 1st step, hold 5 s on next steps, Melt A ([Green][1][1])	

Raw Data For Cycling A. Green



Quantitation data for Cycling A. Green



Threshold cycles (C_t) for NTC, NRT samples, MCF 7 cells and wounded (W) cells irradiated with 16 J/cm^2 and left to incubate 0 h post irradiation.

No.	Colour	Type	C_t
1	Red	W16	29.37
2	Yellow	W16	26.36
3	Blue	MCF 7	27.35
4	Purple	MCF 7	29.70
5	Pink	NRT	30.14
6	Light Blue	NRT	27.64
7	Teal	NTC	29.46
8	Light Red	NTC	29.40



This report generated by Rotor-Gene 6000 Series Software 1.7 (Build 75)
 Copyright ©2000-2006 Corbett Research, a Division of Corbett Life Science. All rights reserved.
 ISO 9001:2000 (Reg. No. QEC21313)

E7 MPG Expression in W Cells Irradiated With 16 J/cm² 3 h Incubation Post Irradiation

Quantitation Report



14 Hilly Street Mortlake NSW 2137 Australia
 T + 61 2 9736 1320
 F + 61 2 9736 1364
 W www.corbettlifescience.com

Experiment Information

Run Name	Expression of MPG in WS1 or MCF7 cells 2008-04-13
Run Start	2008/04/13 03:01:15 PM
Run Finish	2008/04/13 04:13:32 PM
Operator	Alwin
Notes	Expression of MPG in WS1 (W cells irradiated with 16 J/cm ²) or MCF 7 cells 3 h post irradiation
Run On Software Version	Rotor-Gene 1.7.75
Run Signature	The Run Signature is valid.
Gain Green	5.

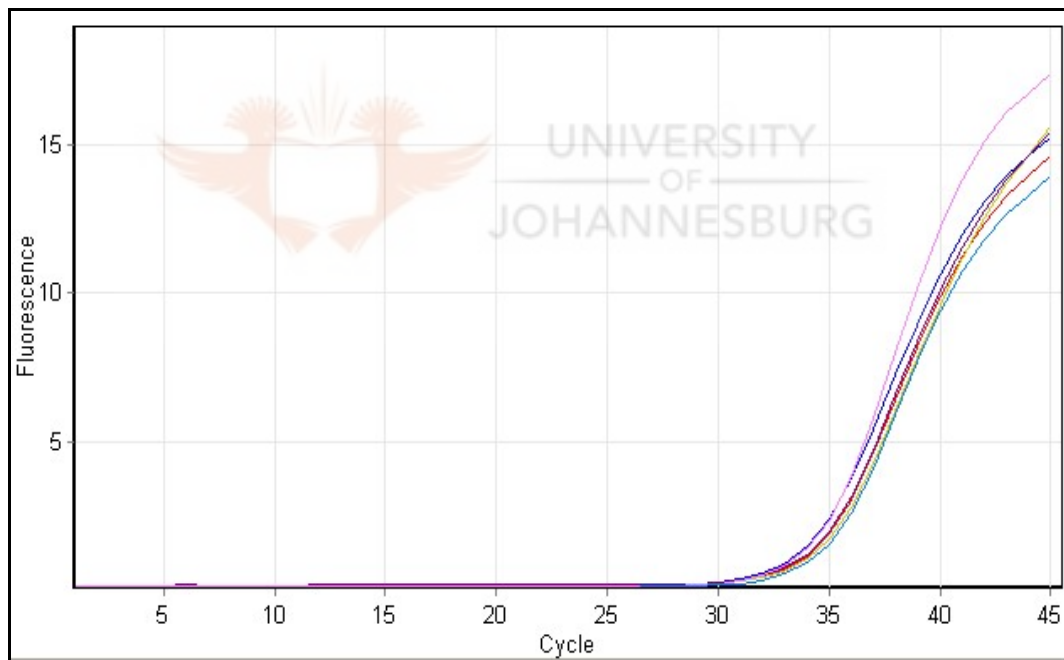
Quantitation Information

Threshold	0.06348
Left Threshold	1.000
Standard Curve Imported	No
Standard Curve (1)	N/A
Standard Curve (2)	N/A
Start normalising from cycle	1
Noise Slope Correction	No
No Template Control Threshold	0%
Reaction Efficiency Threshold	Disabled
Normalisation Method	Dynamic Tube Normalisation
Digital Filter	Light
Sample Page	Page 1
Imported Analysis Settings	

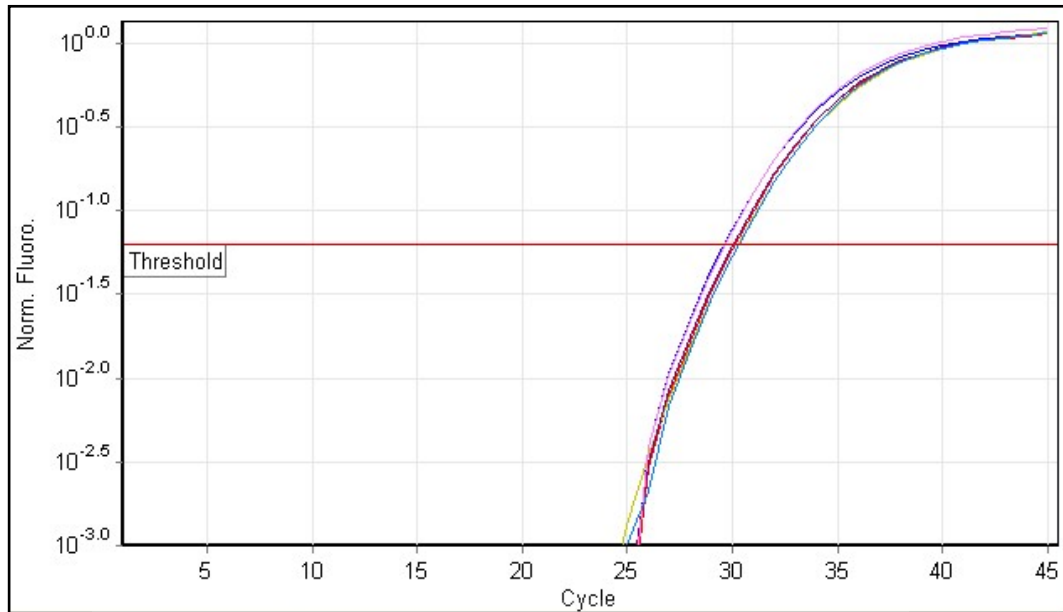
Profile

Cycle	Cycle Point
Hold @ 95°C, 10 min	
Cycling (45 repeats)	Step 1 @ 95°C, hold 5 s
	Step 2 @ 60°C, hold 15 s
	Step 3 @ 72°C, hold 15 s, acquiring to Cycling A([Green][1][1])
Melt (72-95°C) , hold s on the 1st step, hold 5 s on next steps, Melt A([Green][1][1])	

Raw Data For Cycling A. Green



Quantitation data for Cycling A. Green



Threshold cycles (C_t) for MCF 7 cells non irradiated, NRT samples and wounded (W) WS1 cells irradiated with 16 J/cm² and left to incubate 3 h post irradiation,

No.	Colour	Type	Ct
1	Red	W16	30.13
2	Yellow	W16	30.30
3	Blue	MCF 7	29.63
4	Purple	MCF 7	30.05
5	Pink	NRT	29.68
6	Cyan	NRT	30.32



This report generated by Rotor-Gene 6000 Series Software 1.7 (Build 75)
 Copyright ©2000-2006 Corbett Research, a Division of Corbett Life Science. All rights reserved.
 ISO 9001:2000 (Reg. No. QEC21313)

E8 MPG Expression in W Cells Irradiated on day 1 With 16 J/cm² 8 h Incubation Post Irradiation

Quantitation Report



14 Hilly Street Mortlake NSW 2137 Australia
 T + 61 2 9736 1320
 F + 61 2 9736 1364
 W www.corbettlifescience.com

Experiment Information

Run Name	Expression of MPG in WS1 or MCF 7 cells 2008-04-11 (1)
Run Start	2008/04/11 07:26:22 AM
Run Finish	2008/04/11 08:43:35 AM
Operator	Alwin
Notes	Expression of MPG in WS1(W cells irradiated with 16 J/cm ²) or MCF 7 cells 8 h post irradiation
Run On Software Version	Rotor-Gene 1.7.75
Run Signature	The Run Signature is valid.
Gain Green	5.

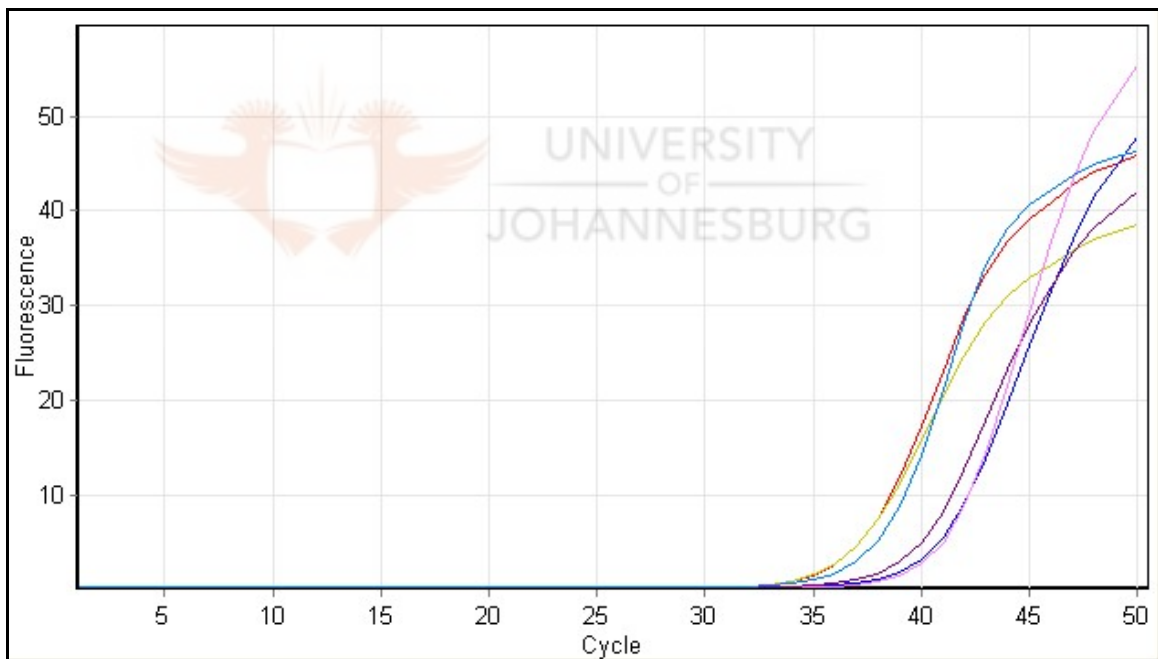
Quantitation Information

Threshold	0.02838
Left Threshold	1.000
Standard Curve Imported	No
Standard Curve (1)	N/A
Standard Curve (2)	N/A
Start normalising from cycle	1
Noise Slope Correction	No
No Template Control Threshold	0%
Reaction Efficiency Threshold	Disabled
Normalisation Method	Dynamic Tube Normalisation
Digital Filter	Light
Sample Page	Page 1
Imported Analysis Settings	

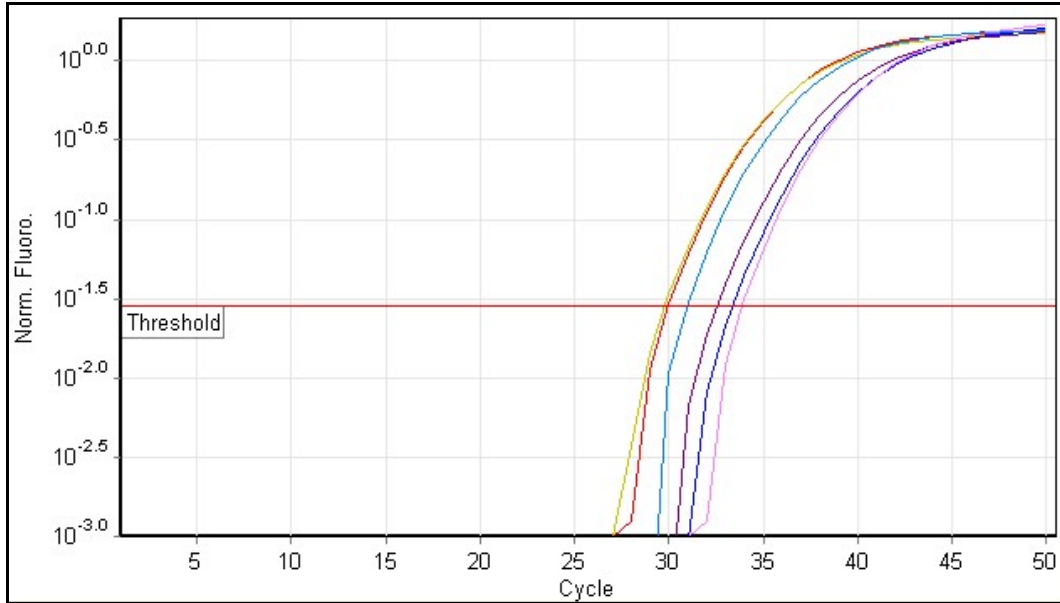
Profile

Cycle	Cycle Point
Hold @ 95°C, 10 min	
Cycling (50 repeats)	Step 1 @ 95°C, hold 5 s
	Step 2 @ 60°C, hold 15 s
	Step 3 @ 72°C, hold 15 s, acquiring to Cycling A([Green][1][1])
Melt (72-95°C) , hold on the 1st step, hold 5 s on next steps, Melt A ([Green][1][1])	

Raw Data For Cycling A. Green



Quantitation data for cycling A. Green



Threshold cycles (C_t) for NRT sample, MCF 7 cells and wounded (W) WS1 cells irradiated with 16 J/cm^2 and left to incubate 8 h post irradiation.

No.	Colour	Type	Ct
1	Red	W16	29.95
2	Yellow	W16	29.78
3	Blue	MCF 7	33.37
4	Purple	MCF 7	32.54
5	Teal	NRT	33.87
6	Pink	NRT	30.94



This report generated by Rotor-Gene 6000 Series Software 1.7 (Build 75)
 Copyright ©2000-2006 Corbett Research, a Division of Corbett Life Science. All rights reserved.
 ISO 9001:2000 (Reg. No. QEC21313)